

UNCLASSIFIED

AD 287 052

*Reproduced
by the*

**ARMED SERVICES TECHNICAL INFORMATION AGENCY
ARLINGTON HALL STATION
ARLINGTON 12, VIRGINIA**

Best Available Copy



UNCLASSIFIED

200307030-91

581 025

NOTICE: When government or other drawings, specifications or other data are used for any purpose other than in connection with a definitely related government procurement operation, the U. S. Government thereby incurs no responsibility, nor any obligation whatsoever; and the fact that the Government may have formulated, furnished, or in any way supplied the said drawings, specification or other data is not to be regarded by implication otherwise as in any manner licensing the holder or any other person or corporation, or conveying any rights or permission to manufacture, use or sell any patented invention that may in any way be related thereto.

8003073008

287 052

COLD REGIONS SCIENCE AND ENGINEERING
Part II: Physical Science
Section B

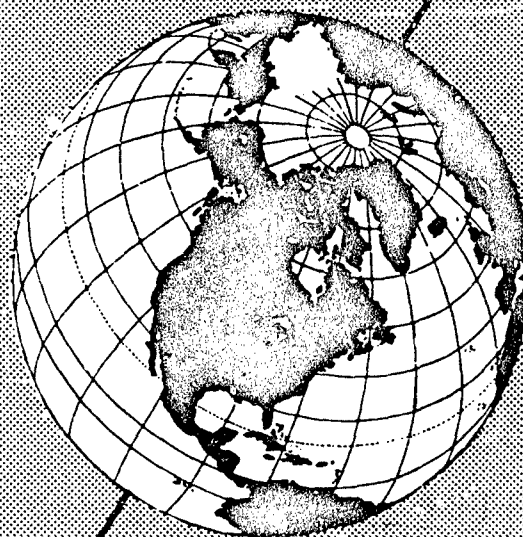
65-1-3

II-B
July 1962

287 052

The Physics and Mechanics of Snow as a Material

CATALOGED BY ASTIA
AS AD INJ




U. S. ARMY
COLD REGIONS RESEARCH AND
ENGINEERING LABORATORY
Corps of Engineers

ASTIA Availability Notice

Qualified requestors may obtain
copies of this report from ASTIA.

COLD REGIONS SCIENCE AND ENGINEERING

F. J. Ganger, Editor

Part II: Physical Science

Section B

IL-B

July 1962

The Physics and Mechanics of Snow as a Material

by Henri Bader

with a section by Daisuke Kuroiwa


ASTIA
RECEIVED
NOV 1 1962
TISIA A

**U. S. ARMY COLD REGIONS RESEARCH
AND ENGINEERING LABORATORY**
Corps of Engineers
Hanover, New Hampshire

PREFACE

This monograph summarizes existing knowledge on the properties of snow as a material; its properties as a cover will be found in II-C1, "Snow and Ice on the Earth's Surface", now under preparation.

The paper has been reviewed and approved for publication by the Office of the Chief of Engineers, U. S. Army.


W. L. NUNNESSER
Colonel, Corps of Engineers
Director

Department of the Army Project 8S-66-02-001

CONTENTS

	Page
Preface	ii
Editor's foreword	vi
A. Metamorphism	1
B. Structure	9
C. Texture	10
D. Index properties	12
E. Permeability	13
F. Classification	17
G. Mechanics	29
H. Thermal properties	58
References - Chapters A-H	60
J. Electrical properties of snow	63
References - Chapter J	78

ILLUSTRATIONS

Figure		
1.	Phase diagrams	2
2.	Metamorphism of a snow crystal in a closed atmosphere	4
3.	Symmetrical metamorphism of a snow crystal in a small air space	5
4.	Graph of diameter of crystal of Figure 3	5
5.	Depth hoar crystals 100 days old	7
6.	Wet spring snow, large composite grains	7
7.	Screened fractions of granular snow	7
8a.	Thin section of 10-yr-old névé	10
8b.	Thin section of 70-yr-old névé	10
9.	Porosity and density vs mean number of adjacent grains per grain	11
10.	Cumulative mass graph of grain size distrib. in alpine snows	11
11.	Graph of permeability K versus K/n	18
12.	Group of permeability parameter a versus grain size d	18
13.	The field of snow in the graph of permeability versus porosity	18
14.	Effect of temperature on creep rate of snow for different values of activation energy	31
15.	Creep compression of snow as a function of time at constant load and temperature	32
16.	Viscosity of new snow as a function of density (g/cm^3) at different temperatures	32
17.	Effect of density on creep rate of snow, for different values of exponent b	32
18.	Snow density as a function of depth on a polar glacier	32
19.	Viscosity as a function of snow grain size for different densities and temperatures	33
20.	Cross-section number m of snow as a function of density	33
21.	Tensile strength of snow as a function of temperature	37
22.	Effect of temperature on tensile strength of snow of different grain sizes	37
23.	Tensile strength of snow versus density	38
24.	Tensile strength versus density for low density snows	38
25.	Shear strength of snow versus density	38
26.	Torsional shear strength of snow versus density	38

CONTENTS (Cont'd.)

ILLUSTRATIONS

Figure		Page
27.	Effect of normal pressure on shear strength of snow ----	40
28.	Shear strength versus normal pressure for a snow a density $\gamma = 0.45$ -----	40
29.	Shear strength and apparent internal friction ($\tan \rho_s$) of two snow types -----	40
30.	Crushing strength of snow versus density -----	42
31.	Stress versus plate penetration in snow. Repeated structural collapse in small increments -----	42
32.	Resistance to compressive collapse (under frictionless lateral confinement) of new snow -----	42
33.	Collapse compression of new snow, $\gamma_0 = 0.07$ at -2.5°C ---	44
34.	Collapse compression of granular snow, $\gamma_0 = 0.32$ at -3°C ---	45
35.	Collapse compression of wet snow -----	46
36.	Minimum work of disaggregation per unit volume of snow versus density -----	47
37.	High speed collapse compression of snow -----	47
38.	Dynamic friction of snow on snow versus normal pressure on contact area -----	48
39.	Dynamic friction of snow on snow versus velocity of relative motion of contact areas -----	48
40.	Graph of stress effect functions -----	49
41.	Strain, parallel to uniaxially applied constant stress versus time -----	50
42.	Rheological model for behavior shown in Figure 41 -----	50
43.	Comparison of creep under uniaxial tension and compression for different stresses -----	53
44.	Change in length of cylindrical snow samples versus stress, at different elapsed times -----	53
45.	Strain rate versus density (g/cm^3) of two snow samples under incremental increase of uniaxial stress -----	54
46.	Depth-density relation for snow (to ice) at Site 2, Greenland -----	55
47.	Young's modulus of snow versus density, obtained from vibrating bars. Site 2, Greenland -----	56
48.	Young's modulus by vibration of snow and ice versus density, for an extended range of densities. Site 2 and Tuto, Greenland -----	56
49.	Poisson's ratio and Young's modulus versus density, obtained from seismic wave velocities. Site 2, Greenland -----	56
50.	Thermal conductivity k versus density γ -----	56

CONTENTS (Cont'd.)

ILLUSTRATIONS

Figure	Page
J-1. Complex dielectric constants of various kinds of ice ----	64
J-2. Complex dielectric constants of various kinds of snow --	65
J-3. Relation between static and high-frequency dielectric constants of snow and density ratio ρ -----	67
J-4. Variation of dielectric constant of snow with lapse of time -----	68
J-5. Variation of apparent electrical conductivity of snow with time -----	70
J-6. Time dependence of direct current flowing through a snow condenser -----	71
J-7. Change of potential of probe electrodes inserted into snow condenser -----	72
J-8. Temperature dependence of the thickness of solution film in equilibrium with ice sphere -----	72
J-9. Relation between $\Delta \epsilon$ and free water content in snow ----	73
J-10. An interference method for determining the dielectric constant of snow -----	73
J-11. $\tan \delta$ of snow at frequency range $10^5 - 10^{10}$ cps -----	75
J-12. Decrease of receiver current due to snow accretion or icing -----	76
J-13. Scattering of a 12 cm wave due to snow accretion on a feedhorn -----	77

TABLES

Table		Page
I. Snow conversion — Density to absolute porosity in percent -----		14
II. Permeability of new snow upon compaction in increments -----		16

EDITOR'S FOREWORD

This is the third section of "Cold Regions Science and Engineering" to appear. It summarizes existing knowledge on the properties of snow as a material: its properties as a cover will be found in II-C1, "Snow and Ice on the Earth's Surface", now under preparation.

Dr. Bräder has written most of this section but Dr. Kuroiwa was available to write on the Electrical Properties of Snow as a Specialist in that subject.

Sections of the work will appear as they become ready, not necessarily in numerical order, but fitting into this plan.

- I. Environment
 - A. General
 - B. Regional
- II. Physical Science
 - A. Geophysics
 - 1. Micrometeorology
 - 2. Exploration Geophysics
 - B. The Physics and Mechanics of Snow as a Material
 - C. The Physics and Mechanics of Ice
 - 1. Snow and ice on the earth's surface
 - 2. Ice as a material
 - D. The Physics and Mechanics of Frozen Ground
 - 1. Properties of frozen soils
 - 2. Permafrost
- III. Engineering
 - A. Snow engineering
 - B. Ice engineering
 - C. Frozen-ground engineering
 - D. General engineering
- IV. Miscellaneous

F. J. SANGER

15 June 1962

SNOW AS A MATERIAL

by

Henri Bader

Snow is a porous, permeable aggregate of ice grains. The grains can be predominantly single crystals or close groupings of several crystals. The pores are filled with air and water vapor. In wet snow the grains are coated with liquid water.

The characteristic property of snow is its inherent thermodynamic instability. Consequently most of the interesting physical parameters inevitably change with time. This process of change is called snow metamorphism.

A. METAMORPHISM

Snow metamorphism is a change of texture and structure, an evolution beginning with the deposition of snow and ending only when it has ceased to exist, either by ablation or by changing to relatively dense ice.

A few salient conditions and properties of the material are responsible for metamorphism.

- a) Temperature proximity to the melting point. Even in the coldest natural environment, the temperature is relatively close to the melting point.
- b) High vapor pressure.
- c) Crystallinity and anisotropism.
- d) Low viscosity.
- e) Porosity.

Consider a snow grain (ice crystal) in a small closed dry air space. The temperature is close to the melting point of ice (say within 50C). This means that we have a high state of thermal oscillation of the water molecules around their lattice position; the lattice is close to breakdown. The lattice force field, which restrains the water molecules from straying away from fixed lattice positions, weakens near the crystal surface, and the surface becomes covered with a quasi-liquid layer^{1,2} within which individual molecules and groups of molecules can move around. One might say that the lattice becomes fuzzy close to the surface. The random thermal agitation of molecules at the ice surface often results in imparting to individual molecules velocities sufficiently high to kick them out of the surface layer into the surrounding air space, where they become a component of the gas phase. As the water vapor concentration in the air space increases, an increasing number of water molecules impinge back onto the ice surface, and those that hit with low velocity at points where the thermal agitation happens to be low at the moment of impingement are reincorporated into the boundary layer. A dynamic equilibrium is established in a very short time, in which the number of molecules leaving the ice surface to move into the gas space is equal to the number falling back into the surface layer. The concentration of water vapor in the gas phase is given in terms of vapor pressure, which is strongly temperature-dependent.

Figure 1 shows this dependence. It also shows that ice has a lower vapor pressure than supercooled water of the same temperature, which means that ice and water cannot co-exist in equilibrium at temperatures below the melting point. If, for instance, a piece of ice and a dish of supercooled water were placed side by side under a bell-jar at -5C, then the water would tend to evaporate until the vapor pressure in the air in the jar reached 3.17 mm of mercury. But the air would then be supersaturated with respect to the piece of ice, which has a vapor pressure of only 3.03 mm, and more vapor molecules would fall into the ice surface layer than would be ejected from it. A vapor pressure gradient would be established between the air over the water dish and the air over the piece of ice, and water vapor would move from the dish to the ice by diffusion.

^{1,2}See References

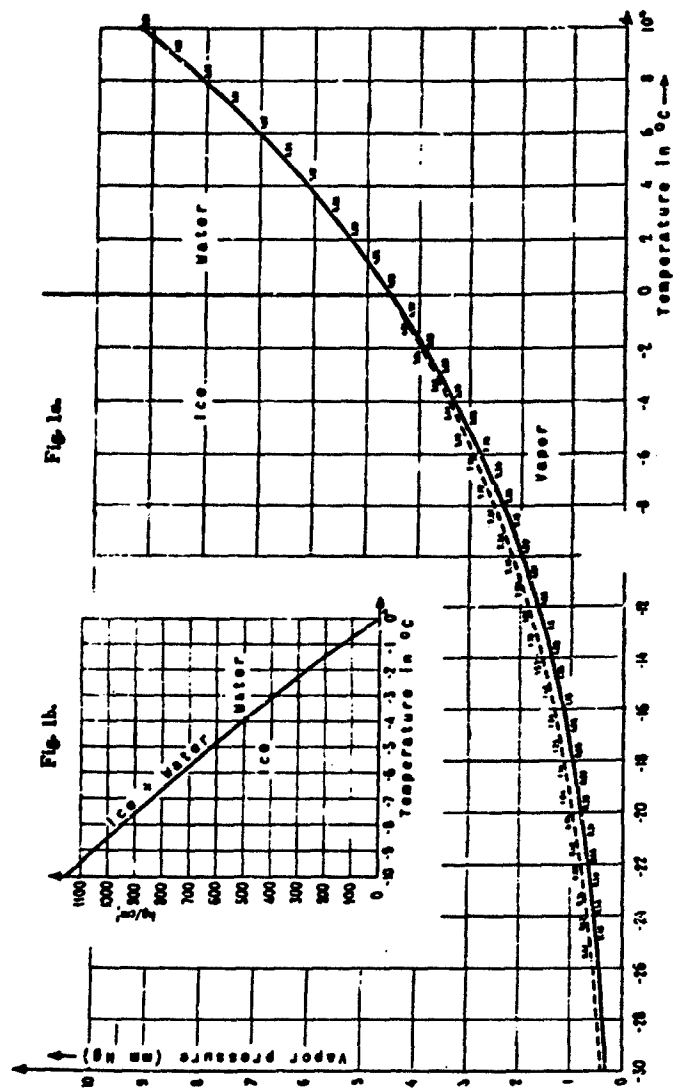


Figure 1. Phase diagrams. a. Phase diagram of the system ice-water-vapor. (Dashed line shows the vapor pressure of supercooled water.) b. Phase diagram of system ice-water.

Discussion of another aspect of this hypothetical experiment is pertinent to the understanding of the principles governing snow metamorphism. It concerns the rate of transfer of water substance over the vapor phase. The highly dynamic nature of the equilibrium between water or ice surface and vapor in the surrounding air space signifies that a disturbance of this equilibrium by addition to or removal of water vapor from the air space will be quickly compensated by condensation or evaporation at the surface. Experiments² indicate that a dry air layer about $\frac{1}{2}$ mm thick over ice is saturated to 80% in $\frac{1}{4}$ sec by evaporation from the ice surface. One might then suppose that, if a flat piece of ice were suspended $\frac{1}{2}$ mm over the surface of the dish of supercooled water, the rate of growth of ice at the expense of water would be very rapid. It would actually begin at a very rapid rate, but immediately the water surface would begin to cool down because of the loss of latent heat of evaporation (600 cal/g) and the ice surface would warm up because of a gain in heat of condensation (sublimation, 680 cal/g). This would lower the difference in vapor pressure between the two surfaces and proportionally slow down the rate of vapor transfer. The rate of heat flow from the interior of the water towards the water surface and from the ice surface towards the interior of the ice block would then become the dominant factor in controlling the rate of vapor transfer.

In summary, one important fact is that mass transfer over the vapor phase is accompanied by energy transfer. If two ice grains of different temperature are brought close together, the cold one, having a lower vapor pressure, will grow at the expense of the warmer one by vapor transfer, until the temperature difference is wiped out by the corresponding heat transfer. Now consider a rod of ice in which a constant temperature difference is maintained between both ends. There are four heat transfer mechanisms, two of which involve mass transfer.

- a) Heat flows in the rod by conduction.
- b) Heat flows in the surrounding air by conduction \pm convection.
- c) Evaporation at the warm end and condensation at the cold end transfer heat and mass via the vapor phase. The heat transfer is equal to the latent heat of sublimation of the transported mass.
- d) Water molecules will creep along the quasi-liquid surface layer from the warm end of the rod, where thermal agitation is strong, towards the cold end, where it is weaker. The mass removed from the surface layer at the warm end must be replaced by quasi-liquefaction of the underlying crystalline ice; thus the emerging transfer accompanying surface molecular creep has the latent heat of fusion as a maximum value, but is perhaps smaller, because the layer is not quite liquid.

The quoted values of vapor pressure are those for equilibrium over flat surfaces. Convex surfaces have higher, and concave surfaces lower, vapor pressure than flat ones. The magnitude of the curvature effect, as calculated from theory for liquids appears to be negligibly small for curvatures larger than about 10μ . Observation, however, indicates that it is important in snow when the grain curvature is as large as a few hundred microns. Figure 2 is a series of photographs of a snow crystal placed on a microscope slide, surrounded by a vaseline ring, and covered with a thin cover glass, which did not touch the crystal.² The slide was stored at temperatures always below -2.5°C . Attention is drawn to the following interesting features of Figure 2.

- a) The frozen cloud elements (diameter approximately 30μ) picked up by the falling snow crystal vanish very quickly. They do so partly by evaporating because they have a higher vapor pressure corresponding to their small radius of curvature, and partly by flowing into the quasi-liquid surface layer.
- b) The sharp points of the branches become blunt. There is a general tendency for material to evaporate or creep away from positions where curvature radii are small: hence the branches separate from the main body of the crystal where they are thin, and then become rounded. The larger spheres then grow at the expense of the smaller ones, exclusively by vapor transfer, since there is no contact.

Proof that surface creep is significant was obtained by similar experiments³ where vapor transfer was suppressed by immersing the snow crystals in kerosine. Metamorphism was then a few times slower than in air.

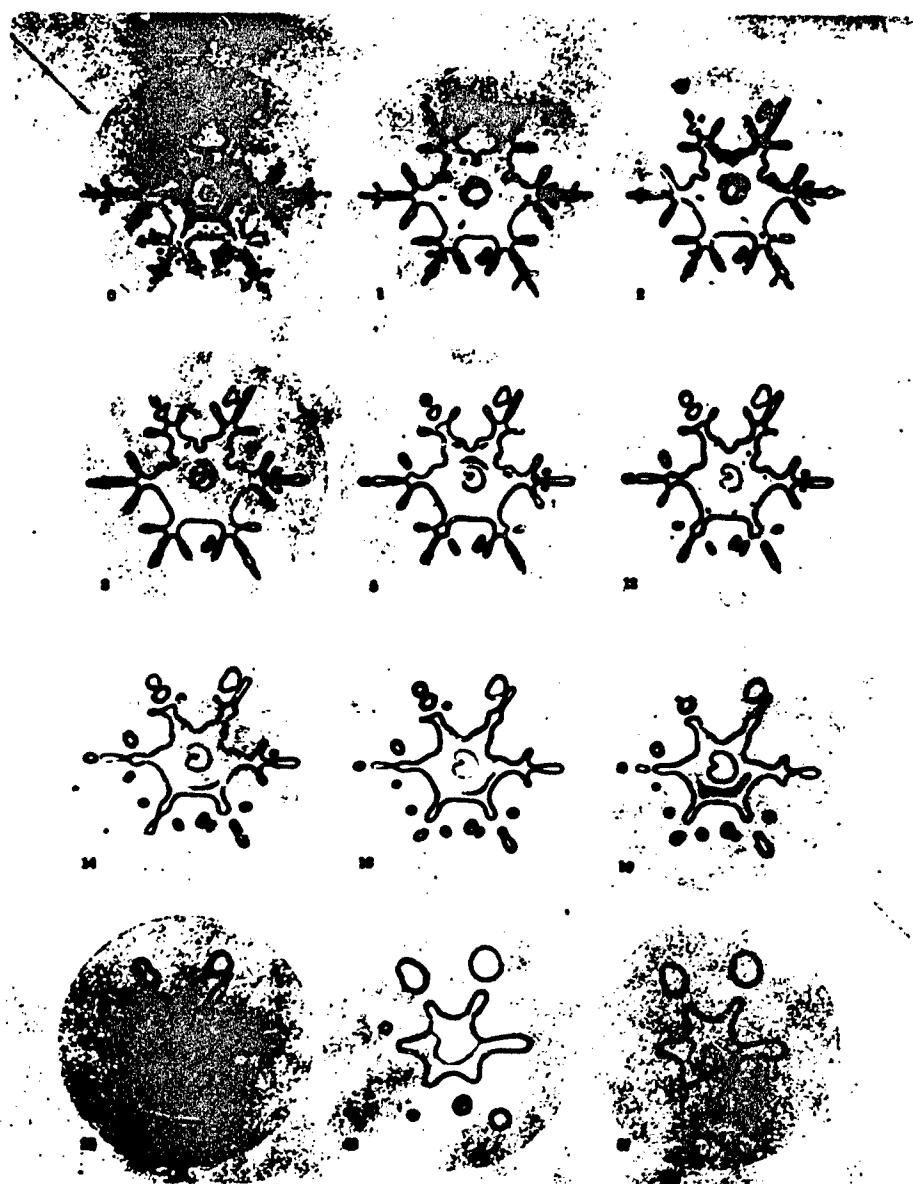


Figure 2. Metamorphism of a snow crystal in a closed atmosphere. Magnification 15x. Temperature below -2.5°C . Numbers indicate age in days.

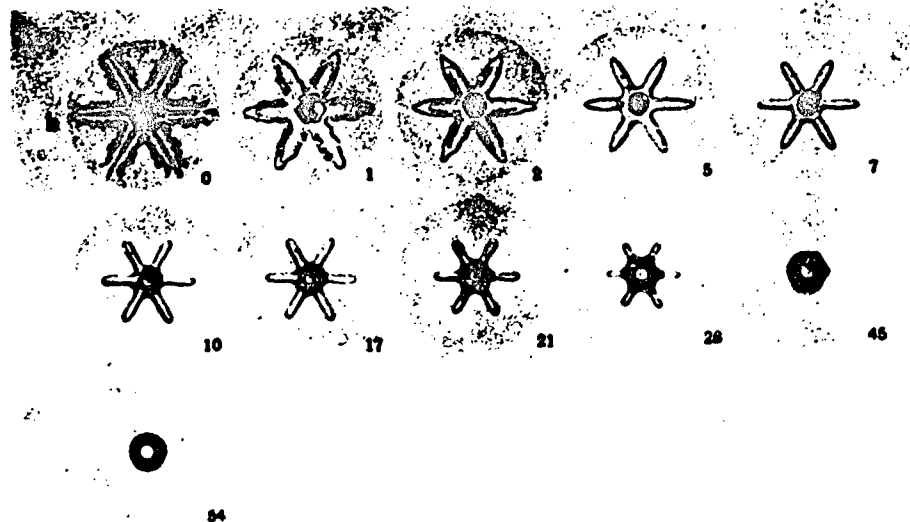


Figure 3. Symmetrical metamorphism of a snow crystal in a small air space. Magnification 15...

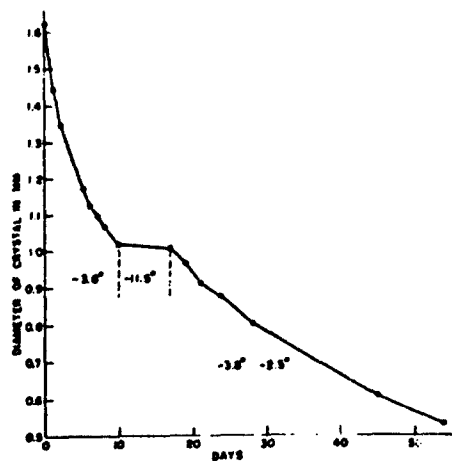


Figure 4. Graph of diameter of crystal of Figure 3.

sufficiently low to suppress surface tension effects, any ice crystal will assume the equilibrium shape of a hexagonal prism of approximately equal width and height. Old snow grains tend to become equidimensional and to develop crystallographic faces if they are large or if the temperature is low.

Figure 3, also of a crystal in a small air space, shows symmetrical behavior, given aided by the fact that only the radial center (white spot) was in contact with the glass slide. As a model of metamorphism, it reveals three interesting features. One is that the rate of change is highly temperature-dependent; there was very little change during 7 days at -11.5°C (Fig. 4). Another is that the rate of change decreases with time. The third is that at temperatures very close to the melting point, surface tension in the quasi-liquid surface layer can overcome the tendency of the lattice to form crystallographic elements (planes, edges and vertices). The 45-day picture is of a flat hexagonal prism with rounded edges, which in 9 days at -2.5°C changes to a cylinder. This would not have happened if the temperature had been a few degrees lower, or if the crystal had been much larger. Furthermore, if the temperature had been much lower, the edges of the prism would have become sharper. It is most probable that, given enough time at a temperature

As already stated, the surface of an ice crystal surrounded by air is covered by a very thin quasi-liquid layer in which the water molecules can move fairly freely, in contrast to conditions in the interior of the crystal, where they occupy distinct lattice positions. When two crystals are brought into contact, the thin surface layers merge and molecular mobility diminishes as the constraining force-fields of the lattices acting from both sides gain the upper hand. The quasi-liquid layer does not completely vanish unless the lattices of the two crystals fit together perfectly (i. e., the crystallographic axes happen to be strictly parallel). An amorphous interface (grain boundary) remains, which is normally plane and visible as a thin line in section. The formation of this relatively stable intergrain boundary can occur within minutes under optimum conditions. It is favored by pressure and high temperatures and retarded by low temperature which slows molecular diffusion.

The intergrain boundary bonds the two crystals. The strength of the bond is not sensibly different from that of the crystal itself; and there is no detectable difference between bond formed with or without melting and no reason for assuming that they should be different. The dry bond, however, forms more slowly than the wet one. When a piece of snow is broken or crushed, failure occurs predominantly at the grain bonds, which are weak sections only because they are small. The larger the individual and total grain contact areas, the stronger the snow. The original contact area (bond) between two convex grain surfaces is very small. It probably very soon attains its maximum strength per unit area, so that increasing strength with time (age-hardening of snow) is due to increasing size of the contact area. It is interesting to note that increase in contact area between two grains is not accompanied by significant reduction of the distance between grain centers.²¹ Thermodynamic processes in snow do not of themselves affect the snow volume. They can, however, change the density by adding to, or subtracting from, the mass in a given volume.

Gravitation causes primary vertical body forces in the snow mass which are transmitted in all directions from grain to grain in the structure.

There are two main effects of these forces:

a) Densification by viscous shear deformation along grain boundaries and grain deformation, which produce denser packing, normally without loss of cohesion. Sudden structural collapse by breaking of bonds occurs when the crushing strength of a snow layer is reached by the weight of overlying snow accumulation. This often happens in "depth hoar," a coarse-grained, poorly bonded, highly viscous type of snow, and is a major cause of avalanching. Other types of snow have sufficiently low viscosity to react to slowly increasing load by densification accompanied by sufficient increase in crushing strength to prevent structural collapse. Densification by plastic mechanical deformation of the single crystal grains is most probably insignificant, except in the case of the dense snow occurring at depths of tens of meters in glaciers.

b) The Riecke effect. This may be an important metamorphism-accelerating factor, but is not known to be so. When a crystal in equilibrium with its liquid or vapor phase is stressed, solubility or vapor pressure differences are produced. More highly stressed parts of the snow crystal surface will melt if wet, or evaporate if dry, and less stressed parts will grow. A spherical grain squeezed between two others will thus tend to flatten more or less elliptically. The result is similar to that produced by plastic deformation of the grains, but is perhaps achieved at lower stresses.

We can distinguish four fairly distinct kinds of snow metamorphism:²²

1) Destructive metamorphism of dry snow. A few days after deposition of the original snow, crystal shape is almost completely lost. Often its only indication is that larger flat snow stars have changed into somewhat flat grains. The end product of destructive metamorphism usually consists of a fine-grained snow of density between 0.15 and 0.25 g/cm³. This is the skier's powder snow. Grains are rounded and weakly bonded. Each grain is a single crystal with only one or two small crystallographic faces. Very few grains are smaller than 0.2 mm, the predominating size being from 0.5 to 1 mm, sometimes somewhat larger.

Further metamorphism of this snow depends, if it stays dry, above all on whether or not it is plastically densified by the load of later snowfalls. If the snow is densified to

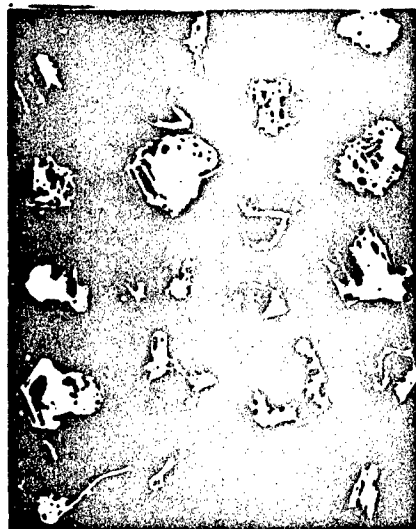


Figure 5. Depth hoar crystals 100 days old
Density 0.26 g/cm^3 . Magnification $3\times$.



Figure 6. Wet spring snow, large
composite grains. Magnification $4\times$.

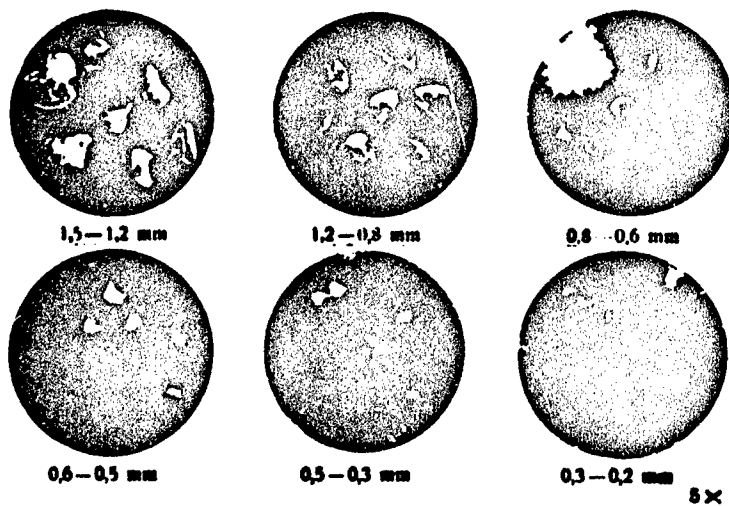


Figure 7. Screened fractions of granular snow.

as much as 0.3 g/cm^3 , further increase in grain size becomes very slow. But the area of grain contact increases and the snow hardens. Only on high polar glaciers, where such snow never melts, do we, in the course of one or two years, observe significant further grain growth and more generous development of crystallographic elements, often accompanied by some reduction in strength. This is slow constructive metamorphism.

2) **Constructive metamorphism** of dry snow consists in growth of grains to significantly more than 1 mm, with development of crystallographic elements (faces, edges, and vertices). It is slow if the density is high. If the density is below about 0.3 g/cm^3 , it can become very rapid when vapor transfer is accelerated by convective air flow in the large pore volume, owing to a strong positive temperature gradient (colder at the top than at the bottom). The end product of constructive metamorphism is a very distinctive snow type known as "depth hoar," or "Schwimmschnee" from the German. Here grain size is between 2 and 8 mm, and single crystals as large as 15 mm are observed. They often show excellent crystallographic development (Fig. 5), large faces and sharp edges and vertices.¹² A variety of shapes can be observed, such as short prismatic or tabular solid crystals, and hollow hexagonal or rectangular cups. Bonding of grains in depth hoar is very poor; it has a high viscosity and low strength, and can be collapsed by shock or surcharge, to the increase of which it cannot react by rapid viscous densification. Depth hoar is a troublesome snow type; it is a major cause of avalanching, is a great hindrance to oversnow traffic, and is most difficult to compact to hard roads and runways. The lightest depth hoar has a density of little less than 0.2 g/cm^3 , and the heaviest little more than 0.3.

3) **Melt metamorphism** characterizes the changes produced in snow by the presence of liquid water. When snow becomes moist, temperature gradients and their effects vanish. But the rate of densification of low-density snow increases because of the constrictive effect of the high surface tension of the water film covering all the grains. All crystallographic elements quickly vanish. Crystals become rounded and, for an unknown reason, some intercrystalline bonds grow very rapidly while others dissolve. Clusters of several grains, which form small denser regions in the snow structure, coalesce to larger polycrystalline grains (see Fig. 6). Bonding between grains is very weak. As meltwater percolates through the snow, crystals normally grow to a maximum size of about 3 mm and composite grains to about 15 mm. Within a few days this metamorphism produces the well-known "rotten" snow of the thaw season.

In the accumulation areas of glaciers, melt metamorphism produces coarse-grained névé, which can acquire any density up to that of ice by slow plastic densification and annual addition of ice mass by freezing of percolating melt water.

When wet snow freezes, it acquires high strength because bond size is increased by the freezing of water preferentially retained at the re-entrant surfaces at the bonds. It again loses strength on becoming wet because bonds decrease in size by preferential melting perhaps mainly due to concentration of temperature-depressing soluble impurities there. Percolating meltwater is not equally distributed in all layers of a snowpack. Some retain very little, while others absorb water almost to saturation and convert to dense ice layers or lenses on refreezing.

4) **Pressure metamorphism.** This is a new term, introduced here to characterize the densification of dry névé on high polar glaciers. It can take névé many decades to change from snow of density around 0.45 to ice of density 0.83 g/cm^3 (this is the density at which the air permeability decreases to zero, and snow changes to ice by definition). Thermodynamic processes, such as grain and grain-bond growth by vapor or surface migration, appear to be of secondary importance during this period of very slow change, the situation being dominated by processes of mechanical deformation under pressure. Hard surface crusts are formed in several ways.

- a) Refreezing of surface layers wetted by thaw, rainfall or wet fog fall-out.
- b) Surface condensation from moist air.
- c) Packed deposition of windborne drift snow.

d) Condensation of vapor moving up from below the surface, by diffusion or convection; crusts between snow layers are perhaps also formed by vapor migration.

Crusts are important diagnostic features in the snow pack, especially as an aid in counting annual layers. There are still unexplained crust formations in dry snow.

B. STRUCTURE

Any snow which has gone through the stage of destructive metamorphism is granular (Fig. 7) and can have any density above about 0.15 g/cm^3 . If such snow is disaggregated and heaped when cold, it will show a porosity of about 0.45 (density 0.5 g/cm^3) similar to that of a heap of dry sand. This demonstrates that, except possibly in the vicinity of density 0.5, the structure of snow as a granular aggregate is not akin to that of a lightly sintered granular heap. Low-density dry snow (less than 0.5), which includes all seasonal snow, has a very irregular structure, perhaps best described as composed of randomly oriented intersecting chains of grains. This type of structure can be derived from one consisting of packed granules, by conceptually removing some of the grains, leaving an irregular lattice. In such a structure a significant number of the grains have a high degree of mobility affecting only a small volume. In other words, there are relatively large pore spaces into which grains can move when the structure is deformed. This property of the structure of low-density snow is important to an understanding of its mechanics. It could be deformed by shearing of grain contact areas, without deformation of individual grains. As the density increases, the average number of grains in contact with each grain increases, and the degree of mobility decreases. At a density of around 0.5 g/cm^3 the condition of close packing is approached, and further densification is not possible without deformation of grains.

The thin section (Fig. 8a) is of dry 10-yr-old névé from 8 m depth in the interior of the Greenland ice sheet.¹³ The grain sections are white, the lines are grain boundaries and the black areas pore space. Density is 0.50 g/cm^3 (porosity 45.4%), mean grain cross-sectional area 0.5 mm^2 , ratio of total length of grain boundaries to total grain perimeter is 0.35. There are 120 grains per cm^2 . Figure 9 is a thin section of dry névé, 70 years old. The density is 0.73 g/cm^3 (porosity 4%), close to that of ice. Mean grain cross-sectional area is 1.0 mm^2 , and grain-boundary to grain-perimeter ratio is 0.63. There are 80 grains per cm^2 .

Assuming that the two snows were originally the same, it took 60 years at -24.5°C with pressure increasing linearly from 0.3 to 2.8 kg/cm^2 at the rate of $0.04 \text{ kg/cm}^2\text{-yr}$ to halve the porosity and double the mean grain cross-sectional area. Figure 9 gives the relation between density and the mean number of grain contacts per grain (in thin section).¹³ It appears to show a discontinuity at density 0.5 g/cm^3 . Since thin sections of snow of density lower than 0.3 g/cm^3 show mainly isolated grain sections and, except for studies of grain crystal axis orientation, yield almost no information on the structure. A large number of very closely spaced parallel sections must be made, and the structure model cannot be well presented in print.¹⁰

Description and statistical treatment of pertinent parameters of snow structure are not yet sufficiently well developed to permit good translations of data from two-dimensional thin sections to the three-dimensional structure.¹² This inherently difficult problem is complicated by the fact that the snow structure is very often anisotropic. Structure anisotropism is of two types. The first is geometric, for instance parallelism of flattened grains, and has hardly been studied. The second refers to orientation patterns of the crystallographic c-axis of the grains, determinable by optical means. We can sometimes find a primary vertical preferred orientation due to preferred sedimentation of plate or star snow crystals in horizontal position. The same preference develops during destructive and constructive metamorphism, where c-axis position parallel to the maximum temperature gradient appears to be advantageous to grain growth. In dry snow, pressure metamorphism favors the development of grains with vertical c-axes, but it is not known whether grains tend to rotate to this position or whether those with vertical axes grow at the expense of differently oriented ones.

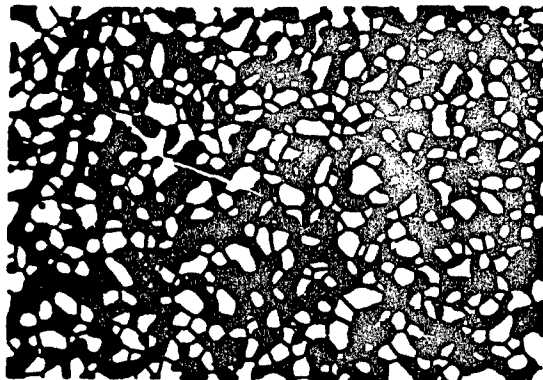


Figure 8a. Thin section of 10-yr-old névé. Density 0.5 g/cm³. Pore area is black. Magnification 3.8x. (From Fuchs, ref. 13).

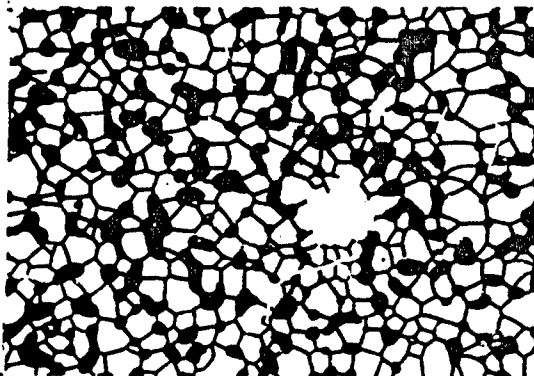


Figure 8b. Thin section of 70-yr-old névé. Density 0.73 g/cm³. Magnification 3.8x. (From Fuchs, ref. 13)

Shearing deformation produces strong orientation to parallelism of basal planes (normal to c-axis) with the shear plane, while tension leads to a structure with grain basal planes predominantly parallel to the direction of tensile stress.¹

A thorough basic study of snow metamorphism and snow mechanics in relation to snow structure is yet to be done.

C. TEXTURE

Snow crystal shape has already been discussed under metamorphism. In relatively new dry snow, up to several months old, the grain is predominantly a single crystal, but in older dry snow there is a tendency towards formation of grains consisting of several crystals. The process is apparently a dry "fusion" of several close neighbors to a more or less irregularly shaped, internally strongly bonded unit, which then becomes the new grain of the snow structure. In the course of decades, as this snow is compressed to ice on high polar glaciers, one of the crystals of the grain slowly grows at the expense of the others, until we again have a single crystal grain. For determination of grain size distribution, weakly bonded granular snow can be mechanically

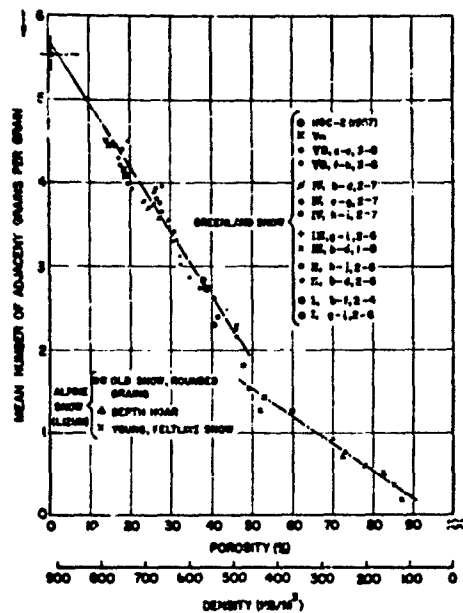


Figure 9. Porosity and density vs mean number of adjacent grains per grain. (From Fuchs, ref. 13)

Curve	Age (days)	Density (g/cm ³)
1a, 1b	6	.214
2a, 2b	15	.292
3	42	.323
4a, 4b	96	.285
5a, 5b	118	.357
6a, 6b	175	.228

There are many ways of determining and defining grain size and grain size distribution, and in quantitative work on snow, a generally accepted convention has not yet been established. When snow is screened into fractions, we will define the mean grain diameter \bar{d} of a fraction in terms of the length of the side of the square mesh opening. If the fraction passes through squares of side length M and is retained on squares of side m , then:

$$\bar{d} = \sqrt{Mm}.$$

If W is the weight of a fraction, and the mixture is separated into n fractions of mean grain diameters \bar{d}_i , then the mean diameter \bar{d}_m of the mixture is:

$$\bar{d}_m = \left[\sum_{i=1}^n (w_i \bar{d}_i) \right] / \sum_{i=1}^n (w_i)$$

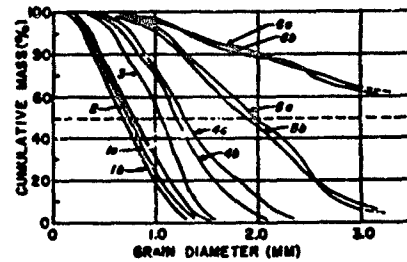


Figure 10. Cumulative mass graph of grain size distribution in alpine snows. (From DeQuervain, ref. 11)

disaggregated, and screened² or elutriated¹¹. The majority of size analyses show an approximately linear graph of cumulative mass versus grain diameter, with the curved ends often seen in graphs of soil analyses. The average diameter lies close to the 50% cumulative mass value, the mass of grains smaller than 0.2 mm is very small, and the maximum size is close to twice the average size. The linear portion of the cumulative distribution curve reaches from about $\frac{1}{3}$ average diameter (based on mass, not on number of grains) to $1\frac{1}{3}$ average diameter and covers 80% to 90% of total mass. Figure 10 shows a number of distribution curves for Alpine snows as follows:

If grains are counted and measured under the microscope,¹⁹ a rather complicated computation has to be made to obtain $\underline{d_g}$ as determined by screening, because the grains are not spherical. If measurements are made on thin sections of snow, determination of $\underline{d_g}$ becomes still more difficult. This subject requires research, because well bonded snow cannot be disaggregated for screening without excessive breaking of grains. Definition of grain shape, pertinent to the definition of grain size, is another aspect of snow texture which requires attention.

D. INDEX PROPERTIES²⁴

Identification of snow type for any given purpose is not a well developed subject, and a great deal of systematic work, consisting of determination of a large number of parameters on many different snows, would have to be done to make it so. The following index properties are considered:

1) Density (specific gravity) is mass per unit volume, usually expressed in g/cm³, but engineers sometimes prefer lb/ft³ (1 g/cm³ = 62.4 lb/ft³). Density is measured by weighing a known volume, or melting a known volume of snow and measuring the volume of melt water. By careful use of the standard SIPRE 500 cm³ snow tube (stainless steel 58/60 mm, 198 mm long) density is easily measured to three significant figures. For the purpose of correlation with other properties, two significant figures are often insufficient. Density is by far the most significant index property of snow.

2) Porosity and void ratio

Porosity is the ratio of volume of voids to snow volume. This is the absolute porosity \underline{n} , and is calculated from the snow density γ and the ice density γ_i :

$$\underline{n} = \frac{\gamma_i - \gamma}{\gamma_i} = \frac{0.917 - \gamma}{0.917} = 1 - 1.090\gamma.$$

Table 1 gives values of the absolute porosity \underline{n} (in percent) for densities between 0.030 and 0.917 g/cm³. The relative porosity refers to the volume of communicating pores, and is almost equal to absolute porosity for low- or medium-density snow. Only in very high-density snow, above 0.7 g/cm³, does the volume of the isolated pores become significant. No measurements of relative porosity of high-density snow have yet been made.

The void ratio, \underline{e} , is the ratio of the volume of voids to the volume of the solid substance.

$$\underline{e} = \frac{\gamma_i - \gamma}{\gamma} = \frac{\underline{n}}{1 - \underline{n}}.$$

3) Hardness is the resistance to penetration by a rigid object. The most commonly used instrument is the drop-hammer actuated Swiss Rammsonde, a tube with a conical tip.² The penetrating cone has a 60-deg angle and a base diameter of 40 mm. The ram hardness number is expressed in kilograms, and runs up to a few thousand for very hard snow of density 0.5 g/cm³. The Canadian hardness gage, a hand-pushed spring-loaded circular plate, has been much used in softer snows to measure the crushing strength in situ. The Canadian hardness number is expressed in kg/cm². Both these instruments penetrate at rates sufficiently high to eliminate effects of plastic deformation. The slow CBR Test (California Bearing Ratio), developed for soils, is used only in very hard snow.

4) Grain size is determined by visual inspection (with hand lens) of grains spread out on a plate having a 1 mm grid, by measurements under the microscope, or by screening or elutriation. Grain size is usually given in mm, but often only qualitative statements are made, such as reference to fine-, medium-, coarse-, or very coarse-grained snow. This refers to the predominating grain diameter, and here the classification of Schaefer, Klein and De Quervain²² is gaining popularity.

<u>Predominating grain diameter (mm)</u>	<u>Designation</u>
< 0.5	very fine grained (vfg)
0.5 to 1.0	fine grained (fg)
1.0 to 2.0	medium grained (mg)
2.0 to 4.0	coarse grained (cg)
> 4.0	very coarse grained (vcg)

5) Grain shape is observed mainly for distinguishing between different types of new snow, for identification of depth hoar, and for deciding that a given dry snow has or has not been previously wet.

6) Permeability is given in terms of the inverse of the resistance to the passage of air through snow. It is a most useful parameter for definition of snow type, but has not been used much for lack of a field instrument. Permeability is discussed in a separate section.

7) Ultimate strength. Tensile, shear and crushing strengths must be measured at high rates of loading to eliminate the effects of plastic yielding (testing time of the order of 10 sec). For practical purposes, tensile strength is equal to cohesion (shear strength at zero normal pressure). Relatively simple instruments have been built for field use, but the necessity of many tests to compensate for wide scatter (standard deviations of 30% are common) has limited their use.

8) Temperature. This is not usually considered to be an index property in classification of materials. In snow, however, the value of many parameters is so highly temperature-dependent, that the latter must be included. Its maximum value is 0C; reported positive values are erroneous.

- 9) Newtonian viscosity.
- 10) Liquid water content.
- 11) Elastic parameters.
- 12) Structural parameters.
- 13) Thermal conductivity.
- 14) Dielectric properties.

Items 9-14 are only mentioned here because they have been too difficult to measure with useful accuracy in the field.

Good reports of snow investigations in the field should include at least determination of density, hardness, grain size, grain shape (or descriptive terms implying grain shape, such as "granular" or "depth hoar") and temperature.

E. PERMEABILITY

The permeability of snow^{2,4,16} is an important property; its value covers a wide range and is very sensitive to changes in density, texture, or structure. It is measured as permeability to flow of air, and coefficient K of air permeability is defined as follows:

$$K = \frac{QL}{A \Delta P} = \frac{v}{i} \text{ cm/sec}$$

where

Q = volume rate of air flow (cm³/sec)

A = cross section of snow sample (cm²) normal to direction of air flow.

L = length of sample in direction of air flow (cm)

ΔP = air pressure head (cm, in terms of height of water column)

v = air velocity cm/sec (calculated over cross section A)

i = air pressure gradient (cm water / cm length of sample)

SNOW AS A MATERIAL

Table I

SNOW CONVERSION TABLE
DENSITY TO ABSOLUTE POROSITY IN PERCENT

Porosity = 1 - 1.09 density

	0	1	2	3	4	5	6	7	8	9
030	96.7	94.6	92.5	90.4	88.3	86.2	84.1	82.0	79.9	77.8
040	95.6	93.5	91.4	89.3	87.2	85.1	83.0	80.9	78.8	76.7
050	94.5	92.4	90.3	88.2	86.1	84.0	81.9	79.8	77.7	75.6
060	93.5	91.4	89.3	87.2	85.1	83.0	80.9	78.8	76.7	74.6
070	92.4	90.3	88.2	86.1	84.0	81.9	79.8	77.7	75.6	73.5
080	91.3	89.2	87.1	85.0	82.9	80.8	78.7	76.6	74.5	72.4
090	90.2	88.1	86.0	83.9	81.8	79.7	77.6	75.5	73.4	71.3
100	89.1	87.0	84.9	82.8	80.7	78.6	76.5	74.4	72.3	70.2
110	88.0	85.9	83.8	81.7	79.6	77.5	75.4	73.3	71.2	69.1
120	86.9	84.8	82.7	80.6	78.5	76.4	74.3	72.2	70.1	68.0
130	85.8	83.7	81.6	79.5	77.4	75.3	73.2	71.1	69.0	66.9
140	84.7	82.6	80.5	78.4	76.3	74.2	72.1	70.0	67.9	65.8
150	83.6	81.5	79.4	77.3	75.2	73.1	71.0	68.9	66.8	64.7
160	82.5	80.4	78.3	76.2	74.1	72.0	69.9	67.8	65.7	63.6
170	81.4	79.3	77.2	75.1	73.0	70.9	68.8	66.7	64.6	62.5
180	80.3	78.2	76.1	74.0	71.9	69.8	67.7	65.6	63.5	61.4
190	79.2	77.1	75.0	72.9	70.8	68.7	66.6	64.5	62.4	60.3
200	78.1	76.0	73.9	71.8	69.7	67.6	65.5	63.4	61.3	59.2
210	77.0	74.9	72.8	70.7	68.6	66.5	64.4	62.3	60.2	58.1
220	75.9	73.8	71.7	69.6	67.5	65.4	63.3	61.2	59.1	57.0
230	74.8	72.7	70.6	68.5	66.4	64.3	62.2	60.1	58.0	55.9
240	73.7	71.6	69.5	67.4	65.3	63.2	61.1	59.0	56.9	54.8
250	72.6	70.5	68.4	66.3	64.2	62.1	60.0	57.9	55.8	53.7
260	71.5	69.4	67.3	65.2	63.1	61.0	58.9	56.8	54.7	52.6
270	70.4	68.3	66.2	64.1	62.0	59.9	57.8	55.7	53.6	51.5
280	69.3	67.2	65.1	63.0	60.9	58.8	56.7	54.6	52.5	50.4
290	68.2	66.1	64.0	61.9	59.8	57.7	55.6	53.5	51.4	49.3
300	67.1	65.0	62.9	60.8	58.7	56.6	54.5	52.4	50.3	48.2
310	66.0	63.9	61.8	59.7	57.6	55.5	53.4	51.3	49.2	47.1
320	64.9	62.8	60.7	58.6	56.5	54.4	52.3	50.2	48.1	46.0
330	63.8	61.7	59.6	57.5	55.4	53.3	51.2	49.1	47.0	44.9
340	62.7	60.6	58.5	56.4	54.3	52.2	50.1	48.0	45.9	43.8
350	61.6	59.5	57.4	55.3	53.2	51.1	49.0	46.9	44.8	42.7
360	60.5	58.4	56.3	54.2	52.1	50.0	47.9	45.8	43.7	41.6
370	59.4	57.3	55.2	53.1	51.0	48.9	46.8	44.7	42.6	40.5
380	58.3	56.2	54.1	52.0	49.9	47.8	45.7	43.6	41.5	39.4
390	57.2	55.1	53.0	50.9	48.8	46.7	44.6	42.5	40.4	38.3
400	56.1	54.0	51.9	49.8	47.7	45.6	43.5	41.4	39.3	37.2
410	55.0	52.9	50.8	48.7	46.6	44.5	42.4	40.3	38.2	36.1
420	53.9	51.8	49.7	47.6	45.5	43.4	41.3	39.2	37.1	35.0
430	52.8	50.7	48.6	46.5	44.4	42.3	40.2	38.1	36.0	33.9
440	51.7	49.6	47.5	45.4	43.3	41.2	39.1	37.0	34.9	32.8
450	50.6	48.5	46.4	44.3	42.2	40.1	38.0	35.9	33.8	31.7

SNOW CONVERSION TABLE

	0	1	2	3	4	5	6	7	8	9
460	49.8	49.7	49.6	49.5	49.4	49.3	49.2	49.1	49.0	48.9
470	48.7	48.6	48.5	48.4	48.3	48.2	48.1	48.0	47.9	47.8
480	47.7	47.6	47.5	47.4	47.3	47.2	47.1	47.0	46.9	46.8
490	46.6	46.5	46.4	46.3	46.2	46.1	46.0	45.9	45.8	45.7
500	45.5	45.4	45.3	45.2	45.1	45.0	44.9	44.8	44.7	44.6
510	44.4	44.3	44.2	44.1	44.0	43.9	43.8	43.7	43.6	43.5
520	43.3	43.2	43.1	43.0	42.9	42.8	42.7	42.6	42.5	42.4
530	42.2	42.1	42.0	41.9	41.8	41.7	41.6	41.5	41.4	41.3
540	41.1	41.0	40.9	40.8	40.7	40.6	40.5	40.4	40.3	40.2
550	40.0	39.9	39.8	39.7	39.6	39.5	39.4	39.3	39.2	39.1
560	38.9	38.8	38.7	38.6	38.5	38.4	38.3	38.2	38.1	38.0
570	37.8	37.7	37.6	37.5	37.4	37.3	37.2	37.1	37.0	36.9
580	36.7	36.6	36.5	36.4	36.3	36.2	36.1	36.0	35.9	35.8
590	35.7	35.6	35.5	35.4	35.3	35.2	35.1	35.0	34.9	34.8
600	34.6	34.5	34.4	34.3	34.2	34.1	34.0	33.9	33.8	33.7
610	33.5	33.4	33.3	33.2	33.1	33.0	32.9	32.8	32.7	32.6
620	32.4	32.3	32.2	32.1	32.0	31.9	31.8	31.7	31.6	31.5
630	31.3	31.2	31.1	31.0	30.9	30.8	30.7	30.6	30.5	30.4
640	30.2	30.1	30.0	29.9	29.8	29.7	29.6	29.5	29.4	29.3
650	29.1	29.0	28.9	28.8	28.7	28.6	28.5	28.4	28.3	28.2
660	28.0	27.9	27.8	27.7	27.6	27.5	27.4	27.3	27.2	27.1
670	27.0	26.9	26.8	26.7	26.6	26.5	26.4	26.3	26.2	26.1
680	25.8	25.7	25.6	25.5	25.4	25.3	25.2	25.1	25.0	24.9
690	24.8	24.7	24.6	24.5	24.4	24.3	24.2	24.1	24.0	23.9
700	23.7	23.6	23.5	23.4	23.3	23.2	23.1	23.0	22.9	22.8
710	22.6	22.5	22.4	22.3	22.2	22.1	22.0	21.9	21.8	21.7
720	21.5	21.4	21.3	21.2	21.1	21.0	20.9	20.8	20.7	20.6
730	20.4	20.3	20.2	20.1	20.0	19.9	19.8	19.7	19.6	19.5
740	19.3	19.2	19.1	19.0	18.9	18.8	18.7	18.6	18.5	18.4
750	18.2	18.1	18.0	17.9	17.8	17.7	17.6	17.5	17.4	17.3
760	17.1	17.0	16.9	16.8	16.7	16.6	16.5	16.4	16.3	16.2
770	16.0	15.9	15.8	15.7	15.6	15.5	15.4	15.3	15.2	15.1
780	14.9	14.8	14.7	14.6	14.5	14.4	14.3	14.2	14.1	14.0
790	13.8	13.7	13.6	13.5	13.4	13.3	13.2	13.1	13.0	12.9
800	12.8	12.7	12.6	12.5	12.4	12.3	12.2	12.1	12.0	11.9
810	11.7	11.6	11.5	11.4	11.3	11.2	11.1	11.0	10.9	10.8
820	10.6	10.5	10.4	10.3	10.2	10.1	10.0	9.9	9.8	9.7
830	9.5	9.4	9.3	9.2	9.1	9.0	8.9	8.8	8.7	8.6
840	8.4	8.3	8.2	8.1	8.0	7.9	7.8	7.7	7.6	7.5
850	7.3	7.2	7.1	7.0	6.9	6.8	6.7	6.6	6.5	6.4
860	6.2	6.1	6.0	5.9	5.8	5.7	5.6	5.5	5.4	5.3
870	5.1	5.0	4.9	4.8	4.7	4.6	4.5	4.4	4.3	4.2
880	4.0	3.9	3.8	3.7	3.6	3.5	3.4	3.3	3.2	3.1
890	2.9	2.8	2.7	2.6	2.5	2.4	2.3	2.2	2.1	2.0
900	1.8	1.7	1.6	1.5	1.4	1.3	1.2	1.1	1.0	0.9
910	0.8	0.7	0.6	0.5	0.4	0.3	0.2	0.1	0.0	

Permeability is measured at some temperature below freezing and can be reduced to the standard temperature of 0C by a small correction resulting from variation of air viscosity with temperature. Air viscosity drops with temperature, so that the measured permeability is higher, the lower the temperature. The correction is very close to 1% per 3C. No barometric correction is necessary.

For K to be constant, $Q/\Delta P$ must be constant, i. e. measurement must be made within the laminar flow range. Experiments show that the upper limit is $v = 5$ cm/sec for fine-grained snow and $v = 1$ cm/sec for coarse-grained snow.

Very coarse-grained depth hoar with $K \approx 1500$ requires measurement under a pressure gradient (i) not exceeding 0.0005. ΔP for a sample 20 cm long is then 0.1 mm of water so that measurement to 0.01 mm is necessary for a 10% accuracy in K ; but for most snows the accuracy then is close to 1%. A good snow permeameter measures Q to better than 1%, and ΔP to 0.01 mm of water pressure. It is convenient to use SIPRE standard snow tubes with a cross section of 24.6 cm² which is large enough to render edge effects negligible if there is no gap between snow and cylinder wall.

K_0 is the air permeability of snow at its natural porosity n_0 . It is an empirical fact, not yet theoretically understood, that if a snow sample in a tube is crushed (densified) in increments with successive measurements of n and the corresponding K the following relation holds:

$$K = \frac{anN}{N-n} \quad \text{where } a \text{ and } N \text{ are constants.}$$

The parameters a and N are easily determined graphically by plotting K/n against K , and drawing a line through the points, which are usually surprisingly well lined up. a is then the intercept on the K/n axis, and N is the reciprocal of the slope.

Table II. Permeability of a new snow upon compaction in increments.
New snow from Wilmette, Illinois, sampled 16 hrs after falling. Sample tube length 18.9 cm, cross section 24.6 cm²

	Length of sample (cm)	γ	n	$i \times 10^3$	K	K/n
Natural condition	18.9	0.094	0.897	4.475	261	291
1st compaction to	18.4	0.097	0.894	4.595	254	284
2nd compaction to	17.9	0.099	0.892	5.815	201	225
3rd compaction to	17.4	0.102	0.889	6.175	189	213
4th compaction to	16.9	0.105	0.885	6.55	178	201
5th compaction to	15.9	0.112	0.878	7.66	152	173
6th compaction to	14.9	0.119	0.870	9.09	128	147
7th compaction to	13.9	0.128	0.860	10.72	109	127
8th compaction to	12.9	0.138	0.849	12.73	92	108

Table II is a typical example. Figure 11 is a graph of K versus K/n from Table II, from which $a = 8$ and $N = 0.922$. Points corresponding to lower values of K (greater densification) must begin to fall below the line since they must tend towards the graph origin. The limits of linearity have not been investigated.

Laboratory work⁴ has shown that the value of parameter a depends mainly on grain size. Figure 12 is a log-log plot of a versus grain size (d) calculated from screened fractions as defined under the previous heading "Texture."

The relation is approximately:

$$a = 16.8d^{1.43}$$

and we can now write

$$K \approx \frac{16.8d^{1.63}nN}{N-n}$$

or if K_0 , n_0 , and N have been determined, the mean grain size can be estimated:

$$d \approx \left[\frac{K_0 (N-n_0)}{16.8Nn_0} \right]^{0.614}$$

The parameter N is interpreted as representing a virtual porosity, perhaps the porosity of the loosest possible packing for a given snow texture. For most snows at any stage of metamorphism, the value N/n_0 is close to 1.063, which means that there is a "normal" density, i. e., a "normal" structure, corresponding to a given texture. Wind-packed snow shows abnormally high values of N/n_0 (up to 1.2); in a sense, its density is too high; structure and texture are out of balance. Given enough time, metamorphism in such snows re-establishes the normal ratio N/n_0 .

In sampling very soft new snow, a gap between the sample and the tube often develops, preventing measurement of K_0 . This value can then be calculated by determining a and N as described above, because the first compression closes the gap.

$$K_0 = \frac{an_0N}{N-n_0}$$

If only K_0 and n_0 have been determined, the probable mean grain size can be estimated by using $N/n_0 = 1.063$

$$d \approx \left(\frac{K_0}{283n_0} \right)^{0.614} \text{ mm.}$$

Figure 13 shows the field of snow in the graph of permeability versus porosity, assembled from data from references 2 and 4. All snows fall within the indicated area. The grain-size lines are based on the above equation for d and are no more than guidelines. The graph shows the great value of permeability as an index property.

F. CLASSIFICATION

Almost every worker in snow classifies different types in some manner, yet no proposed classification scheme has been generally adopted. The "International Classification of Snow (With Special Reference to Snow on the Ground)," issued by the Commission on Snow and Ice of the International Association of Hydrology³³ is very useful and slowly gaining favor. But it is not sufficiently quantitative for advanced scientific and engineering purposes. A great deal of new work on standardization of testing techniques, and on correlation of numerical values of different properties will have to be done before a greatly improved classification can be proposed. Summarization of the content of the "International Classification" would not be useful; the complete text is therefore offered in an appendix, with the kind permission of the Commission on Snow and Ice of the International Association of Hydrology and of the Associate Commission on Soil and Snow Mechanics, National Research Council, Canada.

Classification of the forms of falling snow has been done in very great detail,³⁴ based on the great variety of habits (shapes) of the atmospheric ice crystals.

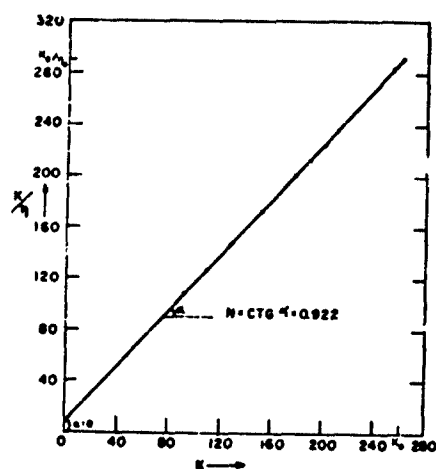


Figure 11. Graph of permeability K versus K/n .

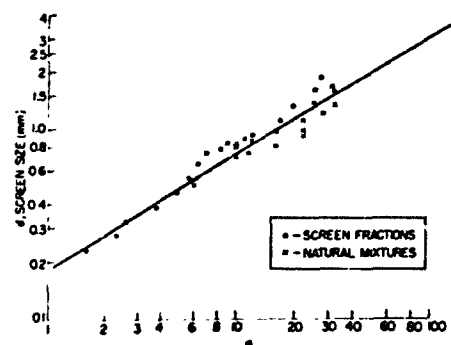


Figure 12. Group of permeability parameter a versus grain size d . (From Bender, ref. 4)

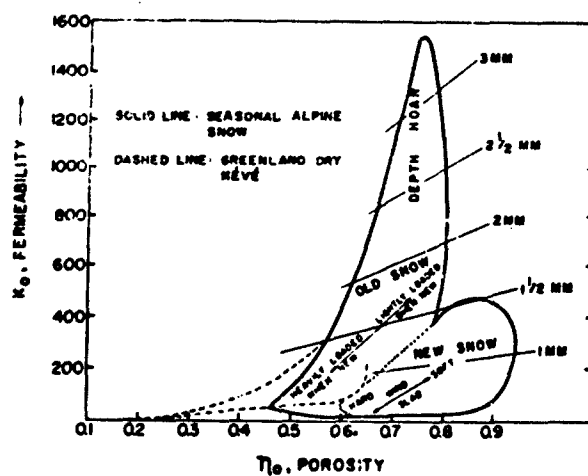


Figure 13. The field of snow in the graph of permeability versus porosity.

THE INTERNATIONAL CLASSIFICATION FOR SNOW

(With Special Reference to Snow on the Ground)

Issued by

The Commission on Snow and Ice

of the

International Association of Hydrology

**Published as Technical Memorandum No. 31 by the
Associate Committee on Soil and Snow Mechanics,
National Research Council, Ottawa, Canada.**

August, 1954

FOREWORD

In recent years the need for a standard system of classifying solid precipitation and fallen snow has become pressing. Mechanized transport over vast snow-ridden areas, the usefulness of accurate snow surveys in the mountain and upland regions of the world, and the intensified scientific study of lying snow - all these factors made it impelling to devise some reliable and simple method of reporting and recording snow.

The seed of the International Snow Classification, which had long been germinating, took firm root during the meetings of the then International Commission on Snow and Glaciers in Oslo in 1948. On that occasion three separate papers on snow data were read and it became clear that a master system must be devised. Accordingly, a committee was set up by the Commission consisting of Dr. V. J. Schaefer, Mr. G. J. Klein, and Dr. M. R. de Quervain with instructions to produce a system that would be generally and internationally acceptable.

With immense labour and application, and after consultations with corporate bodies and private individuals, a tentative scheme was produced. This was placed before the Commission at Brussels in 1951. After some final amendments, authorisation was given for its publication. The Classification is now being considered by the World Meteorological Organisation through its Technical Commission on Aerology (C.Ae) and it is hoped that it will receive also the approval of this body. This publication has been greatly facilitated by the National Research Council of Canada through the good offices of Mr. R. F. Legget, Chairman of its Associate Committee on Soil and Snow Mechanics.

On behalf of the Commission on Snow and Ice I gratefully acknowledge the debt we all owe to the authors of this work.

November 13, 1952
London, England

Gerrid Seligman,
President,
Commission on Snow and Ice

INTRODUCTION

The classification presented herein has been developed by the Committee on Snow Classification in the hope that it may become the generally accepted international system for classifying snow.

The Committee, which was formed at the Oslo Conference of the International Union of Geodesy and Geophysics, regarded the question of an international nomenclature for snow as being outside its province. For this reason symbols were used to designate the various classes and basic features of snow, making the classification independent of language and therefore more convenient for international use. Although the symbols may also be used for teletype messages, it should be emphasized that the latter use was not the primary reason for adopting the symbols.

The classification is similar to several more or less parallel systems which have been developed in different countries and have been in use during the past one or two decades. The best features of these systems have been combined and modified to form a coherent and reasonably simple classification. Much thought and effort have been put into its general arrangement, details, and many groups and individuals directly concerned with snow research have been consulted with a view to making the classification as suitable and generally acceptable as possible. If the classification is as well received as it was in its tentative draft form, there is little doubt that it will be adopted by many groups engaged in the study of snow and its related problems.

An important feature of the classification is that it has been set up as the basic framework which may be expanded or contracted to suit the needs of any particular group ranging from scientists to skiers. It has also been arranged so that many of the observations may be made either with the aid of simple instruments or, alternatively, by visual methods. Since the two methods are basically parallel, measurements and visual observations may be combined in various ways to obtain the degree of precision required in any particular class of work.

Section I, on solid precipitation, is not intended to replace that part of the International Meteorological Code which deals with snow, hail, etc., and care was taken to avoid any conflict between the two systems. Section I is based on the form of the crystal or particle and regards form and size of a particle as two separate features.

(iii)

Section II, dealing with deposited snow, is based on the fundamental features which determine the physical characteristics of a mass of snow and distinguish one type from another.

Sections I and II may be regarded as the fundamental part of the classification.

Section III deals with measurements which are frequently required in describing a snow cover, while Section IV provides a means for describing certain features of the snow surface which may be significant in some problems.

Subsection 1 of Section IV, dealing with surface deposits such as surface hoar, has been included because of its relation to snow lying on the ground. The ice deposits which form on the wings of aircraft are of a similar kind, and specialists in this field are using a more detailed classification than the classification for surface deposits presented here. It may be regarded as an example of an expansion of a section of the present classification.

An attempt has been made to describe clearly each class or feature of snow in the body of the classification. Classification has also been presented in an abstract form which is suitable for convenient reference in the field.

A number of examples explaining the use of the symbols are given in the text, while the use of the graphic symbols is illustrated in Appendix II.

Those interested in the English terminology commonly used in describing snow should refer to "Snow Structure and Ski Fields" by G. Seligman, MacMillan and Co., Limited, London, 1936. If a nomenclature for snow were included as an appendix to this classification, it would closely follow the nomenclature given by Seligman.

SOLID PRECIPITATION

The term "solid precipitation" refers to the various kinds of solid water particles which develop in the atmosphere and fall earthwards, for example, snow crystals, ice pellets. When a sharp distinction is drawn between falling and deposited particles, the term applies to precipitation while it remains airborne; but in the classification presented here, "solid precipitation" is taken to also include freshly deposited particles which have not undergone any perceptible transformation subsequent to being deposited upon the earth.

When different classes of solid precipitation occur together, the relative number of each type may be given as the number of tenths, or hundredths, e.g., 8F2D4+2F8D1.5 designates 80 per cent stellar crystals of 4 mm. average diameter mixed with 20 per cent graupel of 1.5 mm. average diameter.

The International Meteorological Code may be used to indicate the intensity and duration of the precipitation as well as other weather data when this information is required.

The method of classifying solid precipitation is outlined in subsections 1 and 2.

1. Type of Particle

General symbol F

Graphic symbol for snow in general, i.e. F1 to F7









TABLE I


CLASSES OF SOLID PRECIPITATION

Description	Symbol	Graphic Symbol
<u>Plate</u> A plate is a thin, plate-like snow crystal the form of which more or less resembles a hexagon or, in rare cases, a triangle. Generally all edges or alternative edges of the plate are similar in pattern and length.	1	
<u>Stellar Crystal</u> A stellar crystal is a thin, flat snow crystal in the form of a conventionalized star. It generally has six arms but stellar crystals with three or twelve arms occur occasionally. The arms may lie in a single plane or in closely spaced parallel planes in which case the arms are interconnected by a very short column.	2	
<u>Column</u> A column is a relatively short prismatic crystal, either solid or hollow, with plane, pyramidal, truncated or hollow ends. Pyramids, which may be regarded as a particular case, and combinations of columns are included in this class.	3	

(Table 1, continued)

Description	Symbol	Graphic Symbol
<p><u>Needle</u></p> <p>A needle is a very slender needle-like snow particle of approximately cylindrical form. This class includes hollow bundles of parallel needles, which are very common, and combinations of needles arranged in any of a wide variety of fashions.</p>	4	
<p><u>Spatial Dendrite</u></p> <p>A spatial dendrite is a complex snow crystal with fern-like arms which do not lie in a plane or in parallel planes but extend in many directions from a central nucleus. Its general form is roughly spherical.</p>	5	
<p><u>Capped Column</u></p> <p>A capped column is a column with plates of hexagonal or stellar form at its ends and, in many cases, with additional plates at intermediate positions. The plates are arranged normal to the principal axis of the column. Occasionally only one end of the column is capped in this manner.</p>	6	
<p><u>Irregular Crystal</u></p> <p>An irregular crystal is a snow particle made up of a number of small crystals grown together in a random fashion. Generally the component crystals are so small that the crystalline form of the particle can only be seen with the aid of a magnifying glass or microscope.</p>	7	
<p><u>Graupel</u></p> <p>Graupel, which includes the soft hail, small hail, and snow pellets of the meteorologist, is a snow crystal or particle coated with a heavy deposit of rime. It may retain some evidence of the outline of the original crystal although the most common type has a form which is approximately spherical.</p>	8	
<p><u>Ice Pellet</u></p> <p>Ice pellets are frequently called "sleet" in North America. An ice pellet is a transparent spheroid of ice and is usually fairly small. Some ice pellets do not have a frozen centre which indicates that, at least in some cases, freezing takes place from the surface inwards.</p>	9	

(Table 1, continued)

Description	Symbol	Graphic Symbol
Hail A hailstone* is a grain of ice, generally having a laminar structure and characterized by its smooth glazed surface and its translucent or milky-white centre. Hail is usually associated with those atmospheric conditions which accompany thunderstorms. Hailstones are sometimes quite large. *In English, hail, like rain, refers to a number at one time, while hailstone, like raindrop, refers to an individual.	0	

Modifying features of classes F1 to V0 may be included by adding one or more of the following subscripts.

TABLE II
MODIFYING FEATURES

Feature	Symbol Subscript
Broken crystals	p
Rime-coated particles not sufficiently coated to be classed as graupel	r
Clusters, such as compound snow flakes, composed of several individual snow crystals	f
Wet or partly melted particles	w

2. Size of Particle

General symbol D

The size of a crystal or particle is its greatest extension measured in millimeters. When many particles are involved, e.g., a compound snow flake, it refers to the average size of the individual particles.

Example: F4fD2.5 or \longleftrightarrow f D2.5 designates a cluster or clusters composed of needles, the average size of the needles being 2.5 mm.

SECTION II

DEPOSITED SNOW

A snow cover is generally composed of layers of different types of snow each of which is more or less homogeneous within its own boundaries. Section II deals with the classification of the type of snow in any one layer.

A mass of snow is very porous and it may or may not contain some water in the liquid state which is usually referred to as "free water". In the general case, therefore, snow may be regarded as a mixture of ice, air, and water, the ice being in the form of crystals or grains which are usually interknit or welded together to form a structure which possesses some degree of strength. The physical characteristics of a mass of snow, like those of many other materials, depend upon the relative proportions of its constituents, its structure, and its temperature. Taking physical characteristics as the criterion, the primary features which classify a type of deposited snow are those given in Table III.

TABLE III
PRIMARY FEATURES OF DEPOSITED SNOW

Feature		Units	Symbol
Specific gravity, or Density		non-dimensional g/cm ³ , or kg/m ³ .	G
Free water content		% by weight, or see Table IV	W
Impurities		% by weight	J
Structure	Grain shape	see Table V	F
	Grain size	millimeters	D
	Strength represented by:		
	Compressive yield strength,	g/cm ² .	Kp
	Tensile strength	g/cm ² .	Ks
	Shear strength at zero normal stress, or	g/cm ² .	Ks
	Hardness	according to instrument	R
	Snow temperature	degrees Centigrade	T

The above features are discussed in some detail in the following subsections.

1. Specific Gravity

General symbol G

Specific gravity is the ratio of the weight of any volume of a substance to the weight of an equal volume of water and is therefore non-dimensional. Density may be used as an alternative. It should, however, be expressed either in grams per cubic centimeter or in kilograms per cubic meter; the former having the same numerical value as specific gravity while the latter avoids the inconvenience of the decimal point. For example: a specific gravity of 0.235 is equivalent to a density of 0.235 grams per cubic centimeter or 235 kilograms per cubic meter. Using symbols, this may be given as G 0.235 or G 235 provided the dimensions used are clearly indicated or understood.

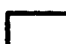
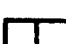



2. Free Water Content

General symbol W

There are several methods of measuring the free water content of snow but, since fairly elaborate apparatus is usually required in order to obtain reasonable accuracy, these methods are generally used only in a laboratory. Measurements of free water content are expressed as a percentage by weight.

In field tests, reliance usually has to be placed upon simple observations. Table IV is given as the basis of observations of this kind and, although this method was primarily intended for use in the field, it is also of considerable value in the laboratory.

TABLE IV
FREE WATER CONTENT

Term	Remarks	Symbol	Graphic Symbol
Dry	Usually T is below 0°C, but dry snow can occur temperature up to and including 0°C. When its structure is broken down by crushing and the loose grains are lightly pressed together as in making a snow ball, the grains have little tendency to cling to each other.	a	
	T = 0°C. The water is not visible even with the aid of a magnifying glass. When lightly crushed, the snow has a distinct tendency to stick together.	b	
Wet	T = 0°C. The water can be recognised by its meniscus between adjacent snow grains, but water cannot be pressed out by moderately squeezing the snow in the hands.	c	
Very Wet	T = 0°C. The water can be pressed out by moderately squeezing the snow in the hands but there still is an appreciable amount of air confined within the snow structure.	d	
Slush	T = 0°C. Snow flooded with water and containing a relatively small amount of air.	e	

3. Impurities

General symbol J

This subsection has been included in the classification in order to cover those cases in which the kind and amount of an impurity have an influence upon the physical characteristics of the snow. In these cases the kind of impurity should be fully described and its amount given as a percentage by weight. Common impurities are: dust, sand, organic material, salt, etc.

Graphic symbol

4. Grain Shape



General symbol F

In the classification, numerical symbols (F1, F2, etc.) have been used for solid precipitation while alphabetical symbols (Fa, Fb, etc.) have been used for deposited snow. However, whenever a distinction between the various types of freshly deposited snow is required, the classification given in Table I may be used and, when necessary, the relative proportions of the various types may be expressed as the number of tenths as explained in Section I.

TABLE V
GRAIN SHAPE

Description	Symbol	Graphic Symbol
<p><u>Class "a"</u></p> <p>Class "a" refers to freshly deposited snow composed of crystals, or parts of broken crystals, of types F1 to F7 (Table I). Snow which has lost its crystalline character while falling to earth, and graupel, ice pellets, and hail do not belong to this class. Class "a" snow is generally very soft.</p>	a	
<p><u>Class "b"</u></p> <p>This class refers to snow during its initial stage of settling. It has not reached the very fine grain-size condition which is generally regarded as the conclusion of the initial stage of transformation. Although it has lost a great deal of its crystalline character, some crystalline features can be observed. Class "b" snow is usually fairly soft.</p>	b	
<p><u>Class "c"</u></p> <p>When snow is transformed by melting, or melting followed by freezing, it completely loses all crystalline features and its grains become irregular and more or less rounded in form. This is Class "c" snow. It has no sparkle effect even in bright sunlight and can be readily recognized by its dull appearance. It is usually fairly soft when wet, but can be very hard when frozen. Class "c" snow may have any size of grains from very fine to very coarse.</p>	c	

(Table V, continued)

Description	Symbol	Graphic Symbol
Class "d" At temperatures well below freezing and without any apparent melting, snow is transformed into Class "d" by the process of sublimation which produces irregular grains with flat facets. These facets give the snow a distinct sparkle effect in bright sunlight. In the Arctic, where temperatures are low and persistent winds accelerate the sublimation, practically all of the settled snow is Class "d" and has almost as much sparkle as a deposit of F1 crystals. Class "d" snow is usually fairly hard.	d	
Depth Hoar Depth hoar is characterized by its hollow cup-shaped crystals. These crystals are produced by a very low rate of sublimation during a long uninterrupted cold period and are most frequently found directly below a more or less impermeable crust in the lower part of the snow cover. The strength of a layer of depth hoar is very low.	.	

5. Grain Size

General symbol D

The grain size of a more or less homogeneous mass of snow is the average size of its grains, taking the size of an individual grain as its greatest extension. A simple method suitable for field measurements is to place a fair sample of the grains on a plate which has been ruled in millimeters. The average or typical size is then estimated by comparing the size of the grains with the spacing of the lines on the plate.

The grain size of deposited snow is expressed in millimeters or, alternatively, by the use of the terms or symbols presented in Table VI.

TABLE VI

GRAIN SIZE OF DEPOSITED SNOW

Term	Symbol	Grain Size Range
Very fine	a	less than 0.5 mm.
Fine	b	0.5 to 1.0 mm.
Medium	c	1.0 to 2.0 mm.
Coarse	d	2.0 to 4.0 mm.
Very coarse	e	greater than 4.0 mm.

6. Strength of Structure







General symbol K

The yield strengths in compression, tension, and shear of many materials are generally inter-related by simple ratios, such as 2:2:1 which applies to ductile materials. In this case, the three yield strengths are known when any one of them is given. Investigations, still in progress, indicate that a relation of this kind exists between the yield strengths of snow. It is therefore proposed that the strength of deposited snow be described by any one of the following:

- (a) Compressive yield strength, i.e., the stress under a compressive load at which initial collapse of the snow structure occurs, g/cm^2 .
- (b) Tensile strength, g/cm^2 .
- (c) Shear strength at zero normal stress, g/cm^2 .
- (d) Hardness, in which case the correlation between the readings of the particular hardness instrument and (a), (b), or (c) above should be given.

Since the technique and instruments required for measuring (a) and (d) are considerably less complex than those required for measuring (b) and (c), compressive yield strength and hardness measurements can be expected to be used more frequently than measurements of tensile and shear strength.

TABLE VII
STRENGTH OF DEPOSITED SNOW

Term	Range of Kp. g/cm^2	Symbol	Graphic Symbol
Very low	0 - 10	a	
Low	10 - 100	b	
Medium	100 - 1000	c	
High	1000 - 10,000	d	
Very high	Greater than 10,000	e	
Ice		i	

7. Snow Temperature

General symbol T

The temperature of snow should be given in degrees Centigrade. Sometimes it is desirable to record other related temperatures; the suggested symbols for the more common ones are included below:

Snow temperature	T	degrees Centigrade
Air temperature	Ta	" "
Temperature of snow surface	Ts	" "
Ground temperature	Tg	" "

SECTION III

SNOW COVER MEASUREMENTS

A cross-section of a snow cover may be described by classifying the snow in each layer, as outlined in Section II, and by giving the location of the boundaries of the layers by means of measurements. The location of a layer boundary is generally established by its vertical co-ordinate measured from the surface of the ground but, in certain cases, where only the upper part of the snow cover is of interest or where it is difficult to use the ground as the reference, the snow surface may be taken as the reference.

The symbols H, HS and HN should be used for all vertical measurements regardless of whether they are taken at a place where the snow surface is horizontal or inclined. Vertical measurements are preferred even when the snow lies on a slope. If, however, the measurements are taken along a line perpendicular to an inclined snow surface, this fact should be indicated by using the corresponding symbols M, MS and MN.

TABLE VIII

SNOW COVER MEASUREMENTS

Term	Dimension	Symbol
Vertical co-ordinate (measured from the ground)	cm	H
Total depth of snow cover	cm	HS
Depth of daily new snowfall	m	HN
Measurements corresponding to those above but taken perpendicularly to an inclined snow surface	cm	M, MS, and MN
Inclination of snow surface	angle in degrees	N
Water equivalent of the snow cover	mm	HW
Ratio of snow covered area to total area	tenths	Q
Age of snow deposit	indicate whether hours, days, or years	A

SECTION IV

SNOW SURFACE CONDITIONS





Surface deposits, such as surface hoar, and other features of the snow surface may be described as indicated in the following subsections.

1. Surface Deposits

General symbol V

These deposits are represented by the symbols V1, V2, etc., to avoid confusion with the symbols F1, F2, etc., for solid precipitation.

TABLE IX
SURFACE DEPOSITS

Term and Description	Symbol	Graphic Symbol
<u>Surface Hoar</u> Surface hoar is a deposit of plane, prismatic, or dendritic crystals formed by sublimation of water vapour onto any fixed object the temperature of which is below 0°C. Plane crystals of surface hoar can be distinguished from plates (F1) by their lack of symmetry.	1	
<u>Soft Rime</u> Soft rime is a light, brittle feathery deposit intermediate between surface hoar and hard rime (see definition below) and appears to be a combination of the elements of both hoar and rime.	2	
<u>Hard Rime</u> Hard rime is a frozen deposit of small, supercooled fog droplets on any solid object. The droplets freeze immediately upon contact with the object which gives rime its very fine pebbly texture.	3	
<u>Glassed Frost or Glaze</u> Glassed frost is a smooth, thin, ice coating formed on any solid object by raindrops which have run together before freezing, or by thawing followed by freezing.	4	

2. Surface Roughness

General symbol S


This subsection does not refer to roughness due to the granular nature of snow, but to the roughness of a snow surface caused by the effects of wind, rain, unequal evaporation or unequal melting. The average depth of the irregularities, measured in cm., may be combined with the symbol, for example: Sc 15 or  15.

TABLE X
SURFACE ROUGHNESS

Term	Symbol	Graphic Symbol
Smooth	a	—
Wavy	b	~~~~~
Concave furrows	c	~~~~~
Convex furrows	d	~~~~~
Random furrows	e	~~~~~

3. Penetrability of Surface Layers

General symbol P

Occasionally, an approximate indication is required of the ability of a snow cover to satisfactorily support a certain load. The depth of penetration of some suitable object, such as a ski or a man's foot, may be employed for this purpose. The following symbols are suggested:

Depth of ski track (skier supported on one ski)

PS

Depth of footprint (man standing on one foot)

PP

The depth of penetration should be measured in centimeters or may be expressed by symbols.


rs or may be expressed

TABLE XI
DEPTH OF PENETRATION

Term	Depth Range, cm.	Symbol
Very small	less than 0.5	a
Small	0.5 to 2	b
Medium	2 to 10	c
Deep	10 to 30	d
Very deep	greater than 30	e

ABSTRACT OF THE CLASSIFICATION FOR SNOW

I SOLID PRECIPITATION

TYPE OF PARTICLE		SYMBOL	GRAPHIC SYMBOL
PLATE		F1	⬡
STELLAR CRYSTAL		F2	✳
COLUMN		F3	▭
NEEDLE		F4	↔
SPATIAL DENDRITE		F5	⊗
CAPPED COLUMN		F6	▯
IRREGULAR CRYSTAL		F7	⋈
GRAUPEL		F8	⚡
ICE PELLET		F9	⬠
HAIL		F0	▲

MODIFYING FEATURE	BROKEN CRYSTALS	RIME COATED CRYSTALS	CLUSTERS	WET
SYMBOL SUBSCRIPT	p	r	f	w

SIZE OF PARTICLE D MEASURED IN MILLIMETERS.

II DEPOSITED SNOW

28c

FEATURE	SYMBOL	SUBCLASSIFICATION				
		a	b	c	d	e
SPECIFIC GRAVITY	G					
FREE WATER, %	W	dry	moist	wet	very wet	slush
GRAIN SHAPE	F	51-77 crystals	partly settled	rounded grains	grains with facets	depth hard
GRAIN SIZE, mm.	D	<0.5	0.5-1	1-2	2-4	>4
COMP. YLD. STGTH. g/cm ³	K	0-10	10-10 ³	10 ³ -10 ⁵	10 ⁵ -10 ⁷	>10 ⁷
SNOW TEMPERATURE, °C	ICE LAYER, i		IMPURITIES J%			

III SNOW COVER MEASUREMENTS

	VERTICAL	1 to inclined surfaces	INCLINATION OF SURFACE, N DEGREES	
CO-ORDINATE, cm.	M	M	WATER EQUIVALENT OF COVER, MW mm. OF WATER	
TOTAL DEPTH, cm.	MS	MS	SNOW COVERED AREA, Q TENTHS TOTAL AREA	
DAILY NEW SNOWFALL, cm.	NN	NN	AGE OF DEPOSIT, A HR., DAYS, ETC.	

IV SNOW SURFACE CONDITIONS

SURFACE DEPOSIT	SURFACE HOAR	SOFT RIM	RD RIME	GLAZED FROST
SYMBOL	V1	V2	V3	V4
GRAPHIC SYMBOL	—	∨	∨	∞

SURFACE ROUGHNESS	SMOOTH	WAVY	CONCAVE FURROWS	CONVEX FURROWS	RANDOM FURROWS
SYMBOL	S ₀	S ₁	S ₂	S ₃	S ₄
GRAPHIC SYMBOL	—	~~~~~	~~~~~	~~~~~	~~~~~

SURFACE PENETRABILITY	a	b	c	d	e
RANGE, cm.	<0.5	0.5-2	2-10	10-30	>30

SKI TRACK DEPTH (SKIERS SUPPORTED ON ONE SKI) cm. PS
 FOOT PRINT DEPTH (MAN STANDING ON ONE FOOT) cm. PP

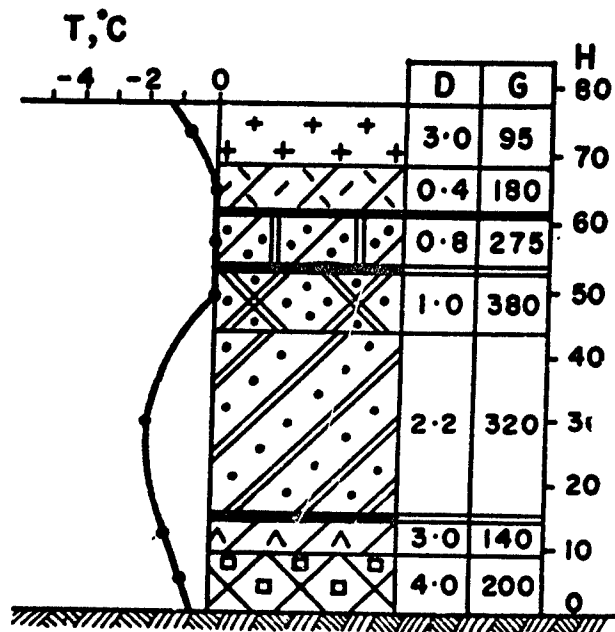
APPENDIX I LIST OF SYMBOLS

		Derived from:
A	Age of a snow deposit	<u>Alter</u> , <u>Age</u>
a	very low, etc.	Always used after the general symbol of a particular quality, such as specific gravity to indicate the degree of that quality.
b	low, etc.	
c	medium	
d	high, etc.	
e	very high, etc.	
D	Size of a particle	<u>Diameter</u>
F	Shape or form of a particle	<u>Form</u>
	with figure : solid precipitation	
	with letter : deposited snow	
f	Cluster of particles; see Table II	<u>Flake</u>
G	Specific gravity, density	<u>Gravity</u> , <u>Gewicht</u>
H	Vertical co-ordinate	<u>Height</u> , <u>Hauteur</u> , <u>Höhe</u>
HN	Depth of daily new snowfall	
HS	Total depth of snow cover	
HW	Water equivalent of snow cover	
i	An ice layer	<u>Ice</u>
J	Impurities	<u>Impurities</u> , <u>Impuretés</u>
K	General symbol for strength of deposited snow	<u>Kohäsion</u>
Kp	Compressive yield strength	see Table VII
Ks	Shear strength at zero normal stress	
Ka	Tensile strength	
M	Measurements taken perpendicularly to an inclined snow surface;	<u>Mächtigkeit</u>
MN	see Table VIII	
MS		
N	Inclination of a snow surface	<u>Neigung</u>
P	General symbol for penetrability of surface	<u>Penetrate</u> , <u>Pénétrier</u>

LIST OF SYMBOLS, continued

		<u>Derived from:</u>
PP	Depth of footprint] see Section IV - 3
PS	Depth of ski track	
p	Fragment of a snow crystal; see Table II	<u>Partager, Part</u>
Q	Ratio of snow-covered area to total area	<u>Quotient</u>
R	Snow hardness, related to a particular instrument	<u>Resistance, Rigidite'</u>
r	Rime-coated particle; see Table II	<u>Rime</u>
S	General symbol for snow surface	<u>Surface</u>
Sa to Se	Snow surface roughness; see Table X	
T	Snow temperature	<u>Temperature</u>
Ta	Air temperature	
Tg	Ground temperature	
Ts	Temperature of the snow surface	
V	Surface deposits, such as surface hoar; see Section V - 1	
W	Free water content of snow	<u>Water, Wasser</u>
w	Partly melted particles; see Table II	

A vertical section of a snow cover may be represented graphically as illustrated below. The appropriate symbols for a particular layer are combined by superposition, while snow temperature is plotted as a curve. Grain size and specific gravity may be tabulated as shown in the example or represented by graphs.



G. MECHANICSNotation

E	=	Young's Modulus
γ	=	Density* of snow
γ_i	=	Density of ice (0.9179 g/cm ³)
ϵ	=	Strain
F	=	Activation energy
R	=	Gas constant
t	=	Time or Celsius (formerly centigrade) temperature
T	=	Kelvin temperature
°C	=	Degree Celsius
e	=	Base of natural logarithms or void ratio
D	=	Snow grain diameter
σ	=	Stress
τ	=	Shear stress or retardation time
η	=	Coefficient of dynamic viscosity
ν	=	Poisson's ratio

*All densities are given in g/cm³ unless otherwise stated.

Introduction

Snow mechanics is a relatively new subject of scientific-technical research, which began to receive attention as an offshoot of soil mechanics in the late thirties, in relation to avalanche defense construction problems. The heavy emphasis on analogy between soil and snow mechanics has perhaps been not altogether fortunate. It was initially very helpful, but snow mechanics may now in some respects have to go its own way. It is presently only in a fair state of development, and a number of fundamental aspects, primarily creep under combined stresses, collapse behavior, and flow dynamics, are not yet well or at all formulated. The difficulties in development of snow mechanics, as a science and for engineering purposes, stem mainly from the following factors:

- a) the very high temperature dependence of many properties of snow.
- b) the thermodynamic instability of snow.
- c) the large density and significant grain size ranges of snow, and the very large dependence of mechanical property parameters on density and grain size.
- d) the freedom of movement of grains in the snow structure.
- e) anisotropism and sample inhomogeneity.

These factors will now be discussed.

a) Temperature. The mechanics of wet snow (temperature very close to 0C, and varying liquid water content) has not yet been investigated quantitatively. Perhaps only two general statements can be made here: Ultimate strength decreases drastically when a snow becomes wet, and viscosity also decreases.

We are concerned here only with dry snow at temperatures lower than a small fraction (not further defined) of a degree below the freezing point of ice at the prevailing pressure.

Temperature has a moderate effect on elastic moduli, which increase with decreasing temperature. The following is reported on young snow.³⁷

$$E_t = E_{t_0} - a(t - t_0)$$

where t is in C.

Modulus	Density (g/cm ³)	Temperature range	a
E ₁	0.16-0.19	-1 to -7C	0.5
E ₂	0.16-0.19	-1 to -7C	0.7
E ₁	0.23-0.25	-1 to -18C	0.07
E ₂	0.23-0.25	-1 to -18C	0.1

E₁ and E₂ are Young's moduli obtained from creep tests under static load, and are explained later under creep mechanics. For Young's modulus E_r , determined from resonance frequency of oscillation of bars, the following values are given.³⁷

Density	Temp range	a
0.29	-1 to -8C	0.1
0.33	-1 to -8C	0.1
0.54	-1 to -8C	0.04
0.63	-2 to -9C	0.07
0.76	-2 to -9C	0.08

The parameter $a = \frac{\partial E}{\partial T}$ decreases at lower temperatures,³⁷ probably exponentially, and appears to be almost independent of density (γ) for $\gamma < 0.25$ g/cm³.

The effect of temperature on ultimate strength has been investigated for the case of tensile strength,⁶ which increases with decreasing temperature. The derivative of strength with respect to temperature decreases, since strength does not increase indefinitely. The magnitude of this temperature effect will be given later.

The effect of temperature on creep rate ($\dot{\epsilon}$) of snow under stress is most important, and adequately given by eq 1, except very close to the melting point.

$$\frac{\dot{\epsilon}_T}{\dot{\epsilon}_{T_0}} = e^{\frac{F}{R} \left(\frac{1}{T_0} - \frac{1}{T} \right)} \quad (1)$$

where T = degrees Kelvin (absolute temperature)

T_0 = reference temperature, at which $\dot{\epsilon}_{T_0}$ has been measured.

R = gas constant = 1.987 cal/mol-degree

F = activation energy = 10,000 to 24,000 cal/mol

$\dot{\epsilon}_T$ = strain rate (creep rate) at temperature T .

The activation energy seems to be somewhat variable, within the range 10,000 to 24,000 cal/mol,^{4, 16, 29, 37} with 14,000 as a fair mean for purposes of comparing creep data obtained at different temperatures. The higher values are limited to some new snows.³⁷

Figure 14 is a graph with $T_0 = 263.3$ ($t_0 = -10^\circ\text{C}$) as reference temperature, using the above equation for different activation energies. The figure shows the enormous effect of temperature on the creep rate. Taking for instance a value of $F = 14,000$, snow under a given stress will creep twice as fast at -10°C than at $-16\frac{1}{2}^\circ\text{C}$, and 200 times faster at -20°C than at -50°C . The lines of Figure 14 would very likely bend sharply upwards as they approach the ordinate of melting temperature.

It is easy to see that analysis of creep even in a homogeneous snow mass can become unmanageable when there are temperature gradients.

b) Thermodynamic instability. The snow structure is thermodynamically inherently unstable, which leads to metamorphism by recrystallization, described in detail previously. For mechanical behavior, the important consequence is increase in density and grain size with time. Density will remain constant or decrease slightly only when there is a loss of mass by sublimation or when tensile stresses dominate. The usual condition is densification under combined stresses, the normal minimum stress being that exerted by the weight of the snow mass itself. Grain growth is favored by applied stress because thermodynamic instability is increased by distortion of snow structure and ice crystal lattice, but it is inhibited by reduction of porosity and permeability upon densification.

c) Density and grain size. The creep rate is highly dependent on density (γ). Since, in most cases, snow densifies as it is deformed, the rate of deformation decreases with time. Figure 15 shows a typical compression versus time curve,³ and Figure 16 shows curves relating viscosity to density.⁶ Such curves are well described by exponential functions.^{3, 22} The rate of creep $\dot{\epsilon}$ (derivative of deformation with respect to time) is proportional to an exponential of the density.^{22, 25, 37}

$$\frac{\dot{\epsilon}}{\dot{\epsilon}_0} = e^{-b(\gamma - \gamma_0)} \quad (2)$$

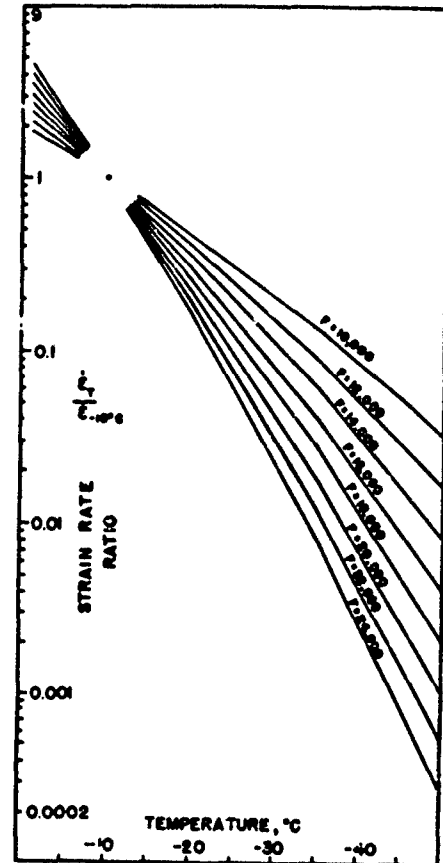


Figure 14. Effect of temperature on creep rate of snow for different values of activation energy F (cal/mol). Density and creep stress constant.

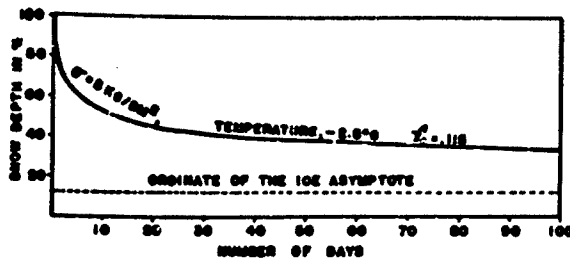


Figure 15. Creep compression of snow as a function of time at constant load and temperature. (γ_0 is the initial density.) (From Bucher, ref. 6)

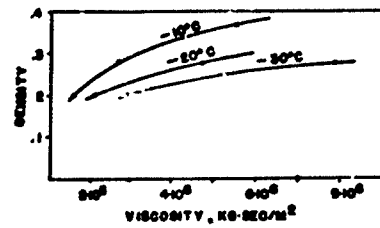


Figure 16. Viscosity of new snow as a function of density (g/cm^3) at different temperatures. (From Bucher, ref. 6)

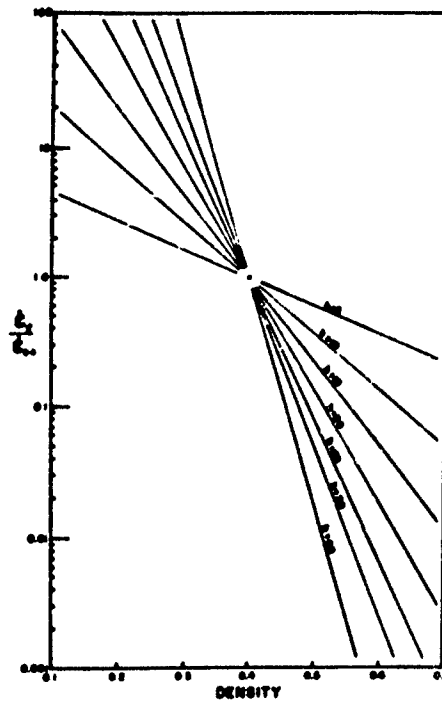


Figure 17. Effect of density on creep rate of snow, for different values of exponent h . Temperature and creep stress constant.

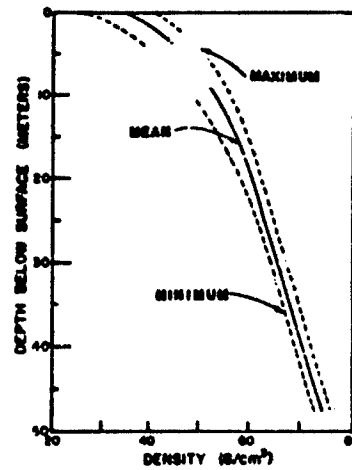


Figure 18. Snow density as a function of depth on a polar glacier. (Site 2, Greenland 77°N 56°W). (From Bader *et al.*, ref 3).

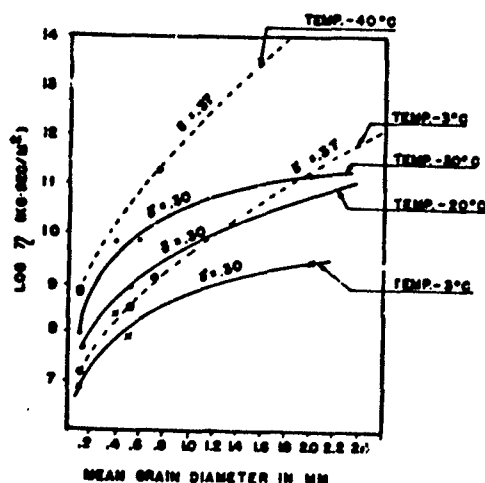


Figure 19. Viscosity as a function of snow grain size for different densities and temperatures. (From Bucher, ref. 6).

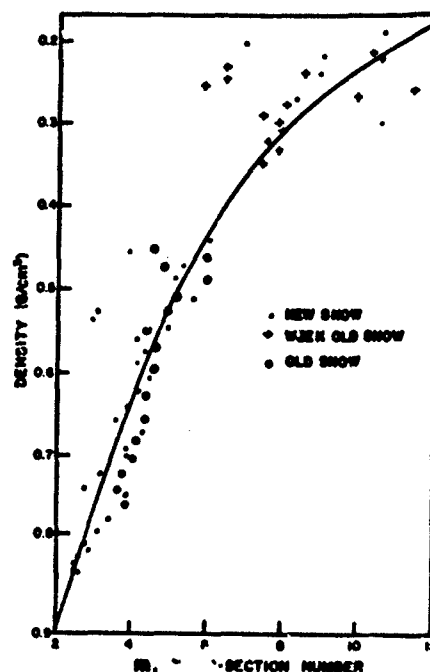


Figure 20. C , section number m of snow as a function of density.

The parameter b varies from perhaps as little as 5 to as much as 40 for different snow type - time sequences. The conditions determining the value of b have not been investigated, since the concept is relatively new. It depends on snow type sequence, and perhaps also on the absolute value of the creep rate and temperature. Values of $b \approx 21$ are very frequently found. Figure 17 is a plot of the equation for different values of b . As an example, for $b = 25$, the creep velocity would decrease by three orders of magnitude during densification by a factor of 2, from 0.25 to 0.52 g/cm³. At $\gamma = 0.4$ a 10% increase in density would drop the creep rate to one-third.

This strong function indicates that, when a snow cover consisting of layers of different densities is slowly compressed, for instance by a footing, the lighter layers will densify much faster than the heavier ones, resulting in a homogenization of the mass with respect to density. This phenomenon is well illustrated by density profiles of deep snow on high glaciers.³ The greater the depth (increasing load and time), the smaller the deviations of density from the mean depth-density curve. Figure 18 shows this condition for Greenland snow at 77N 56W. The parallelism of the maximum and minimum curves below 25 m is attributable to grain size differences. The lower density layers are coarser-grained than the higher density ones, and the salient fact is that, for a given density and stress, coarse-grained snow creeps slower than fine-grained snow. This is well illustrated by Figure 19. (The creep velocity $\dot{\epsilon}$ is inversely proportional to the viscosity η .) This is the only data available, meager for a formulation of the relation between creep velocity and grain size (D). The relation

$$\frac{\dot{\epsilon}_2}{\dot{\epsilon}_1} = \left(\frac{D_1}{D_2} \right)^3 \quad (3)$$

does not fit too badly: the effect would be linear in terms of grain volume.

d) Freedom of movement of grains. In low-density snow there are large pore spaces into which grains can move more or less freely. Thus, for instance, a grain squeezed between one above and one below can often move cut sideways without exerting lateral pressure on a neighboring grain. In consequence, such snow can be vertically compressed with only a very small resultant lateral pressure if lateral dilatation is suppressed.

This phenomenon is most important, for it invalidates, at least for mechanics of low-density snow, the classical theoretical approach, wherein, for plastic deformation, the principal stresses are related to strain rates by analogy to elastic theory. Here the "m" number, variously designated as "cross-section number" or "transverse coefficient" is the viscous or plastic analog to the inverse of Poisson's ratio. The relation of m to density has been determined experimentally by uniaxial compression of snow cylinders,³⁵ and is shown in Figure 20. If z is the length of a snow cylinder, and x is its width, and the cylinder is uniaxially compressed in z , then

$$m = \frac{\frac{1}{z} \frac{dz}{dt}}{\frac{1}{x} \frac{dx}{dt}} = \frac{x \Delta z}{z \Delta x} \text{ for small } \Delta. \quad (4)$$

From this basis an additive theory of snow deformation under combined stresses was developed,^{35, 6, 15} but has been shown to be inadequate.²⁶ Experiments on the relation between principal stresses in confined-side compression reveal that the resulting lateral stress is many times smaller than the one predicted by the additive theory.

This means that we are presently without a useful theory of creep of snow under combined stresses. The freedom of movement of grains could perhaps be formulated in terms of a factor which is a function of density and possibly grain size, but not of temperature. The factor would be large for light snow, and decrease to a minimum value of unity as density increases. Instead of m , we would use a parameter m^* .

$$m^* = \frac{m}{f(\gamma)}$$

$$\text{with the boundary conditions} \quad \gamma = 0, \quad f(0) = \infty \\ \gamma = \gamma_1, \quad f(\gamma_1) = 1$$

m itself will have to be expressed in terms of γ . Its minimum value must be 2 at γ_1 .

In particular, and as a good first approximation, low density snow reacts to triaxial stress in the same manner as to three corresponding independent uniaxial stresses, i. e., the initial strain rate $\dot{\epsilon}_x$ in reaction to a stress σ_x will be almost independent of the strain rates $\dot{\epsilon}_x$ and $\dot{\epsilon}_y$ produced by applied stresses σ_x and σ_y .

A great amount of accurate experimental work will have to be done to clarify triaxial creep mechanics.

e) Anisotropism and sample inhomogeneity. Anisotropism of a vectorial property exists when its value changes with the direction in which it is measured. There are two main sources of snow anisotropism.

1) The individual component ice crystal is anisotropic. Young's modulus varies as much as 15% with direction. Since the basal plane normal to the main crystallographic axis is the only shear creep plane, the effective shear stress varies with angle between applied shear stress and basal plane. Hence snow can be anisotropic with respect to Young's modulus and viscosity when the orientation of the main crystallographic axis of the individual crystals is not random. When recrystallization of a low-density snow takes place under strong temperature gradients, there is a tendency for preferred main-axis orientation parallel to the gradient, i. e., normal to the surface. Long-time pressure

metamorphism - for instance natural densification in deep snow on polar glaciers - also produces preferred orientation, with main axis parallel to the vertical compressive stress.¹³

2) Snow deposited during a snowfall is a very finely layered mass. During deposition, density, structure, and texture fluctuate with fluctuating wind velocity, changing rate of snowfall, changing shape of snow flakes, changing absolute and relative humidity, and changing temperature. Sublimation metamorphism and densification due to gravitation have an initially homogenizing influence, but layering long remains a source of significant anisotropism.

It would be surprising if pressure metamorphism did not produce a structural anisotropism. In creep densification under lateral confinement, for instance in a layer under the load of the overlying snow, the principal stresses are unequal ($\sigma_z > \sigma_x = \sigma_y$). The spatial network of grains developed under this condition is unlikely to be isotropic.

No further reference to anisotropism will be made in the following discussion of snow mechanics because no useful quantitative data have been found in the literature. There can be little doubt, however, that it will loom large in the further development of this science.

It has been found to be almost impossible to obtain or prepare identical snow specimens for laboratory investigation. Quantitative differences in behavior of apparently similar samples, all taken from a natural snow layer, or of specimens of carefully prepared reconstituted snow are very disturbingly large.²⁶

f) Snow type in creep mechanics. The concept of snow type as defined by giving values of density, grain size, permeability, viscosity, etc. breaks down in creep mechanics unless times and deformations are very small, because all these parameters change.

One begins with a given snow type, but ends up with another after the snow has gone through a process of continuous change, at best only mass remaining constant. In snow, as in ice, deformation-time curves (at constant strain) always show an initial transient section with rapidly decreasing creep rate. In ice the curve often straightens out to permit determination of a steady creep rate, but rarely so in snow, where structural changes, particularly grain growth and increasing density constantly lower the creep rate. It becomes necessary to introduce the concept of a continuous time sequence of events occurring in a mass with constantly changing properties, which has not yet been done systematically.

Types of Mechanical Behavior

We can conveniently distinguish between four distinct classes of snow mechanics:

1) Collapse mechanics. Ultimate strength in tension, compression, and shear is given by the stresses causing structural collapse. Here the characteristic feature is sudden loss of cohesion, breaking of the bonds between grains, with or without the development of cracks. In tension and pure shear, the snow mass often breaks in one plane; in compression it sometimes crumbles, but, when unconfined, often shows the conical failure indicating shear surfaces. Disaggregation is an important absorber of energy in snow removal.

2) Flow mechanics. The characteristic phenomenon is continuing rapid deformation after structural collapse. The rigid units are individual grains, or groups of grains forming lumps of different size, which in dry snow often break up further during flow, but in wet snow can re-aggregate to larger coherent masses. In flow, energy is absorbed by dynamic friction between rigid units, by their acceleration, and by further fracture to smaller units. Flow mechanics is involved in rapid sliding along shear planes within a snow mass, produced for instance by failure of abutments; in avalanches of all types; in snow plowing; in crushing of snow under excessive load, by men on foot or skis and by oversnow vehicles; by penetrating hardness-measuring instruments; by ramming of foundation piles; also often in sliding contact between snow and other objects, such as skis, snow shovels, plow blades, and avalanche slope terrain.

Snow is a highly efficient absorber of shock energy, which is largely spent locally in disaggregation and densification by fast flow.

A special type of flow is encountered in loose snow avalanches and rotary snow plowing, where the snow particles are more or less suspended in a fast flowing air stream, which because of low internal friction behaves to some extent like a heavy gas.

3) Creep mechanics. This is deformation under stresses smaller than those leading to structural collapse. The characteristic feature is that there is no rapid change of cohesion.

4) Elasticity mechanics. Here the elastic properties of the mass dominate. We are interested in response to rapid stress changes, primarily wave propagation following explosions for construction and demolition or for seismic sounding.

We will now discuss snow mechanics in more detail, where possible.

1) Collapse Mechanics

The value of strength, expressed in terms of stress (per unit area) measured just before more or less sudden failure of test specimens, must be applied with caution to problems of failure of objects of different size and shape under different stress conditions. In the following discussion of strength, the main interest is in relative value, in the functions rather than in specific values of parameters.

a) Tensile strength. The effect of temperature on tensile strength is not well formulated. Practically the only data available are given in Figures 21 and 22, which show a strong effect for fine-grained snow, and a weak one for coarse-grained snow. Between -10C and -30C, a strength gradient of some -2 1/2 % per 1C does not fit badly to fine-grained snow; it becomes larger at high temperature and smaller at low temperature. The figures show the strong effect of density, but this is better illustrated by determination⁸ made at Site 2, Greenland (77N 56W) in a deep snow-cover sequence. In-situ snow temperature is -24.5C, and the densest snow is from 30 m depth and 40 years old. Tests by three methods, described in reference 8, were made at -10C and corrected to -10C by -2 1/2 % per 1C. Figure 23 summarizes the results. The following equation,⁸ relating strength to density at -10C, will also be useful for shear and crushing strength:

$$\sigma = a \Delta \gamma \left[1 + b (\Delta \gamma)^2 \right] \quad (5)$$

$$\Delta \gamma = \gamma - \gamma_0$$

$\sigma = \sigma_T$ = tensile strength at -10C (by ring test³¹), in psi (multiply σ by 70.3 to obtain g/cm²)

$$a = 503$$

$$b = 2.88$$

$$\gamma_0 = 0.37 \text{ g/cm}^3$$

$$\gamma > 0.4 \text{ g/cm}^3.$$

It would be surprising if the parameter given for the tensile strength equation for the high-density fine-grained Site 2 snow were applicable to snow from other areas, but the variation may not be very large. A tensile strength versus density diagram for lower density snows (Fig. 24) shows a very large scatter.

b) Shear strength. Shear strength of snow is very similar to tensile strength, and, although the numbers given below indicate a lower shear strength, we must nevertheless assume that tensile strength is lower than shear strength, because cylinders in torsion fail with helical fracture surfaces characteristic of tension failure.⁸ The discrepancy can be attributed to test techniques, as described in references 2, 7, 8, 31

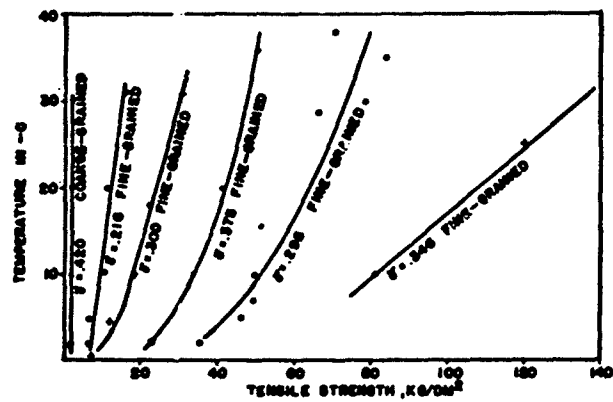


Figure 21. Tensile strength of snow as a function of temperature. (From Bucher, ref. 6).

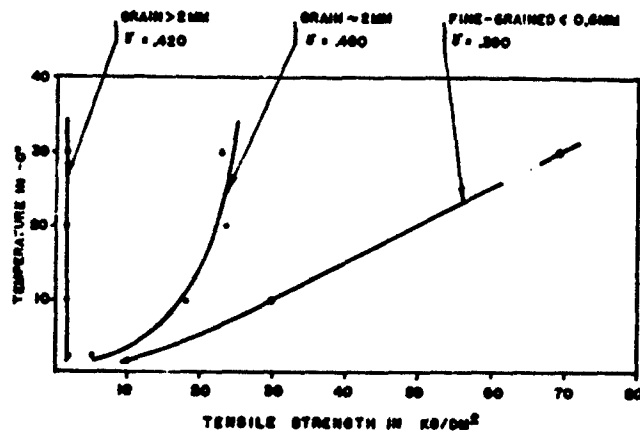


Figure 22. Effect of temperature on tensile strength of snow of different grain sizes. (From Bucher, ref 6).

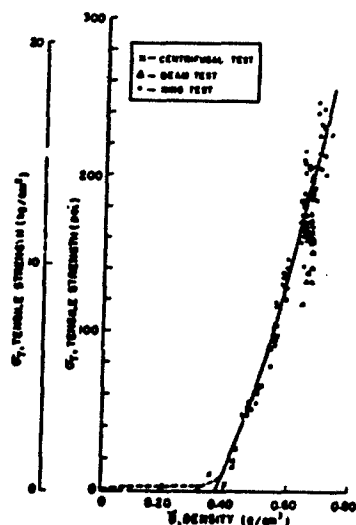


Figure 23. Tensile strength of snow versus density. Site 2, Greenland. (From Butkovich, ref. 8).

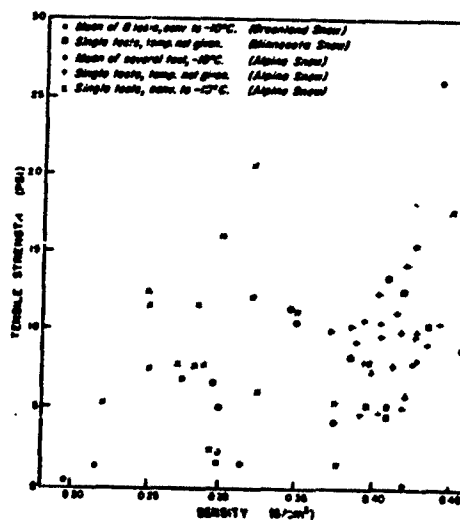


Figure 24. Tensile strength versus density for low density snows. Measurement by centrifugal method.

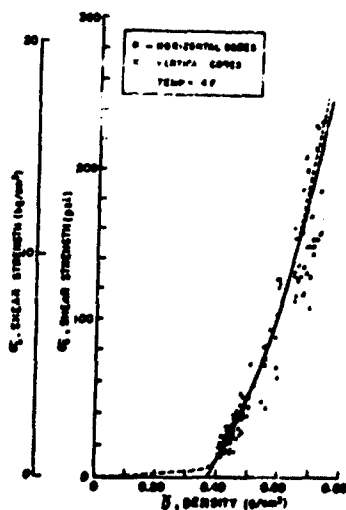


Figure 25. Shear strength of snow versus density. Site 2, Greenland. Measured by shearing out the central section of a cylinder (double shear). (From Butkovich, ref. 8).

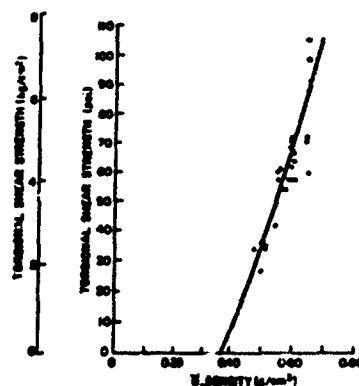


Figure 26. Torsional shear strength of snow versus density. Site 2, Greenland. (From Butkovich, ref. 8)

Figure 25, again of tests made at Site 2, Greenland, shows the relation of shear strength to density. Equation 5 now applies as follows:

$\sigma = \sigma_0$ = shear strength at zero normal pressure in psi at -10C

$a = 333$

$b = 7.04$

$\gamma_0 = 0.37 \text{ g/cm}^3$

$\gamma > 0.4 \text{ g/cm}^3$.

A graph of values of shear strength plotted against density for low-density snow would be very similar to Figure 24. Torsional shear strength of high-density snow was also determined at Site 2, with results shown in Figure 26. The parameters of eq 5 are:

σ = torsional modulus of rupture, in psi . -10C

$a = 230$

$b = 5.73$

$\gamma_0 = 0.37 \text{ g/cm}^3$

$\gamma > 0.5 \text{ g/cm}^3$.

Since the cylinders break on 45-degree helical surfaces, the failure is in tension. Here tensile stress, compressive stress, and shear stress are all equal. The larger difference in values of tensile strength calculated from torsional and ring tests may be due to the difference in general stress distribution.

Using soil mechanics terminology, shear strength at zero normal pressure is often called cohesion.

Shear strength increases when pressure (less than the crushing strength) is applied normal to the plane of failure. Figure 27 shows the effect of pressure on the shear strength of Site 2 snow, the curves corresponding to the following parameters of eq 5:

Normal pressure	a	b	γ_0
0	330	7.04	0.37
30 psi	558	5.44	0.37
60 psi	643	6.13	0.37

Figure 28, giving shear strength versus normal pressure at constant density is important in showing that Coulomb's equation (linear Mohr envelope) is not applicable to cohesive snow. But if the grain bonds are broken by structural collapse, and tests are made before strong new bonds form, we have a material behaving somewhat like sand and the Mohr envelope straightens out.⁵ Figure 29a is for coarse-grained disaggregated snow, where new grain bonds develop slowly; Figure 29b is for fine-grained snow, where they develop quickly. Coulomb's law is used in snow engineering, for instance in avalanche mechanics, and in relation to performance of oversnow vehicles, but is of highly doubtful value to theoretical development. Coulomb's law states that the shear strength is equal to the cohesion plus the product of normal pressure and the tangent of the angle of internal friction.

c) Crushing strength (unconfined uniaxial compressive strength). Testing is usually done on cylindrical specimens with length-to-width ratio larger than 2. Loading rate should be high to minimize densification before failure. Figure 30 summarizes the Site 2 tests. Equation 5 simplifies to

$$\sigma_c = 1418 (\gamma - 0.39), \gamma > 0.4$$

where σ_c = crushing strength at -10C in psi.

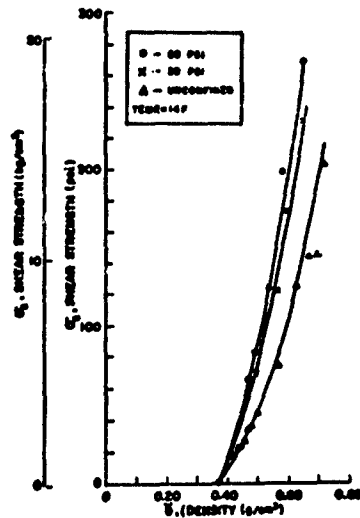


Figure 27. Effect of normal pressure on shear strength of snow. (From Butkovich, ref. 8).

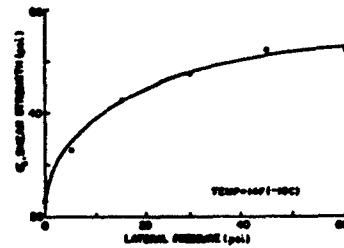


Figure 28. Shear strength versus normal pressure for a snow of density $\gamma = 0.45$. Each point is mean of 10 tests. (From Butkovich, ref. 8).

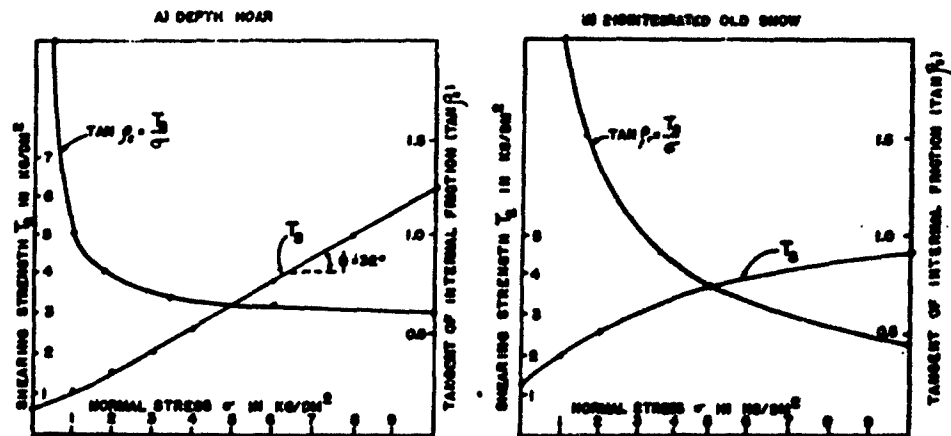


Figure 29. Shear strength and apparent internal friction ($\tan \phi_s$) of two snow types. (From Bader *et al.*, ref. 2)

Conical failure is often noticed in high-density snow, while low-density snow, which is very weak in compression and less homogeneous, fails along irregular surfaces with local crumbling. Comparison of Figures 23 and 30 shows that tensile strength is close to one-half of the crushing strength, which is not surprising because in uniaxial compression the maximum shear stress is approximately half of the compressive stress, and shear and tensile strengths are similar.

Both in nature (snow in an avalanched deposit) and in technology (compacted snow as a construction material) we encounter the phenomenon of age hardening of reconstituted snow. The term reconstituted snow is here used to designate a material produced either by collapse of a cohesive snow structure by rapid deformation, or by redeposition of disaggregated snow. Immediately after its formation, reconstituted snow has very low strength, but it gains strength with time, ultimately attaining approximately that of slowly compressed snow of equal density.

Crushing strength of reconstituted snow as a function of time approaches a maximum value exponentially:¹⁷

$$\sigma_t = \sigma_m - (\sigma_m - \sigma_0)e^{-kt} \quad (6a)$$

σ_t = crushing strength at time t

σ_m = maximum attainable crushing strength

σ_0 = crushing strength at $t = 0$

k = rate coefficient.

The longer it takes for σ_t to reach a given fraction of σ_m , the smaller the value of k , which immediately suggests that the rate coefficient is temperature dependent according to eq 1. The lower the temperature, the smaller the rate of strength increase. The rate of age hardening is accelerated by temperature gradient and pressure, by any process which stimulates internal vapor transfer. In engineering practice (compacted snow roads, trench roofing) it usually takes several days for σ_t to reach $\frac{1}{2} \sigma_m$ at temperatures around -10°C .

d) Compressive strength. For low-density snow, the compressive strength under lateral confinement (for instance axial stress on a snow cylinder filling a rigid tube) is little greater than the corresponding unconfined crushing strength, but the difference increases with density according to a function which has not been determined. It is unlikely that any existing theory relating failure in compression to the value of the principal will be useful for low-density snow. The collapse of a snow structure by failure of individual bonds locally and in rapid sequence, with development of high stress concentrations, destructive shock waves etc., strongly suggests that it will be very difficult to depart from use of purely empirical relations, and a great amount of experimental work will have to be done before such can be formulated.

If a low-density snow is fairly rapidly compressed in a cylinder by a piston in uniform motion, it reacts by collapse in several steps, until the density reaches about 0.5 g/cm^3 . At each collapse stage, there is a sudden loss of piston pressure, followed by a continuous increase. After reaching a density around 0.5, the snow grains are in close packing; the stress then increases very rapidly, as further densification requires deformation of an increasing number of grains. Here we change from a discontinuous process of collapse by breaking of grain bonds to a continuous one of frictional flow.

If an object, such as a plate, is pressed into a large snow mass at a uniform rate, the processes of densification by collapse and flow are both active. The stress in the snow decreases with distance from the plate because it is distributed over increasing areas of the pressure bulb. Collapse takes place in successive thin layer increments as the stress reaches the compressive strength in each, while collapsed layers begin to densify by frictional flow at high pressures. Stepwise collapse is well illustrated by Figure 31, a stress penetration curve for a plate moving at 2 cm/min .¹⁷ The shaded area of

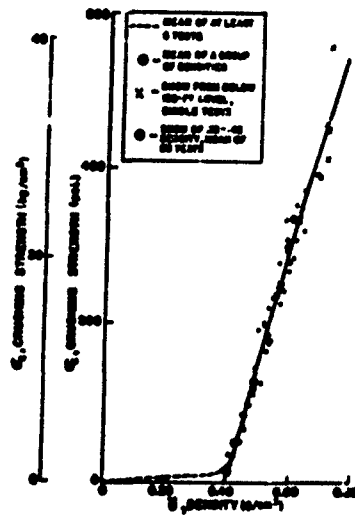


Figure 30. Crushing strength of snow versus density. Site 2, Greenland. (From Butkovich, ref. 6).

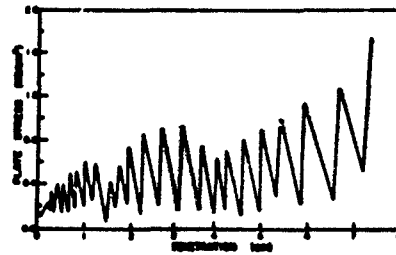


Figure 31. Stress versus plate penetration in snow. Repeated structural collapse in small increments. (From Landauer and Royce, ref. 27).

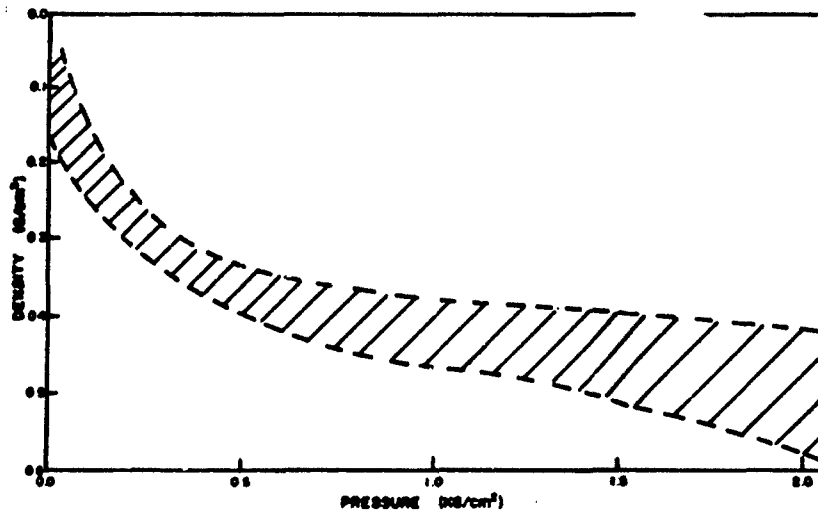


Figure 32. Resistance to compressive collapse (under frictionless lateral confinement) of new snow. Shaded area is range of densities corresponding to given pressure. Initial snow density $0.06 < \gamma < 0.16$. (From Bocher and Roch, ref. 7).

Figure 32 indicates the range of densities to which new snows are compressed by collapse under lateral confinement and negligible lateral friction.⁷ The behavior at -2C of five samples of original density lying between 0.06 and 0.16 g/cm³ falls within the shaded area. Careful work with pressure plates should make it possible to define the limits of the pressure bulb (within which the snow is disturbed). The slow increase of stress with penetration indicates that the diameter of the pressure bulb increases only slowly with distance from the plate. Figures 33 and 34 show the development of essentially conical pressure bulbs in low-density snow,³⁷ reflecting the weakness of shear resistance. In contrast to this, wet snow (Fig. 35) appears to have a high ratio of shear to compressive strength, and a very low viscosity.

e) Work of disaggregation. This is the minimum work that has to be done to break up a unit volume or mass of snow into its individual grains. It applies only to low-density snow ($\gamma < 0.55$), which can be disaggregated without significant grain breakage. Measurements are made by slowly moving a snow cylinder against a slowly revolving spiked wheel and measuring the torque and the rpm.⁸ Figure 36 gives the work of disaggregation for Site 2 snow. Eq 5 can again be used.

e = work of disaggregation in lb/in³

$a = 1.20$

$b = 65.12$

$\gamma_0 = 0.37$

$\gamma < 0.55$.

Hard high-density snow cannot be disaggregated without significant grain breakage. The concept of minimum work of disaggregation then becomes meaningless.

Technical note: It is well known that large rotary snowplows with disaggregators to break up the snow, can process very much less hard snow than soft snow; yet the work of disaggregation is almost negligibly small, requiring, according to the above equation, only 2.3 hp for 1 yd³/sec of 0.5 density snow.

f) High speed collapse mechanics is technically important in snow removal, compaction of snow by moving vehicles, avalanche effects, and explosions in snow. At high speed (meters per second), compressibility and flow of interstitial air, snow-mass inertia, and fast frictional flow become important. This branch of snow mechanics is almost completely undeveloped.

A single significant published paper was found.³⁸ An instrumented, heavy guided cylinder was dropped into snow. The pertinent observations are that the resistance to penetration at velocities of meters per second oscillates (frequency of the order of milli-seconds), and that the pressure bulb shows alternating high- and low-density layers, as illustrated in Figure 37, indicative of a shock wave (with interference phenomena) travelling faster than the penetrating object. It is obvious that analysis must await more experimental work.

2) Flow mechanics

There are insufficient quantitative data available to permit a fruitful exposition of flow mechanics. The only subject on which we have an appreciable volume of publications is marginal to flow mechanics, because in most cases a surface layer only a few grains thick is involved. This is friction of skis on snow, and here the scatter of data and diversity in procedure are so large that one cannot formulate a good theory of friction between solids and snow. Only a few general conclusions are worth summarizing.

a) The coefficient of kinetic friction (ratio of tangential to normal force) of relatively smooth solid surfaces on snow varies mainly between 0.01 and 0.1 but can be

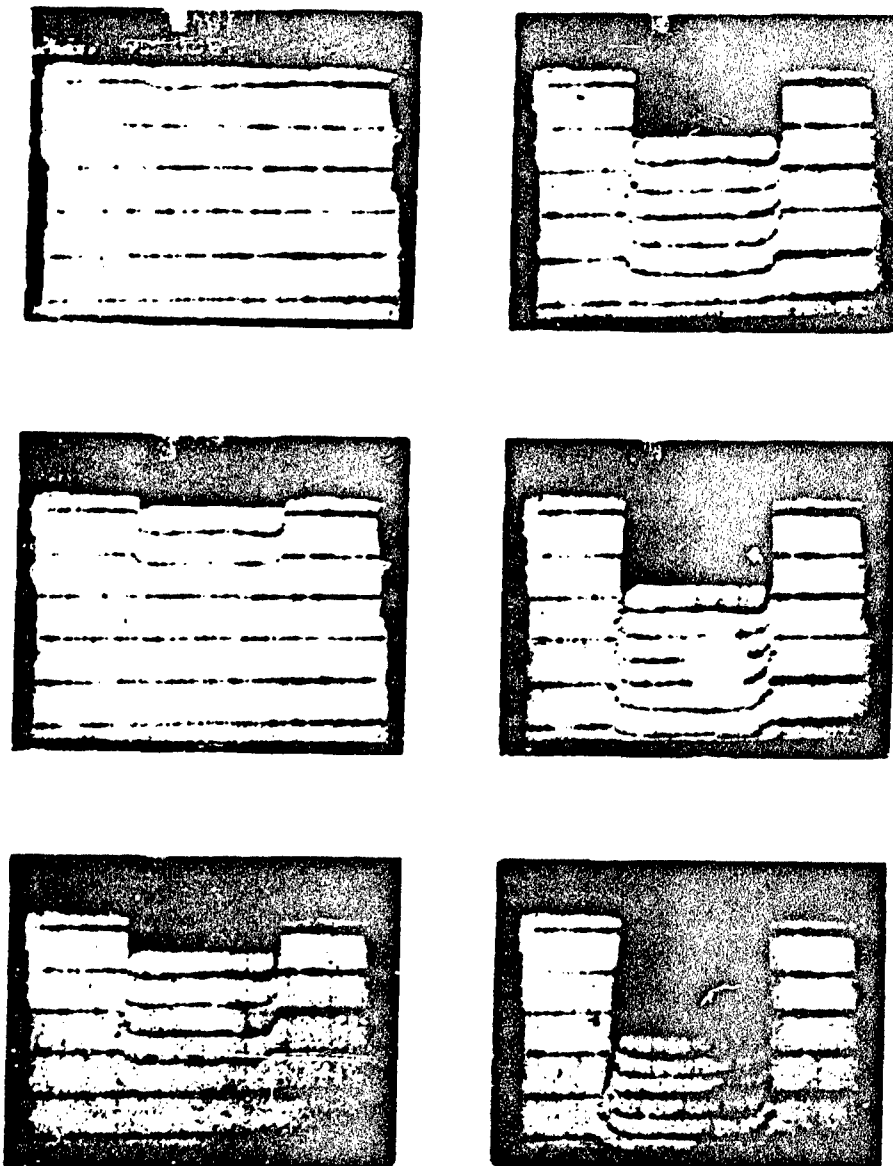


Figure 33. Collapse compression of new snow $\gamma_0 = 0.07$ at -2.5°C .

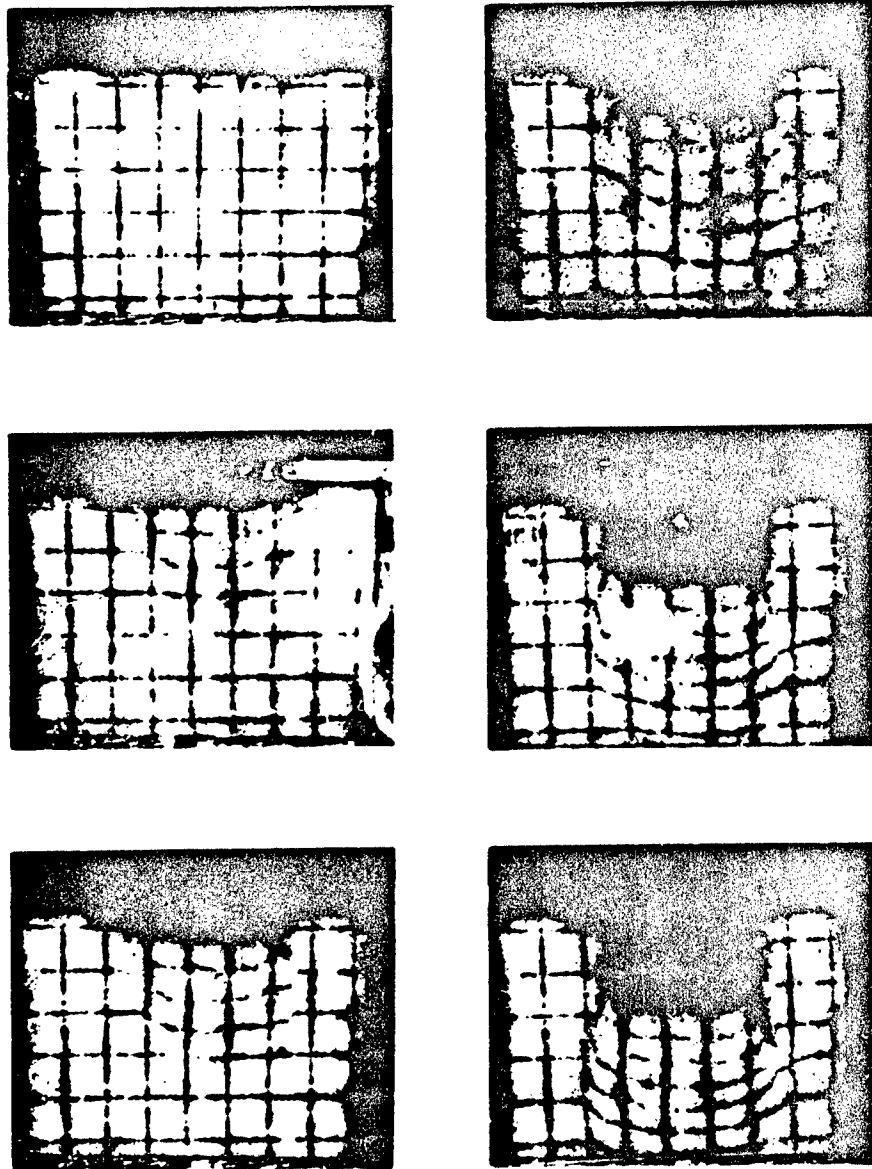


Figure 34. Collapse compression of granular snow, $\gamma_0 = 0.32$ at $-3C$.

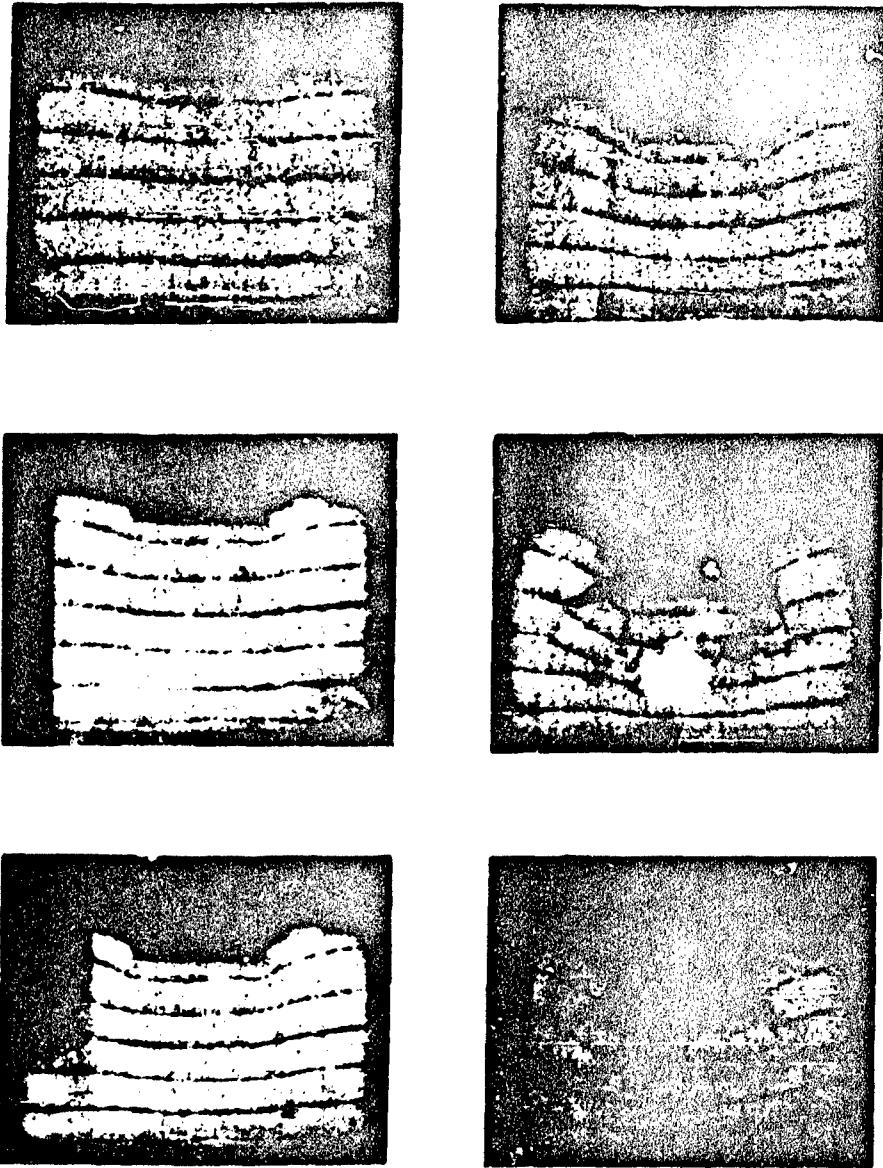


Figure 35. Collapse compression of wet snow.
Meaning of numbers as in Figure 33.

larger. Increasing the degree of solid surface smoothness of non-metallic substances, such as wood, plastics, glass, reduces friction, but not necessarily so for metals.

b) Hydrophobic coatings reduce friction on wet snow, but to a much smaller degree on dry snow.

c) Friction on coarse-grained snow is lower than on fine-grained snow.

d) The coefficient decreases with increasing normal load.

e) The coefficient increases with decreasing temperature.

f) The coefficient increases with velocity, but probably less than linearly.

There is little doubt that the low coefficient of sliding friction results from lubrication by melt water produced by frictional heating, and not by pressure melting.

Figures 38 and 39 summarize the only data available for dynamic friction of snow on snow.⁷ The snow was wet and hard, with a density of from 0.5 to 0.6. The salient feature is an increase of friction with velocity at constant normal pressure, and an increase with normal pressure at constant velocity.

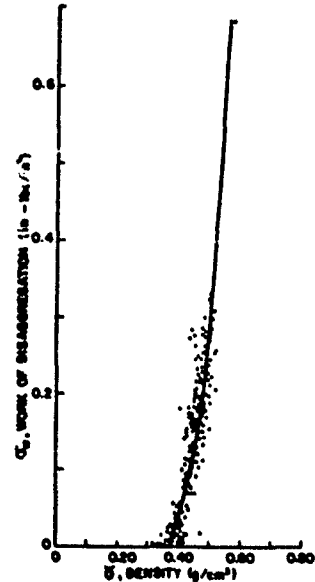


Figure 36. Minimum work of disaggregation per unit volume of snow versus density. Site 2, Greenland. (Butkovich, ref. 8)

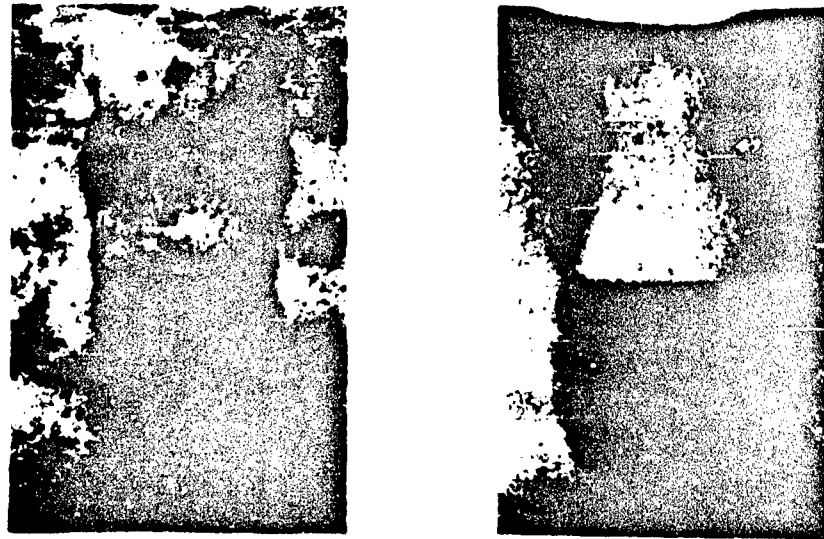


Figure 37. High speed collapse compression of snow. Left: Spray figure showing dark high density layers in pressure bulb. Right: Shade figure of same pressure bulb. (From Yosida, *et al.*, ref. 38)

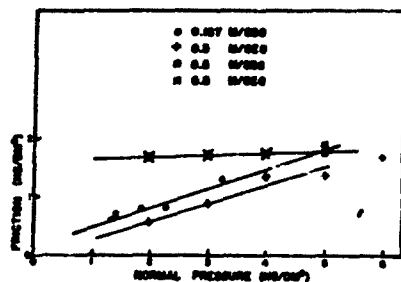


Figure 38. Dynamic friction of snow on snow versus normal pressure on contact area. Hard, wet snow.
(From Bucher and Roch, ref. 7)

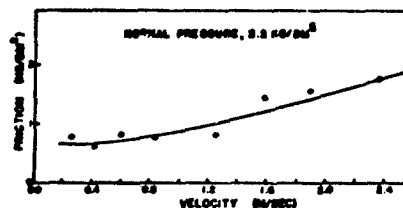


Figure 39. Dynamic friction of snow on snow versus velocity of relative motion of contact areas. Hard, wet snow.
(From Bucher and Roch, ref. 7).

The important natural processes and technologies involving flow for larger masses of snow presently have no theoretical basis worth mentioning.

3) Creep mechanics

In classical mechanics of solids, especially of construction materials, a detectable rate of creep is often considered to be a failure. Not so in snow, where relatively very high creep rates are often tolerable in engineering practice. It becomes reasonable to identify failure with collapse rather than with creep.

By creep, as already stated, we will understand deformation under stresses smaller than those causing structural collapse. Creep mechanics deals with the relations between stress, strain, and time.

Rheologically, snow is a non-Newtonian, visco-elastic substance. It is viscous because it will require permanent time-controlled deformation even at very small stresses; elastic because there is a time-independent deformational component recoverable upon stress release, and non-Newtonian because the strain rate is not a linear function of stress. Strain rate ($\dot{\epsilon}$) increases faster than stress (σ), with the important characteristic that it remains practically constant for stress values up to about 600 g/cm² (8½ psi). Since this is also close to the maximum shear strength of low-density snows, these can be considered Newtonian with respect to viscosity. The scatter of experimental creep data obtained from highly stressed high-density snow is such that the choice of one power series in preference to another cannot be made with great confidence. At the present time, a hyperbolic sine function is gaining favor, because it fits the data rather well, and is supported by theoretical considerations²⁰ based on activation kinetics. The hyperbolic sine is also easier to handle analytically than finite power series.

We can therefore write:

$$\dot{\epsilon} \propto \sigma_0 \sinh \frac{\sigma}{\sigma_0} \quad (7)$$

To obtain some insight into the nature of the function, we write it as a series

$$\sigma_0 \sinh \frac{\sigma}{\sigma_0} = \sigma \left(1 + \frac{(\sigma/\sigma_0)^2}{3!} + \frac{(\sigma/\sigma_0)^4}{5!} + \dots \right)$$

and see that the first term σ dominates (i. e., the viscosity is almost Newtonian) when σ/σ_0 is small.

The series can also be written as

$$\sigma_0 \sinh \frac{\sigma}{\sigma_0} = \frac{\sigma_0}{2} \left(e^{\frac{\sigma}{\sigma_0}} - e^{-\frac{\sigma}{\sigma_0}} \right)$$

where we see that the influence of the second term is small when σ/σ_0 is large; the function then becomes exponential. Since σ/σ_0 must be a real number, σ_0 has the dimension of a stress. A value of about 700 g/cm² (10 psi) has been derived from experiments.²⁵

In Figure 40 we have plotted the following functions:

$$y = \sigma$$

$$y = 700 \sinh \frac{\sigma}{700}$$

$$y = 350 \exp \frac{\sigma}{700}$$

If we are willing to accept a 10% error limit, which is quite reasonable, we can in principle handle any problem where stresses do not exceed 600 g/cm² on the basis of direct proportionality between stress and strain rate, and when stresses are always above 800 g/cm² we can assume proportionality of strain-rate to an exponential function of the stress, which simplifies expression and calculation. For stresses larger than 1000 g/cm² the error drops less than 1%.

Let us now consider the creep properties of a given snow. In order to minimize the effect of density change, total strain must be kept very small. Here a delicate piece of work²⁷ allows an analysis of fundamental creep behavior. A cylinder of relatively new snow of density 0.19 was subjected at -9°C to a uniaxial surcharge stress of 10⁴ dynes/cm² (10 g/cm²) for 7 minutes, and then the surcharge was removed.

Figure 41 shows the result after subtracting the effect of the weight of the snow cylinder by a satisfactory method. When applied stresses are so small that the proper weight of the snow sample cannot be neglected, it can be assumed that there exists a vertical force equal to $\frac{1}{3}$ of the proper weight.²⁵ The behavior is interpretable by a rheological model consisting of single Maxwell and Voigt units in series, as shown in Figure 42.

- 1) Instantaneous elastic strain (O to A in Fig. 41) corresponds to compression of the Maxwell spring.
- 2) Decreasing strain rate (A to B) "transient creep" corresponds to the sum of constant viscous flow in the Maxwell dashpot and decreasing viscous flow in the Voigt dashpot as the Voigt spring is compressed.
- 3) Constant strain rate (B to C) "steady state creep" corresponds to viscous flow in the Maxwell dashpot alone, after the Voigt spring has picked up practically the full load.

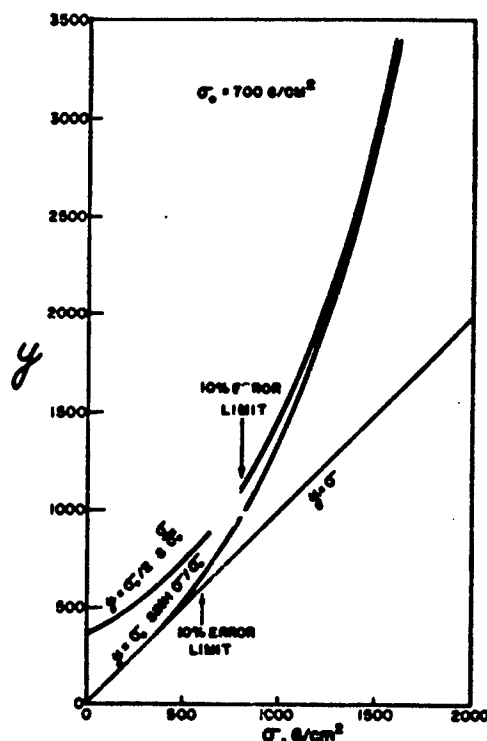


Figure 40. Graph of stress effect functions.

$$y = \sigma$$

$$y = \sigma_0 \sinh \frac{\sigma}{\sigma_0} \text{ for } \sigma_0 = 700$$

$$y = \frac{\sigma_0}{2} \exp \frac{\sigma}{\sigma_0} \text{ for } \sigma_0 = 700$$

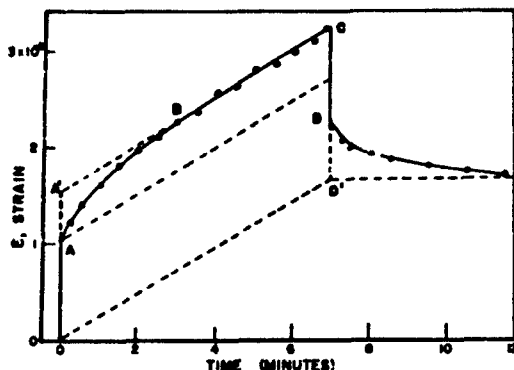


Figure 41. Strain, parallel to uniaxially applied constant stress, versus time. Stress removed at $t = 7$ min. Snow density $\gamma = 0.19$, temperature -9°C . (From Yosida et al., ref. 37)

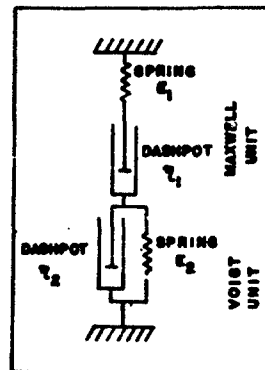


Figure 42. Rheological model for behavior shown in Fig. 41. Maxwell and Voigt rheological units in series. (From Yosida et al., ref. 37)

4) Instantaneous complete recovery (C to D) of original elastic strain (OA) upon stress release corresponds to stretching of Maxwell spring.

5) Slow recovery (D to D') of the strain component (AA'), "elasto-viscous aftereffect" corresponds to relaxation of the Voigt unit.

In terms of the snow structure, it can be visualized that the Maxwell unit represents the behavior of the aggregate as an ideal highly viscous Newtonian fluid, while the Voigt unit represents the complications arising from interference at groups of neighboring grains, where local stresses and strains are constantly changing as the grains move with respect to one another.

The same model has been applied also to the behavior of granular ice at low stress.¹⁸ It must be pointed out, however, that rheologists have developed much more sophisticated theories of visco-elastic behavior.

The Maxwell rheological unit corresponds to the following relation between stress σ , strain ϵ_1 , time t , elastic modulus E_1 , and viscosity η_1 .*

$$\epsilon_1 = \frac{\sigma}{E_1} + \frac{\sigma t}{\eta_1} \quad (8)$$

The first term is OA in Figure 41 and the second the vertical distance from A' to C.

Here for constant stress there is a constant strain rate $\dot{\epsilon} = \partial \epsilon / \partial t$ given by the slope of BC. This is Newtonian flow.

$$\dot{\epsilon}_1 = \frac{\sigma}{\eta_1} \quad (9)$$

The transient creep term is introduced by the Voigt unit

$$\epsilon_2 = \frac{\sigma}{E_2} \left(1 - e^{-\frac{t}{\tau}} \right) \quad (10)$$

where $\tau = \eta_2 / E_2$ is the "retardation time."

The value of the exponential term decreases rapidly, so that $AA' \rightarrow \sigma / E_2$.

*Note that this coefficient is twice that of dynamic viscosity relating to shear, since Poisson's ratio is close to zero here.

The Voigt creep rate is

$$\dot{\epsilon}_2 = \frac{\sigma}{\eta_2} e^{-\frac{t}{\tau}} \quad (10a)$$

The total creep is:

$$\epsilon = \epsilon_1 + \epsilon_2 = \frac{\sigma}{E_1} + \frac{\sigma t}{\eta_1} + \frac{\sigma}{E_2} \left(1 - e^{-\frac{t}{\tau}}\right) \quad (11)$$

and the creep rate

$$\dot{\epsilon} = \dot{\epsilon}_1 + \dot{\epsilon}_2 = \frac{\sigma}{\eta_1} + \frac{\sigma}{\eta_2} e^{-\frac{t}{\tau}} \quad (12)$$

The second term of eq 12 reflects the transient creep rate, which rapidly decreases with time.

At time t_0 , when the load is removed, the stress on the Voigt spring is σ_0 .

$$\sigma_0 = \sigma \left(1 - e^{-\frac{t_0}{\tau}}\right) \quad (12a)$$

The strain recovery by elasto-viscous aftereffect (DD' in Fig. 41) takes place at the decreasing rate $-\dot{\epsilon}_3$.

$$-\dot{\epsilon}_3 = \frac{\sigma_0}{\eta_2} e^{-\frac{t-t_0}{\tau}} \quad (13)$$

and the total recovery at time $t > t_0$ is

$$-\epsilon_3 = \frac{\sigma_0}{E_2} \left(1 - e^{-\frac{t-t_0}{\tau}}\right) \quad (14)$$

If, at time t_0 , the plate exerting the constant stress σ had been locked in relation to the base of the vertical snow cylinder, the stress acting on the plate would have begun to decrease by relaxation. The rate of stress decrease should be

$$\dot{\sigma}_r = \frac{\partial \sigma_r}{\partial t} \quad \text{at constant strain } \epsilon_0.$$

We use eq 11 and obtain, at time $t_0 + \Delta t$

$$\dot{\sigma}_r = - \frac{\epsilon_0 \left(\frac{1}{\eta_1} + \frac{1}{\eta_2} e^{-\frac{\Delta t}{\tau}} \right)}{\left[\frac{1}{E_1} + \frac{\Delta t}{\eta_1} + \frac{1}{E_2} \left(1 - e^{-\frac{\Delta t}{\tau}}\right) \right]^2} \quad (15)$$

The stress itself is:

$$\sigma_r = \frac{\epsilon_s}{\frac{1}{E_1} + \frac{\Delta t}{\eta_1} + \frac{1}{E_2} \left(1 - e^{-\frac{\Delta t}{\tau}}\right)} \quad (16)$$

The validity of the rheological model has not been tested by experimental verification of eq 15 and 16.

In the example shown in Figure 41, the parameters are as follows:

$$\begin{aligned} E_1 &= 0.96 \times 10^7 \text{ dyne/cm}^2 \\ E_2 &= 1.92 \times 10^7 \text{ dyne/cm}^2 \\ \eta_1 &= 2.45 \times 10^9 \text{ dyne-sec/cm}^2 \text{ (poises)} \\ \eta_2 &= 9.80 \times 10^8 \text{ dyne-sec/cm}^2 \text{ (poises)} \\ \tau &= 51 \text{ sec.} \end{aligned}$$

For fine-grained ice at -10C we find values of the following orders of magnitude:¹⁸

$$\begin{aligned} E_1 &\approx 10^{10} & \eta_1 &\approx 10^{14} \text{ poises} \\ E_2 &\approx 10^{11} & \eta_2 &\approx 10^{13} \text{ poises} \\ & & \tau &\approx 10^4 \text{ sec.} \end{aligned}$$

This shows the tremendous change in parameter values to be expected as snow density, structure, and texture change with time and deformation. Here is one of the greatest obstacles to the development of a general theory of creep mechanics of snow. Another, which has already been touched upon, is the paralyzing effect of varying freedom of grain movement within the snow structure on formulation of creep behavior under combined stresses.

Classical theory of creep deformation of solids formulates the relations between stress condition and pure shear strain, incompressibility being (except for Poisson effects) an essential premise. Hence an incompressible body cannot deform under hydrostatic stress condition because shear stresses vanish when the principal stresses become equal. But snow does deform under hydrostatic stress, reacting by a permanent change of volume, densifying apparently according to exactly the same laws applying to creep by shear.²⁴

The modification of classical theory to account for hydrostatic "densification creep" has not been seriously attempted. It is not known, for instance, whether the concept of hydrostatic component ($\frac{1}{3} \Sigma \sigma_i$) remains at all meaningful.

The modified theory will also have to account for a phenomenon which emerged early in snow mechanics:² the fact that rate of elongation under uniaxial tension is much smaller than the rate of shortening under equal compression (Fig. 43).

The significance of this difference in creep rate is accentuated by the small reduction of density during elongation (for instance 3.5% for an elongation of 16.6%² against large densification during compression. It is clear that eq 2, a very strong function, is not valid when the dominating principal stress is tensile and strains are large, which could introduce an insurmountable difficulty into general theory. But eq 2 does apply for small strains, in snows of different densities, in tensile creep. It may also be possible to reconcile the difference between tensile and compressive creep rates by introducing a "shrinkage stress" σ'_s as shown in Figure 44. σ'_s is a tensile stress required to prevent a virtual densification, which is conceived to be taking place during subjection of snow to compressive or tensile stress, but not during a condition of no applied stress. If σ is a uniaxial stress, then the creep rate in compression under $\sigma - \sigma'_s$ is approximately equal to that in tension under $\sigma + \sigma'_s$.

Figure 45 illustrates another frustrating aspect of creep mechanics. It is a new plotting of old data²⁵ on creep under uniaxial stress. Two samples, one of compacted

new snow, the other of compacted old snow, were subjected to increasing, high compression in steps. It is noteworthy that at very high creep rates ($\dot{\epsilon} \approx 10^{-4}$ to 10^{-5} sec $^{-1}$)

a) the exponent multiplier b of eq 2 decreases with increasing stress

b) The hyperbolic sine law (eq 7) may not be valid. If it is valid, then σ_0 will be much larger than the 10 psi previously quoted.

The range of creep rate within which relations 2 and 7 are valid is not known, but most probably includes the maximum deformation rates tolerable in snow engineering (foundations, excavations in snow, and snow roofs). That it does include natural densification creep over the whole range of snow densities in the very deep snow cover of polar glaciers is shown in Figure 46. The points are measured densities at the indicated depths below the surface. The curve was calculated¹ on the basis of validity of the hyperbolic sine law of stress dependence (eq 7, $\sigma_0 = 663$ g/cm 2) and the exponential law of density dependence (eq 2, $b = 21.05$). This theory fails at $\gamma > 0.84$ g/cm 3 , $\sigma > 5$ kg/cm 2 ; but then we no longer have permeable snow, but rather porous ice.

The fact that for the deep pit at Wilkes, Antarctica ($66\frac{1}{2}^\circ$ S, 112° E) the theoretical curve fits well down to $\gamma > 0.9$ g/cm 3 (Fig. 46) indicates that it is the hyperbolic sine law which fails at $\sigma > 5$ kg/cm 2 . At Wilkes $\sigma = 4.3$ kg/cm 2 for $\gamma = 0.9$, σ_0 is the same as at Site 2, Greenland, but $b = 15.77$. The creep rate of snow appears to be highly sensitive to change of rate of stress application (second derivative of stress with respect to time). Samples taken from natural snow that had been subjected to a slowly increasing load for decades³ showed an increase in creep rate of the order of 10^6 when

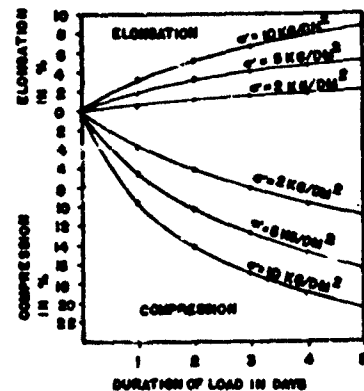


Figure 43. Comparison of creep under uniaxial tension and compression for different stresses. (From Bader et al., ref. 2)

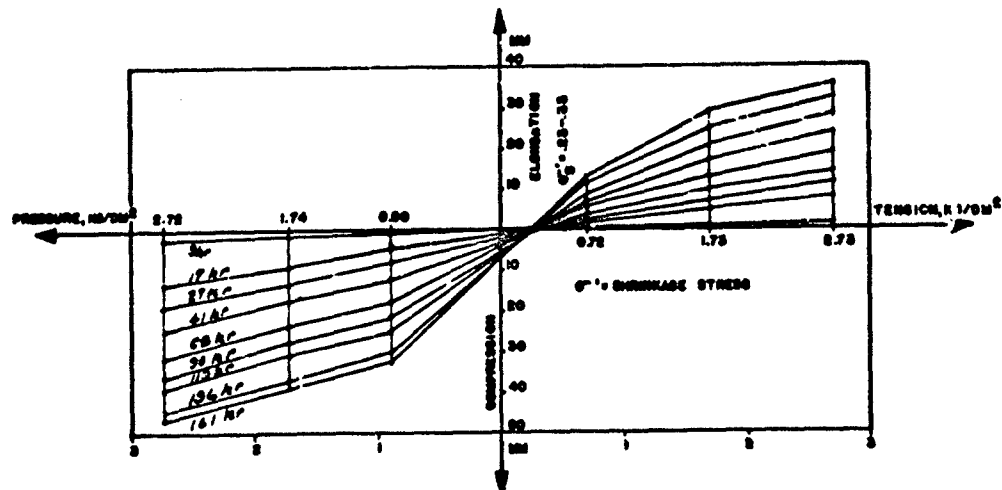


Figure 44. Change in length of cylindrical snow samples versus stress, at different elapsed times. (From Bucher, ref. 6).

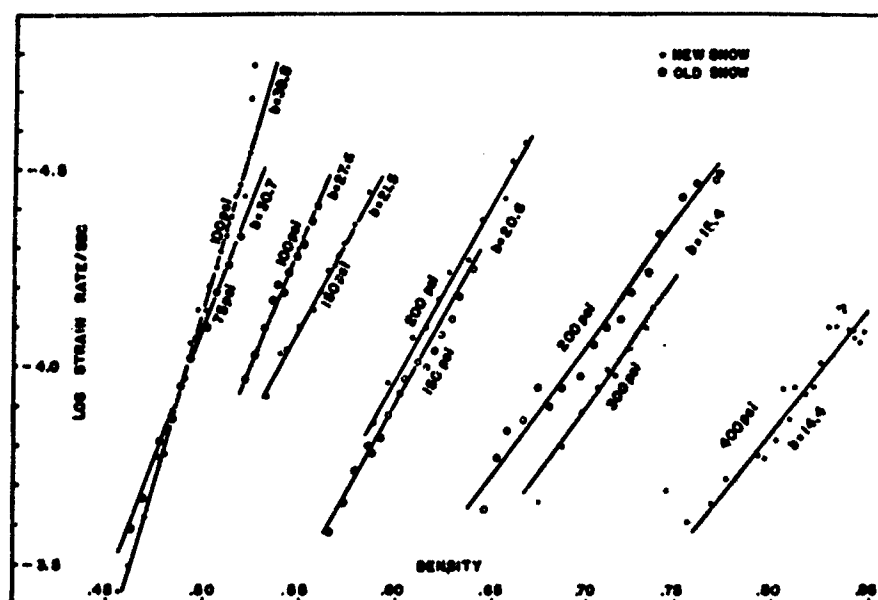


Figure 45. Strain rate versus density (g/cm^3) of two snow samples under incremental increase of uniaxial stress. Creep strain rate is very high.

reloaded several hours after extraction from the snow mass. It is obvious that relaxation processes are most important in creep mechanics; snow really never reaches a steady creep state, it is ever in a transient state of response.

4) Elasticity mechanics

Here we deal with high rates of stress application, where the elastic properties come to the fore. Validity of Hooke's law has been verified experimentally²⁷ for small stresses. Young's modulus (E) at -10°C determined from static load tests, increases from 10^7 dyne/cm² at density $0.2 \text{ g}/\text{cm}^3$ to 10^{10} at density of ice, according to an unknown function. Young's modulus calculated from resonance vibration (approximately 200 cps) of bars is much larger.²⁸ Figure 47 covers the density range 0.27 to $0.6 \text{ g}/\text{cm}^3$, and Figure 48 the whole range from 0.27 to maximum ice density. Two ranges for "ordinary" fine-grained snows are recognized, an exponential one for low density, and a linear one for high density. For Site 2, Greenland-snow test temperature -9°C , we have:

$$E = 6.3 \times 10^6 \exp 14.6 \gamma \text{ dyne}/\text{cm}^2 \text{ for } 0.27 < \gamma < 0.5 \quad (17)$$

and

$$E = (16.4 \gamma - 7.20) \times 10^{10} \text{ dyne}/\text{cm}^2 \text{ for } 0.5 < \gamma < 0.9. \quad (18)$$

The modulus is higher than normal for wind-packed snow (very fine grain) and lower for coarse-grained snow. Thus for a given density, E decreases with increasing grain size.

Young's modulus is dependent on test vibration frequency,²⁹ usually decreasing by some 10% between 200 and 300 cps and then remaining fairly constant from 300 to

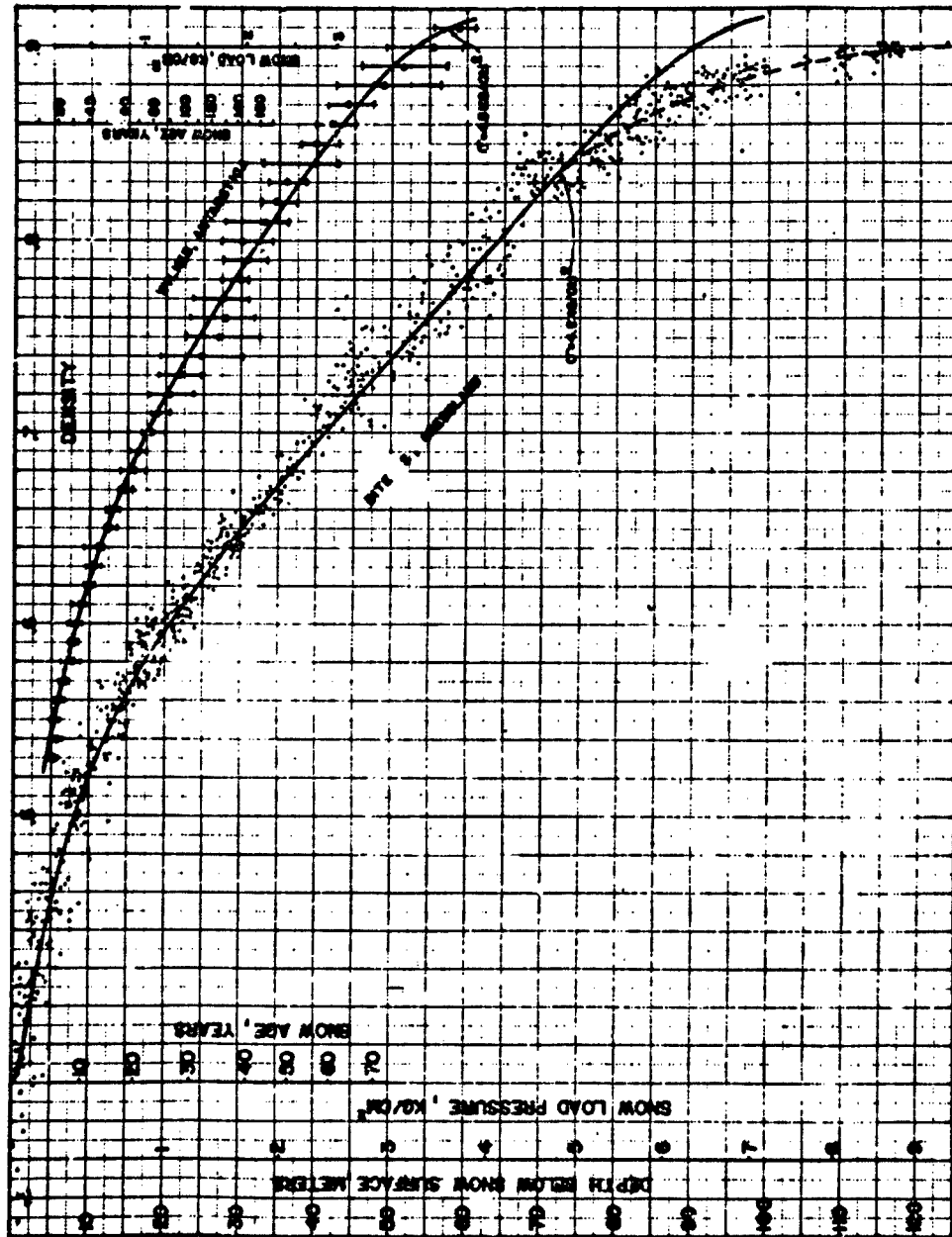


Figure 46. Depth-density relation for snow (to ice) at Site 2, Greenland (77° N 56° W). Temp -34.5°C. Curve is calculated from theory. The curve for Wilkes, Antarctica (66° S 102° E) is also shown.

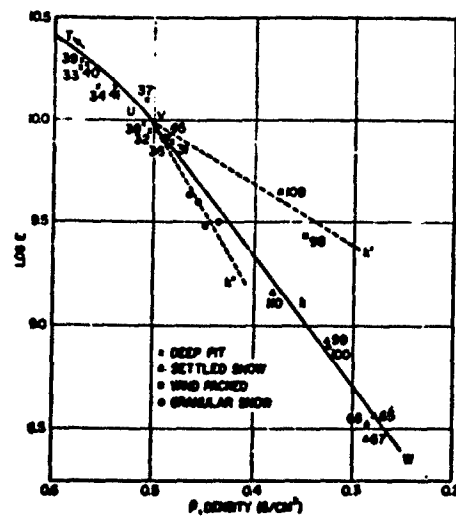


Figure 47. Young's modulus of snow versus density, obtained from vibrating bars. Site 2, Greenland. (From Nakaya, ref. 29)

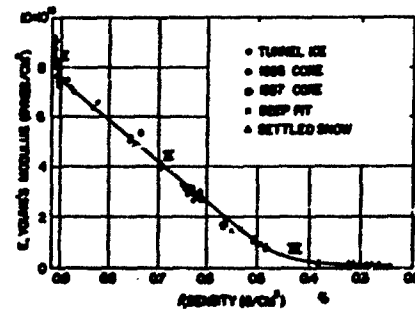


Figure 48. Young's modulus by vibration of snow and ice versus density, for an extended range of densities. Site 2 and Tuto, Greenland. (From Nakaya, ref. 29)

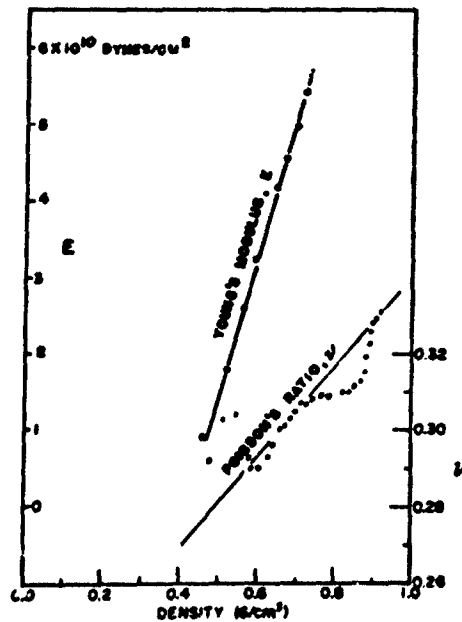


Figure 49. Poisson's ratio and Young's modulus versus density, obtained from seismic wave velocities. Site 2, Greenland.

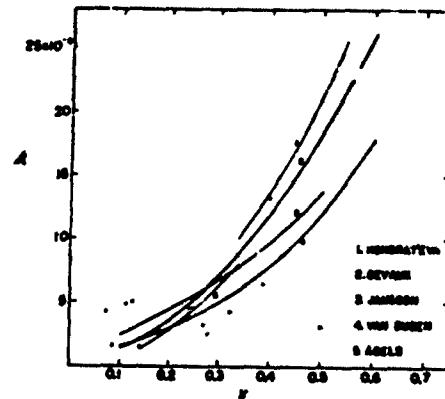


Figure 50. Thermal conductivity k versus density ρ .

600 cps. The smaller value at zero cycles may indicate the existence of a maximum somewhere between 0 and 200 cps.

Seismic depth-sounding at Site 2, Greenland,⁸ gave information on elastic moduli as a function of depth, which can be converted to one of density by means of the depth-density relation (Fig. 46). Values of Young's modulus E and Poisson's ratio ν are shown in Figure 49. The deviation of ν from the line is hardly real, and we write:

$$\nu = 0.22 + 0.122\gamma \quad 0.4 < \gamma < 0.72 \quad (19)$$

$$E = (18.5\gamma - 7.85) \times 10^{10} \text{ dyne/cm}^2 \quad 0.4 < \gamma < 0.72 \quad (20)$$

These values of E are a little higher than those obtained from vibrating bars (eq 18). Seismic records show no frequency dependence between 70 cps and 500 cps.

In large snow masses, sonic waves propagate according to the equations used in seismic sounding:

$$\text{compressional wave velocity } v_p = \sqrt{\frac{E}{\gamma} \cdot \frac{1-\nu}{(1+\nu)(1-2\nu)}} \quad (21)$$

$$\text{shear wave velocity } v_s = \sqrt{\frac{E}{\gamma} \cdot \frac{1}{2(1+\nu)}} \quad (22)$$

Substituting from eq 19 and 20, we can write expressions for wave velocity as a function of density, for Site 2 snow, $0.45 < \gamma < 0.72$

$$v_s = 2.74 \times 10^5 \sqrt{\frac{\gamma - 0.424}{\gamma(1 + 0.1\gamma)}} \text{ cm/sec} \quad (23)$$

$$v_p = v_s \cdot \sqrt{\frac{6.394 - \gamma}{2.295 - \gamma}} \text{ cm/sec} \quad (24)$$

Relations between Equivalent Parameters

For convenience in transformation between interchangeably used parameters, the following relations are given:

$$\gamma = \text{density, g/cm}^3 \quad 0 < \gamma < 0.917$$

$$V = \text{specific volume, cm}^3/\text{g} \quad \infty > V > 1.090$$

$$n = \text{porosity, dimensionless} \quad 1 > n > 0$$

$$e = \text{void ratio, dimensionless} \quad \infty > e > 0$$

$$\gamma_i = 0.917, \text{ density of ice}$$

$$V_i = 1.090, \text{ sp. vol. of ice}$$

$$\gamma = \gamma_i (1 - n) = \frac{\gamma_i}{e + 1} = \frac{1}{V}$$

$$V = \frac{1}{\gamma} = \frac{V_i}{1 - n} = V_i (e + 1)$$

$$n = \frac{\gamma_i - \gamma}{\gamma_i} = \frac{e}{e + 1} = \frac{V - V_i}{V}$$

$$e = \frac{\gamma_i - \gamma}{\gamma} = \frac{n}{1 - n} = \frac{V - V_i}{V_i}$$

Conversion Table

Several dimensional systems are used in text and figures. The following conversion table is given to facilitate transformation.

$$1 \text{ psi} = 7.03 \text{ kg/dm}^2 = 7.03 \times 10^{-2} \text{ kg/cm}^2 = 70.3 \text{ g/cm}^2 = 6.90 \times 10^4 \text{ dynes/cm}^2$$

$$1 \text{ kg/dm}^2 = 10^{-2} \text{ kg/cm}^2 = 10 \text{ g/cm}^2 = 9.81 \times 10^3 \text{ dynes/cm}^2 = 0.142 \text{ psi}$$

$$1 \text{ kg/cm}^2 = 10^2 \text{ kg/dm}^2 = 10^3 \text{ g/cm}^2 = 9.81 \times 10^5 \text{ dynes/cm}^2 = 14.2 \text{ psi}$$

$$1 \text{ g/cm}^2 = 0.1 \text{ kg/dm}^2 = 10^{-3} \text{ kg/cm}^2 = 9.81 \times 10^2 \text{ dynes/cm}^2 = 1.42 \times 10^{-2} \text{ psi}$$

$$1 \text{ dyne/cm}^2 = 1.02 \times 10^{-3} \text{ g/cm}^2 = 1.02 \times 10^{-4} \text{ kg/dm}^2 = 1.02 \times 10^{-6} \text{ kg/cm}^2 \\ = 1.45 \times 10^{-5} \text{ psi}$$

$$1 \text{ kg/m}^3 = 10^{-3} \text{ g/cm}^3$$

$$1 \text{ g/cm}^3 = 10^3 \text{ kg/m}^3$$

$$1 \text{ kg sec/m}^2 = 98.1 \text{ dynes sec/cm}^2 \text{ (poises)}$$

$$1 \text{ dyne sec/cm}^2 = 1.02 \times 10^{-2} \text{ kg sec/m}^2$$

$$1 \text{ degree Fahrenheit} = 5/9 \text{ of } 1 \text{ degree Celsius (formerly Centigrade)}$$

$$\text{Degrees F} = 32 + 9/5 \times \text{degrees C}$$

$$\text{Degrees C} = 5/9 (\text{degrees F} - 32)$$

$$\text{Degrees Kelvin} = 273.2 + \text{degrees C}$$

$$1 \text{ g/cm}^2 = 2.048 \text{ lb/ft}^2$$

$$1 \text{ g/cm}^3 = 62.43 \text{ lb/ft}^3$$

H. THERMAL PROPERTIES

The specific heat of the gas in the pores of snow is of the order of a thousandth of that of the ice content; hence the specific heat of snow is almost equal to that of ice ($\approx 0.5 \text{ cal/g-c}$).

Latent heats of melting and sublimation of snow and ice ($\approx 80 \text{ cal/g}$ and $\approx 700 \text{ cal/g}$ respectively) are also almost equal. The values for ice are discussed in another section.

It is possible that high precision measurement on snow, especially in the vicinity of the melting point, would show small deviations from the heat values of ice, due to the effects of small grain size and large interphase surface. The effect of interstitial gas would then also be felt.

No measurements of thermal coefficients of expansion of snow have been found. One would expect them to be somewhat smaller than those of ice (linear, $\approx 50 \times 10^{-6}$ per 1°C).

The thermal conductivity of snow is not well known; measurement is difficult, and the value is not only a function of density, but depends also on structure, texture, and interstitial air flow. Thermal conductivity of wet snow must be zero, because it is isothermal. Heat can penetrate wet snow by only two means, short wave radiation and percolation of melt water (release of latent heat upon refreezing). Thus a wet snow layer is an efficient one-way valve for heat which can get in (down), but not out (up).

In contrast, heat flow down through a dry snow layer under a temperature gradient is smaller than heat flow up under an equal, but inverse gradient. Let us list the mechanisms of heat transfer in dry snow.

- A. Conduction through the ice network.
- B. Conduction through the interstitial air.
- C. Radiant energy transfer between grains along temperature gradient.
- D. Via mass transfer in the vapor phase by diffusion along water vapor pressure gradient.
- E. Via mass transfer of air and vapor in convective flow.

The magnitude of the components A and C does not depend on whether heat flows up or down.

When the upper surface of the snow layer is warmer than the lower one, the interstitial air is stable ($E = 0$) and components B and D contribute to downward heat flow. But when the top is colder than the bottom, the interstitial air mass is unstable and convective flow can set in. Component E can become much larger than $B = D$.

Reference 24 is a good discussion of the problem of heat transfer with a list of references. The following information is extracted:

- a) of the component ($A + B + D$), B accounts for about $\frac{1}{4}$ at $\gamma = 0.33 \text{ g/cm}^3$
- b) Component D is almost independent of density, and can comprise as much as $\frac{1}{4}$ of the heat transfer in a snow cover
- c) Component D cannot be smaller than B.
- d) Component C is probably not significant; the temperature is too low for high radiation flux.

A number of different empirical equations relating the conductivity to density alone have been proposed. Four are listed in reference 36, together with individual field and laboratory measurements; a fifth comes from reference 23. The empirical equations for k represented in Figure 50, are:

Abels (1894)	$k = 0.0068\gamma^2 \text{ cal/cm-sec-C}$	$0.14 < \gamma < 0.34$
Jansson (1901)	$k = 0.00005 + 0.0019\gamma + 0.006\gamma^4$	$0.08 < \gamma < 0.5$
Van Dusen (1929)	$k = 0.00005 + 0.0010\gamma + 0.0052\gamma^3$?
Devaux (1933)	$k = 0.00007 + 0.007\gamma^2$	$0.1 < \gamma < 0.6$
Kondrat'eva (1945)	$k = 0.0085\gamma^2$ (artificially compacted snow)	$0.35 < \gamma$

The desirability of new determinations of thermal conductivity of snow under well defined conditions is evident. The relative influence of the factors listed above should be further investigated. Grain size may influence conduction through the ice network (factor A) sufficiently to have to be taken into the conductivity equation.

The reflection, absorption and scattering of radiant energy by snow will be discussed elsewhere. Here it is only mentioned that snow has an albedo (ratio of reflected to incident intensity of visible radiation) range of above 0.9 for clean new snow to about 0.5 for clean melting old snow. Dry snow without crusts is an almost perfect diffuser in the visible range (ref. 14) and both dry and wet snow are essentially black bodies in the infrared. Dry snow is relatively highly transparent to radiation of some radar and radio frequencies.

REFERENCES - Chapters A-H

1. Bader, H. (In Preparation) Theory of densification of snow on high polar glaciers II, U. S. Army Cold Regions Research and Engineering Laboratory, Corps of Engineers, Research Report 108.
2. ———; Haefeli, R.; Bucher, E.; Neher, J.; Eckel, O., and Thams, Chr. (1939) Der Schnee und seine Metamorphose (Snow and its metamorphism), Beitrage zur Geologie der Schweiz, Geotechnische Serie, Hydrologie, Lieferung 3. U. S. Army Snow Ice and Permafrost Research Establishment, Corps of Engineers, Translation 14, 1954, 313p.
3. ———; Waterhouse, R. W.; Landauer, J. K.; Hansen, B. L.; Bender, J. A., and Butkovich, T. R. (1955) Excavations and installations at SIPRE Test Site, Site 2, Greenland, USA SIPRE, Corps of Engineers, SIPRE Report 20, 32p.
4. Bender, J. A. (1957) Air permeability of snow, USA SIPRE, Corps of Engineers, Research Report 37, 19p.
5. Bentley, C. R.; Pruneroy, P. W., and Dorman, H. J. (1957) Seismic measurements on the Greenland Ice Cap. Part I: Studies at 76°59'N 56°05'W, Annales de Géophysique, vol. 13, no. 4, p. 253-275.
6. Bucher, E. (1948) Beiträge zu den theoretischen Grundlagen des Lawinenverbaus (Contribution to the theoretical foundations of avalanche defense construction), Beitrage zur Geologie der Schweiz, Geotechnische Serie, Hydrologie, Lieferung 6. USA SIPRE, Corps of Engineers, Translation 18, 1956, 109p.
7. ——— and Roch, A. (1946) Reibungs und Packungswiderstände bei raschen Schneebewegungen (Friction and resistance to compaction of snow under rapid motion), Mitteilungen des Eidgenöss. Institut für Schnee und Lawinenforschung, Davos-Weisshofjoch, 9p.
8. Butkovich, T. R. (1956) Strength studies of high-density snow, 3A SIPRE, Corps of Engineers, Research Report 18, 19p.
9. DeQuervain, M. (1945) Schnee als kristallines Aggregat (Snow as a crystalline aggregate), Experientia, vol. 1, no. 7, p. 207-212.
10. ——— (1948a) Das Korngefüge von Schnee (The grain structure of snow), Mitteilungen des Eidgenöss. Institut für Schnee und Lawinenforschung, vol. XXVII, no. 6, p. 1-12.
11. ——— (1948b) Korngrößenanalyse von Altschnee durch Sedimentation (Grain size analysis of old snow by sedimentation), Schweizerische Monatszeitung, vol. 66, no. 7, p. 117-118.
12. Eugster, H. P. (1952) Beitrag zu einer Gefügeanalyse des Schnees (Contribution to a textural analysis of snow), Beitrage zur Geologie der Schweiz, Geotechnischen Serie, Hydrologie, Lieferung 5, 64p.
13. Fuchs, Alfred (1959) Some structural properties of Greenland snow, USA SIPRE, Corps of Engineers, Research Report 42, 24p.
14. Giddings, J. C. and LaChapelle, E. (1961) Diffusion theory applied to radiant energy distribution and albedo of snow, Journal of Geophysical Research, vol. 66, no. 1, p. 181-189.
15. Haefeli, R. (1942) Spannungs- und Plastizitätserscheinungen der Schneedecke (Stress and plasticity phenomena in the snow cover), Schweiz. Arch. für Angewandte Wiss. und Technik, Nr. 9-12.
16. Ishida, T. and Shimizu, H. (1955) Sekitsetsu no tsuki teikō (Daippo) [Resistance of air flow through snow layers (Part I)], Tetsu-kagaku (Low Temperature Science Laboratory) Series A, vol. 14, USA SIPRE Translation 60, 1958, 8p.

REFERENCES - Chapters A-H (Cont'd)

17. Jellinek, H. H. G. (1957) Compressive strength properties of snow, USA SIPRE, Corps of Engineers, Research Report 34, 16p.
18. ——— and Brill, R. (1956) Viscoelastic properties of ice, Journal of Applied Physics, vol. 27, no. 10, p. 1198-1209.
19. ——— and Schlueter, W. (1957) Particle size distribution of pulverized snow, USA SIPRE, Corps of Engineers, Research Report 29, 8p.
20. Kauzmann, W. (1941) Flow of solid metals from the standpoint of the chemical-rate theory, Transactions of the American Institute of Mining and Metallurgical Engineers, vol. 143, p. 57-83.
21. Kingery, W. D. (1960) Regelation, surface diffusion, and ice sintering, Journal of Applied Physics, vol. 31, no. 5, p. 833-838.
22. Kojima, K. (1957) Sekisetsu-so no nensei asshuku, III (Viscous compression of natural snow layers III), Telson-kagaku (Low Temperature Science), Series A, vol. 16, p. 167-196.
23. Kondrat'eva, A. S. (1945) Teploprovodnost' snegovogo pokrova i fizicheskie protsessy, proiskhodiaschie v nom pod vlianiem temperaturnogo gradienta (Thermal conductivity of the snow cover and physical processes caused by the temperature gradient), Akademii Nauk SSSR. USA SIPRE Translation 22, 1954, 13p.
24. LaChapelle, E. (1960) Critique on heat and vapor transfer in snow, U. S. Department of Agriculture, Forest Service, Alta Avalanche Study Center, Project C, Report no. 1, 12p.
25. Landauer, J. K. (1955) Stress-strain relations in snow under uniaxial compression, USA SIPRE, Corps of Engineers, Research Paper 12, 9p.
26. ——— (1958) Creep of snow under combined st USA SIPRE, Corps of Engineers, Research Report 41, 18p.
27. ——— and Royse, F. (1956) Energy of snow compaction and its relation to trafficability, USA SIPRE, Corps of Engineers, Research Paper 14, 11p.
28. Nekaya, U. (1954) Snow crystals, natural and artificial, Cambridge, Mass.: Harvard University Press, 510p.
29. ——— (1959) Viscoelastic properties of snow and ice from the Greenland Ice Cap, USA SIPRE, Corps of Engineers, Research Report 46, 29p.
30. ——— and Matsumoto, A. (1953) Evidence of the existence of a liquidlike film on ice surfaces, USA SIPRE, Corps of Engineers, Research Paper 4, 6p.
31. Ripperger, E. A. and Davids, N. (1947) Critical stresses in a circular ring, Transactions of the American Society of Civil Engineers, vol. 12, p. 619-635.
32. Schaefer, V. J.; Klein, G. J. and DeQuervain, M. R. (1951) Entwurf einer internationalen Schneeklassifikation ausgearbeitet durch das Komitee für Schnee-klassifikation (Outline of an international snow classification), Union Géodésique et Géophysique, Association Internationale d'Hydrologie Scientifique. Assemblée Générale de Bruxelles, 1951, vol. 1, p. 129-141.
33. ——— (1954) The international classification for snow (With special reference to snow on the ground), The Commission on Snow and Ice of the International Association of Hydrology. Associate Committee on Soil and Snow Mechanics. National Research Council, Ottawa, Canada, Technical Memorandum 31.
34. Snow Ice and Permafrost Research Establishment (1954) Instructions for making and recording snow observations, Corps of Engineers, U. S. Army, Instruction Manual No. 1, 4th revision.

REFERENCES - Chapters A-H (Cont'd)

35. University of Minnesota (1951a) Preliminary investigations of some physical properties of snow, USA SIPRE, Corps of Engineers, SIPRE Report 7, 48p.
36. _____ (1951b) Review of the properties of snow and ice, USA SIPRE, Corps of Engineers, SIPRE Report 4, 156p.
37. Yosida, Z. et al. (1956) Physical studies on deposited snow II. Mechanical properties (1), Contribution no. 307, Institute of Low Temperature Science, Hokkaido University, Japan, no. 9, p. 1-81.
38. _____ (1957) Physical studies on deposited snow III. Mechanical properties (2), Contribution no. 361, Institute of Low Temperature Science, Hokkaido University, Japan, no. 11, p. 1-41.

J. ELECTRICAL PROPERTIES OF SNOW

by

Daisuke Kuroiwa

Introduction

Snow can be considered to be a "mixed dielectric" composed of air and ice. (Wet snow is a three-component system of air, ice, and water.) As mentioned in previous Chapters A and B, the snow cover on the ground changes its internal structure with time. It is to be expected that the dielectric properties of snow will become very complicated because of the continuing metamorphism. Since the main part of the dielectric material of the snow is ice, a brief description of recent studies of the dielectric properties of ice are given first. Then, the dielectric properties of the deposited snow are described from the viewpoint of the "mixed dielectric," bearing a close relation to its internal structure; and finally the dielectric behavior of snow in the high frequency range is treated as one of the problems of radio and microwave engineering in snowy regions.

Dispersion of the dielectric constant of ice

A great number of measurements have been conducted by various authors such as Wintsch (1932), Smyth and Hitchcock (1932), Murphy (1934), Kuroiwa (1951), Auty and Cole (1952), Humbel, Jona, and Scherrer (1953) and Granicher (1957) since J. Errera made his first experiment on the frequency dependence of the dielectric constant of ice in 1924. The anomalous dispersion of the dielectric constant of ice in the audio region is expressed by the well known Debye formula for polar dielectrics.

$$\epsilon^* = \epsilon' - j\epsilon'' = \epsilon_\infty + \frac{\epsilon_0 - \epsilon_\infty}{1 + j\omega\tau} \quad (1)$$

$$\epsilon'(\omega) = \epsilon_\infty + \frac{(\epsilon_0 - \epsilon_\infty)}{2} \left(1 + \frac{1}{1 + \omega^2\tau^2} \right)$$

$$\epsilon''(\omega) = \frac{(\epsilon_0 - \epsilon_\infty)\omega\tau}{1 + \omega^2\tau^2}$$

where ϵ^* is the complex dielectric constant of ice, ϵ' and ϵ'' are real and imaginary parts of ϵ^* , respectively. ϵ_0 is called the "static dielectric constant" or "direct current dielectric constant" and ϵ_∞ is the "high-frequency dielectric constant" or "optical dielectric constant." τ is the relaxation time, ω the angular frequency. These are important constants fundamental to dielectrics.

The characteristic constants ϵ_0 , ϵ_∞ and τ can be determined approximately in the following way. If we eliminate ω from eq (1):

$$\left(\epsilon' - \frac{\epsilon_0 - \epsilon_\infty}{2} \right)^2 + \epsilon''^2 = \left(\frac{\epsilon_0 - \epsilon_\infty}{2} \right)^2 \quad (2)$$

This is an equation of a circle expressed by ϵ' and ϵ'' . Consequently, if measured values of ϵ' and ϵ'' are plotted for each frequency in rectangular coordinates, their loci will form a semicircle of diameter $(\epsilon_0 - \epsilon_\infty)$ with its center on the ϵ' -axis at the location of $1/2(\epsilon_0 + \epsilon_\infty)$. This is the so-called "Cole-Cole" circle. The typical Cole-Cole circles of various kinds of ice obtained by Auty and Cole (1952) are shown in Figure J-1. The number shown at each point on the circles shows the frequency in kc; frequency increases from right to left on the circles. The two intersections of individual semicircles with the ϵ' -axis gives ϵ_0 and ϵ_∞ respectively. Curve (a) represents ϵ^* of ice which has cracks perpendicular to the direction of the applied electric field; curve (b) that of ice which is completely pure, with no cracks and bubbles; curves (c) and (d) that of ice which is slightly contaminated with impurity, but

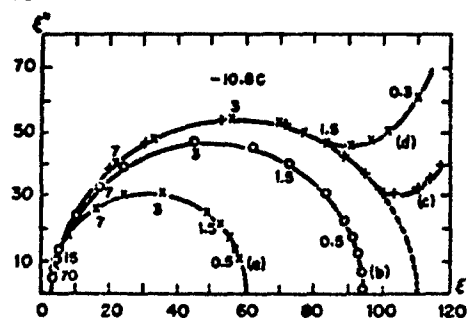


Figure J-1. Complex dielectric constants of various kinds of ice (Auty and Cole, 1952).

water. Humbel *et al.* (1953) also found that the dielectric constant of contaminated ice could reach the value of about 1000 at low frequency range while that of pure ice lay near 90.) However, no influences of the contamination or cracks are observed in high-frequency dielectric constants obtained from extrapolation of the Cole-Cole circle. (This fact does not mean that the high frequency dielectric constant is not influenced at all by cracks or contamination, because the Cole-Cole circle is only an approximate method for obtaining ϵ_{∞}).

The determination of τ is as follows: as seen from eq (1), ϵ'' takes a maximum value for the frequency ω_{\max} which satisfies $\omega\tau = 1$. If the frequency which gives a maximum ϵ'' on the frequency dependence curve is designated by ω_{\max} , one obtains $\tau = 1/\omega_{\max}$. The anomalous dispersion of the dielectric constant of ice in the audio-frequency range was explained by Granicher *et al.* (1957), assuming that the dipole orientation of water molecules in the ice crystal can be achieved through lattice imperfections. The relaxation time τ is the time required for the dipole orientation in an ice crystal, and is expressed by

$$\tau = A \exp(E/kT) \quad (3)$$

where A is the frequency factor due to lattice vibration $5.3 \times 10^{14} \text{ sec}^{-1}$, E the activation energy required for the orientation of dipole ($=13.2 \text{ Kcal/mol}$), k the Boltzmann constant, and T the absolute temperature, $^{\circ}\text{K}$.

Since the ice crystal belongs to the hexagonal system, an anisotropy of the dielectric constant in the directions of the crystal axes is to be expected. According to the experimental study of Humbel *et al.* (1953), the dielectric constant of a single crystal of ice in the direction parallel to c -axis was about 10% higher than that in the direction perpendicular to the c -axis, but the anisotropy was lost with decreasing temperature. (At a temperature below -90°C , it became isotropic.)

As shown in Figure J-1, ϵ_{∞} , the high-frequency or the optical dielectric constant, is 3.2. This value does not agree with the square of the optical index of refraction of ice ($1.31^2 = 1.72$). Recently the measurement of ϵ_{∞} of ice was extended to $1.25 \sim 3.2 \text{ cm}$ wavelength by Lamb and Turney (1949) and Cumming (1952); however its value still remains at 3.18.

Dielectric properties of snow in the audiofrequency range.

Cole-Cole circle of ϵ^* of snow. In order to measure the dielectric constant of snow, a block cut from naturally compacted snow was placed tightly in a condenser box as a dielectric between electrodes. The measured values of ϵ^* for various kinds of snow are given in Figure J-2. Curve 1, Figure J-2a shows how rapidly the dielectric

has neither cracks nor air bubbles. Designating (b) as giving the standard value of ϵ^* of pure ice, and estimating ϵ_0 and ϵ_{∞} , one obtains $\epsilon_0 = 95$ and $\epsilon_{\infty} = 3.2$. In case (a), where cracks exist in the interior of the specimen, $\epsilon_0 = 60$ and $\epsilon_{\infty} = 3.2$. In cases (c) and (d), contaminated ice, $\epsilon_0 = 110$, and $\epsilon_{\infty} = 3.2$. As shown in Figure J-1, chemical impurity increased ϵ_0 to a value greater than that of pure ice. On the contrary, cracks and air bubbles diminished ϵ_0 to a value smaller than that of pure ice. (The influence of chemical impurities on the dielectric constant of ice is remarkable. Smyth and Hitchcock (1932) found that it was increased by more than 20% when potassium chloride was added to the water in so small an amount as 15 mg to a liter of

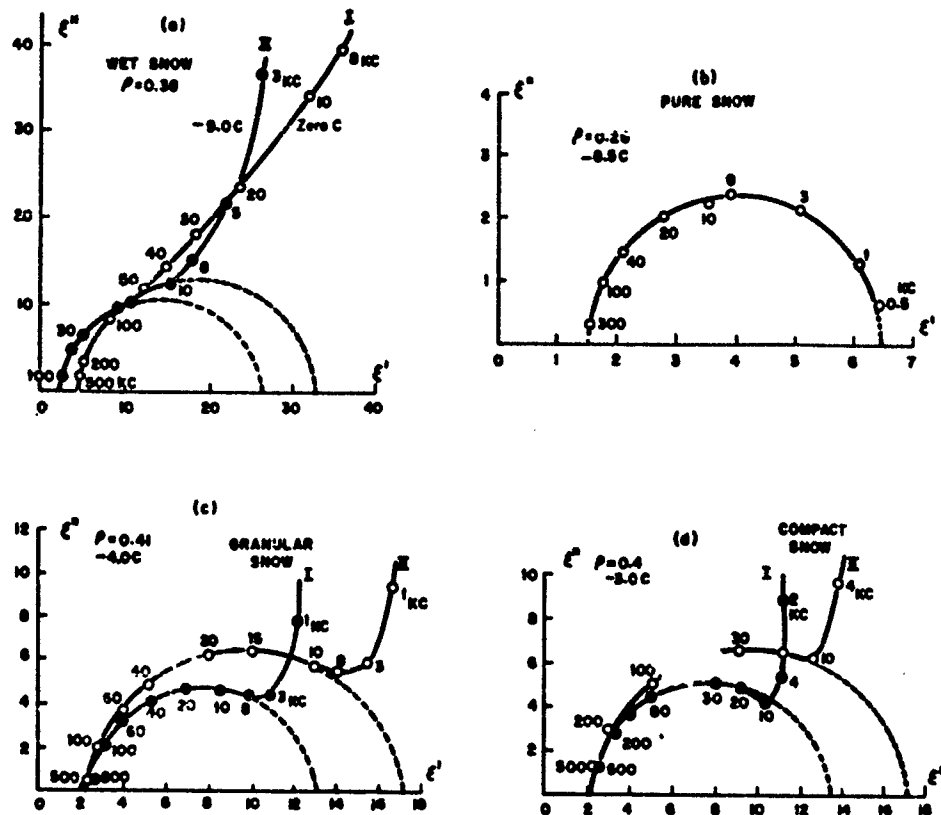


Figure J-2. Complex dielectric constants of various kinds of snow.

constant of wet snow increases with diminishing frequency, which must be ascribed chiefly to the increase of ionic conductivity due to the presence of liquid water. ϵ_0 and ϵ_∞ of wet snow (obtained from extrapolation of the Cole-Cole plot) are 33 and 4 respectively. After finishing the first measurement, the same specimen was placed in a cold room and the second measurement was carried out at a temperature of -9.0°C (Fig. J-2a, curve II). Here we get $\epsilon_0 = 26$ and $\epsilon_\infty = 1.8$. The difference in ϵ_∞ between wet snow and dry snow must also arise from the presence of liquid water in wet snow. In fact, the dielectric constant of water remains about 80 up to microwave range, whereas in the case of ice the dispersion occurs in the audiofrequency range. Figure J-2b shows ϵ^* of "pure snow," a very loose assemblage of hoar frost crystals which was carefully prepared in a cold room, without any contamination being introduced. As is expected, ϵ^* of pure snow forms a complete semicircle. Figure J-2c and J-2d represent the ϵ^* -curves of granular and compact snow, respectively, immediately after the snow was packed into the condenser (curve I) and about half a day later (curve II). Although the temperature of snow and macroscopic density were constant in both cases, the dielectric constant increased with the elapsed time. ϵ_0 , obtained from extrapolation of the Cole-Cole circle, increased

from 13 to 17 in granular snow, and from 13.5 to 17 in compact snow. However, no change of ϵ_m was observed in either case. The time dependence of the dielectric constant of snow is explained by the fact that the ice particles in snow become more and more coherent as time elapses, being connected by ice bonds formed mainly through sintering processes. Adhesion between snow particles and electrodes also will increase with time, with a resultant increase in static dielectric constant of snow. (The detailed explanation will be given later.)

Wiener's theory for the mixture of dielectrics. The snow, considered to be a "mixture of dielectrics," consists of two media - ice and air. In general, the mean electric field \bar{E} of the mixture is given by the following relationships

$$\left. \begin{aligned} E &= pE_1 + (1-p)E_2, \\ \epsilon E &= \epsilon_1 pE_1 + \epsilon_2 (1-p)E_2 \end{aligned} \right\} \quad (4)$$

where E_1 and E_2 are the mean electric fields of the media 1 and 2, respectively, ϵ is the resultant dielectric constant of the mixture, ϵ_1 and ϵ_2 are the dielectric constants of each component medium, and p is the proportion of the volume occupied by medium 1 to the total volume.

Putting $E_1/E_2 = U = \epsilon_2 + u / \epsilon_1 + u$, we obtain

$$\epsilon = \frac{\epsilon_1 p U + \epsilon_2 (1-p)}{pU + (1-p)} \quad (5)$$

$$\text{or} \quad \frac{\epsilon-1}{\epsilon+u} = \frac{p(\epsilon_1-1)}{\epsilon_1+u} + \frac{(1-p)(\epsilon_2-1)}{\epsilon_2+u}$$

This is Wiener's equation for the mixture of dielectrics. The resultant dielectric constant of the mixture is not only a function of p , but also depends on the parameters U or u . The magnitude of u , the so-called "form number" (Formzahl - German), is closely related to the structure of the dielectric mixture. If medium 1 is dispersed in medium 2 with a small volume concentration p , u is determined only by the shape of dispersoid 1. To determine how u varies with an arbitrarily varying shape of the dispersoid is a difficult problem, but we can grasp the idea of the physical meaning of u from the following considerations: Assume that the shape of the dispersoid particle is cylindrical. Then, if the cylinders were arranged between the two electrodes of a condenser with their axes parallel to the direction of the applied field, u would be infinitely large, since, in this case, the resultant dielectric constant ϵ of the mixture comes out to be

$$\epsilon = p\epsilon_1 + (1-p)\epsilon_2 \quad (u = \infty) \quad (6)$$

which, as is to be expected, gives the average value of the two dielectric constants, and expresses the maximum value attainable for the resultant dielectric constant of the mixture with given concentration. If the shape of the dispersoid particle is spherical, $u = 1$. If the dispersoid consists of thin plates with their planes perpendicular to the direction of the applied field, $u = 0$, and

$$\epsilon = \frac{\epsilon_1 \epsilon_2}{\epsilon_1(1-p) + \epsilon_2 p} \quad (u = 0) \quad (7)$$

which is the minimum possible value of ϵ .

If we assume an equivalent circuit for these snow condensers, eq 6 and 7 mean a parallel connection and a series connection of the ice condensers and the air condensers, respectively.

According to these considerations, increase of form number u implies the increase of lengthwise arrangement of the dispersoid in the direction of the applied field.

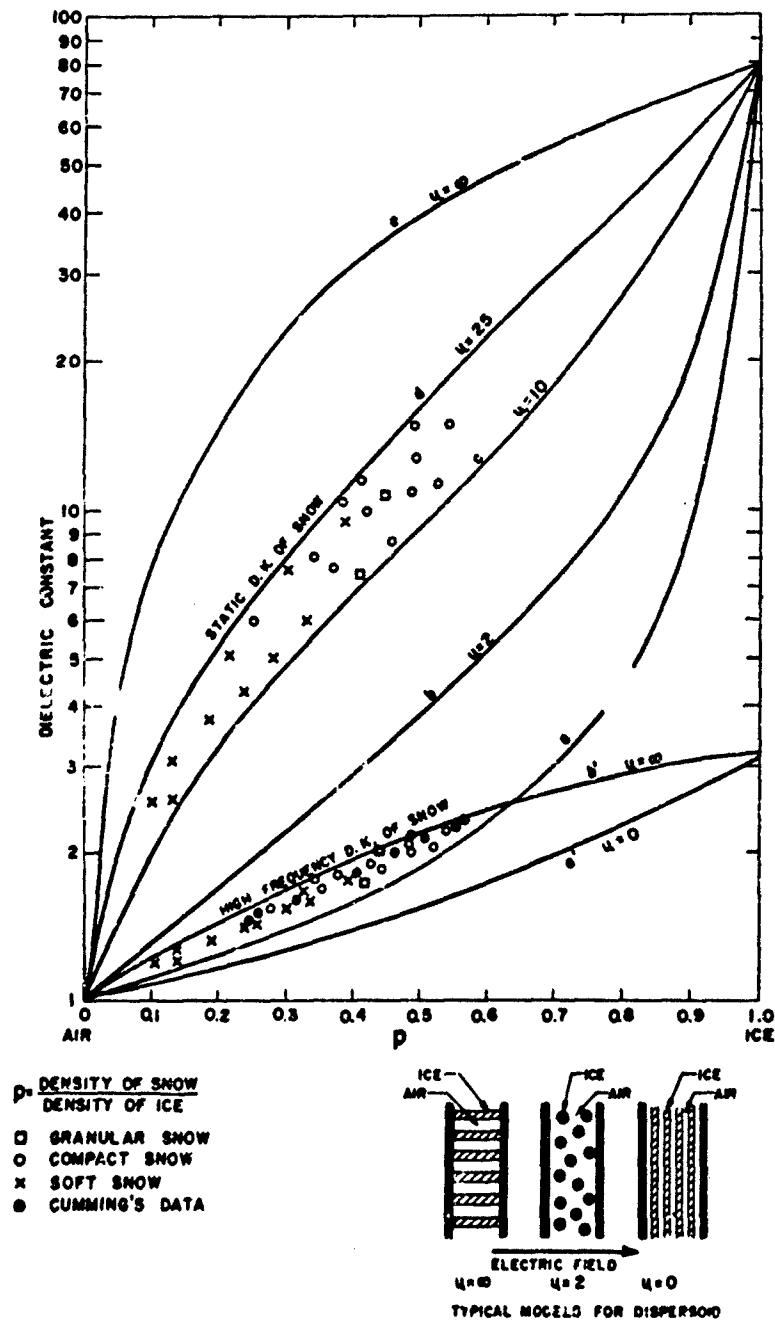


Figure J-3. Relation between static and high-frequency dielectric constants of snow and density ratio p .

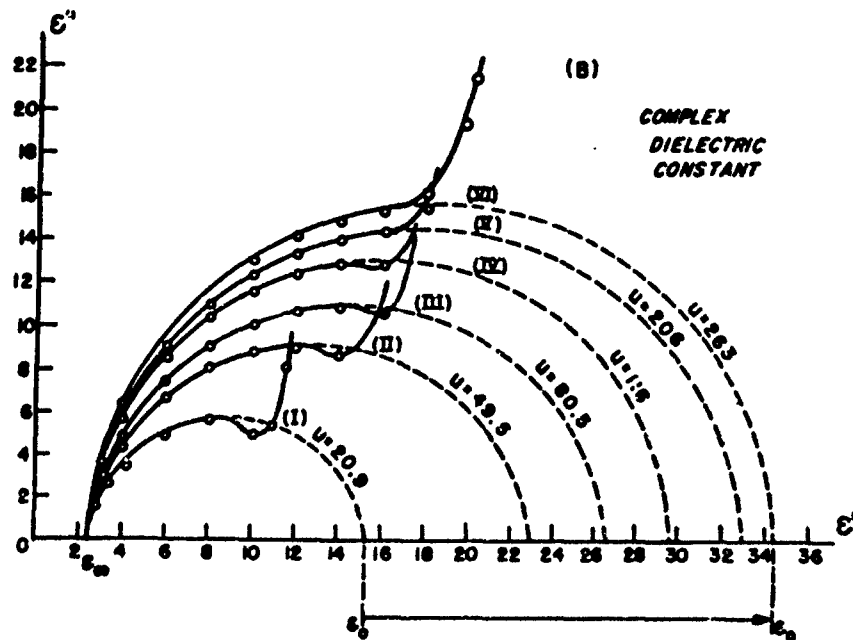
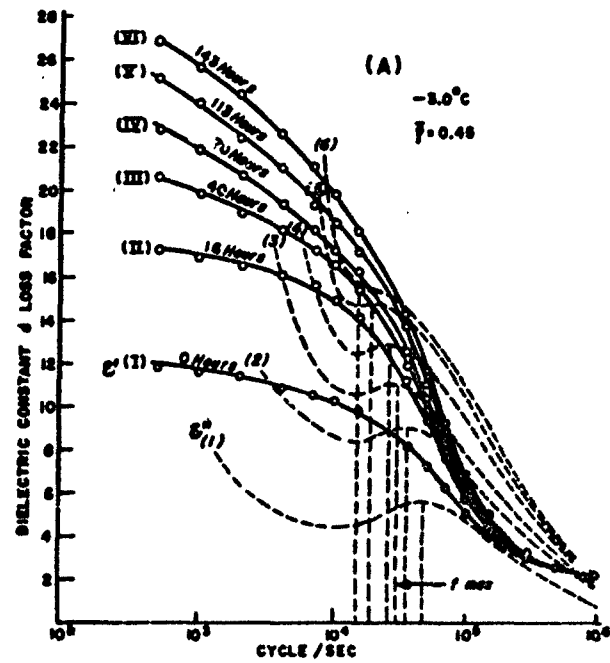


Figure J-4. Variation of dielectric constant of snow with lapse of time.

Static and high frequency dielectric constants of the natural snow as a function of p . In Figure J-3, ϵ_0 and ϵ_∞ of various kinds of snow are plotted against p , the ratio of the density of snow to that of ice: p gives the proportion occupied by ice particles in a unit volume of snow. All the data were obtained immediately after the snow was placed in the condenser. It is seen that the values of both ϵ_0 and ϵ_∞ show a general tendency to increase with increasing p , being scattered within a narrow band, as indicated in the figure. Curves (a), (b), (c), (d) and (e) represent the relationship between ϵ_0 and p calculated from eq 5, using values of $u = 0, 2, 10, 25$, and ∞ , respectively. (In this calculation, $\epsilon_1 = 20$ for ice, and $\epsilon_2 = 1.0007$ for air were used.) The observed values of ϵ_0 of natural snow were dispersed between (c) and (d), implying that their form number ranged from 10 to 25. The observed values for ϵ_∞ were scattered close to curve (b') calculated by using $u = \infty$, $\epsilon_1 = 3.2$ for ice, and $\epsilon_2 = 1.0007$ for air. The form number for ϵ_∞ came in the range 2.5 to 10. Curve (a') illustrates the minimum value of ϵ_∞ calculated as $u = 0$. The black circles indicated in Figure J-3 represent the Cumming's results (1952) for the wavelength of 3.2 cm. A good agreement is found between ϵ_∞ obtained from extrapolation of the Cole-Cole circle and that measured directly by microwave techniques. Three arrangements of the dispersoid for the cases of $u = \infty, 2$ and 0 are shown schematically in the lower right corner of Figure J-2.

Variations of ϵ^* and electrical conductivity of snow due to ice bonding. The ice particles in deposited snow become more and more coherent as time elapses, being connected by ice bonds; this has a great influence upon the dielectric properties of snow. Curves (c) and (d) in Figure J-2 show this effect but the following experiment demonstrates this phenomenon more clearly.

A block of compact snow was pulverized to powder to break up the ice bonds, and then was packed to an average density of 0.45 g/cm^3 in the condenser. The temperature was kept constant at -3.0°C . The observed variations of ϵ' and ϵ'' with frequency are illustrated in Figure J-4a, the lapse of time after the first measurement being taken as the parameter. Figure J-4b gives the corresponding Cole-Cole diagram for ϵ^* . ϵ_0 obtained through extrapolation is found to increase from 15 to 34 as time elapses, while ϵ_∞ remains constant. The form number u , as indicated in this figure, also increases with time from $u = 20.9$ to 263, which implies that ice bonds were progressively formed between ice particles and likewise between the electrode and ice particles. The mutual cohesion of ice crystals is at first only insignificant, but as time goes on ice bonds begin to grow, so that the crystals are eventually linked together. Figure J-5 shows the variation of apparent electrical conductivity K_{a-c} of the same specimen as a function of time. K_{a-c} of snow increased with time, though the electrical conductivity of ice itself does not change with time. Such an aging effect on K_{a-c} of snow must be explained by shortening of electrical paths due to the ice bonding. Schematic diagrams of ice bonding taking place in the snow condenser are shown in Figure J-5. Ice bonding under the constant temperature is achieved mainly through sintering processes described by Kingery (1960) and Kurihwa (1961).

Dielectric aftereffect and direct-current conductivity of snow. It is easily understandable that many difficulties in measuring d-c conductivity will arise from the complexity of its internal structure. In addition, natural snow contains chemical impurities; for instance, the following chlorine ion content can be observed in 1 liter of melted snow: several hundred milligrams near the sea coast, several tens of milligrams in an urban district and a few milligrams well inland. The chemical impurities greatly influence the d-c conductivity of snow. When a d-c voltage is abruptly applied to a condenser filled with a dielectric, the total current I passing through the condenser, in general, can be written in the following form:

$$I = I_0 + I_t + I_d \quad (8)$$

where I_0 is an instantaneous current, I_t a time-dependent current, and I_d a time independent current or d-c conduction current. At the moment of application of the d-c potential, I_0 flows as a result of instantaneous displacement of interatomic electric charges, then I_t follows immediately, indicating an exponential decrease with lapse of

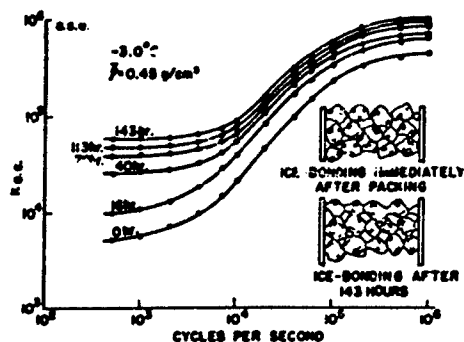


Figure J-5. Variation of apparent electrical conductivity, K_{a-c} , of snow with time.

A snow block cut out from the bottom layer of snow cover deposited in an urban district was used as a specimen. Its density was 0.4 g/cm^3 . The initial currents are shown in Figure J-6. Figure J-6a illustrates the time dependency of I as a function of the applied voltages at constant temperature -12°C . Since it was impossible to determine I_0 and I_t accurately for times shorter than $2 \times 10^{-3} \text{ sec}$, part of the curve is shown by dotted lines. The observation of I_t was continued for 5 min after application of the voltage but the decrease of I_t still continued. The inserted graphs, d, show the decrease of I_t at $5 \cdot 10^{-3} \text{ sec}$, $5 \cdot 10^{-2} \text{ sec}$, $5 \cdot 10^{-1} \text{ sec}$, 5 sec and 5 min against the applied voltages. Figure J-6b represents the records of I_t vs time for different temperatures at constant applied voltage 290 v. As will be seen in curves a, b, c, and d, I_t decreases remarkably with decreasing temperature, implying that d-c conductivity of snow strongly depends on the space charge polarization. In both experiments, therefore, was very difficult to determine the time-independent current I_d . But, if we define the current at 5 min after the d-c voltage application, the d-c resistivity of this snow comes out to be $4.28 \times 10^9 \text{ ohm} \cdot \text{cm}^{-1}$ (at -12°C). The behavior of the space charges in natural snow containing some chemical impurities is demonstrated more concretely by the following experiment.

As shown in Figure J-7, two probe electrodes T_1 and T_2 were inserted into the snow condenser. T_1 was located at $1/5$ the distance between the two electrodes of the condenser, T_2 at the center position between them. A potential of 300 v was applied to the snow condenser, and the voltage change with time between probes and outer electrodes was measured by an electrometer. Curves T_1 , T_2 represent the voltage change of the probes T_1 and T_2 , respectively. The potential T_1 increased with increasing time, but that of T_2 was kept constant. According to Joffe (1928), the change of voltage of the probe T_1 is explained by the migration of the space charges with time. Sikena (1957) measured the d-c conductivity of snow using sandwich electrodes and observed a similar phenomenon. A reasonable explanation has not yet been given for the mechanism of the space charge migration in snow; however, the following mechanism may be proposed for the electrical conductivity of snow. As was pointed out by Murphy and Lowry (1930), electrical conduction in solid dielectrics composed of microscopic cellular structures is achieved through a thin liquidlike film which can be considered to exist on the interfacial surfaces, where many ions are absorbed as shown schematically in Figure J-8. After the application of the electric field, these ions can move towards the applied field and cause polarization. Nakaya and Matsumoto (1953) suggested the existence of liquid water film on the ice surface even at temperatures below 0°C . In the case of snow, the liquid film can be considered to be a liquid solution film containing some chemical impurities. Its thickness will increase with increasing temperature. At higher temperature, the increase of freely movable ions results in the increase of the electrical conduction of snow. In fact, snow particles are connected by ice bonds. The space charges can be transferred through long

time. (The time required for I_t to drop to $1/e$ of its initial value is the relaxation time $\tau = 1/\omega_{\text{max}}$, where ω_{max} is an angular frequency which gives the maximum value of dielectric loss.) After a certain period, I_t approaches a time-independent current I_d given by a true resistivity or d-c resistance of the dielectrics. These phenomena are called dielectric aftereffect. If the material is pure and has a single relaxation mechanism, I_d or d-c conductivity can easily be measured. On the contrary, if the material is impure and has a complex relaxation mechanism like a snow, discrimination between I_t and I_d becomes very difficult because of ionic conduction due to chemical impurities.

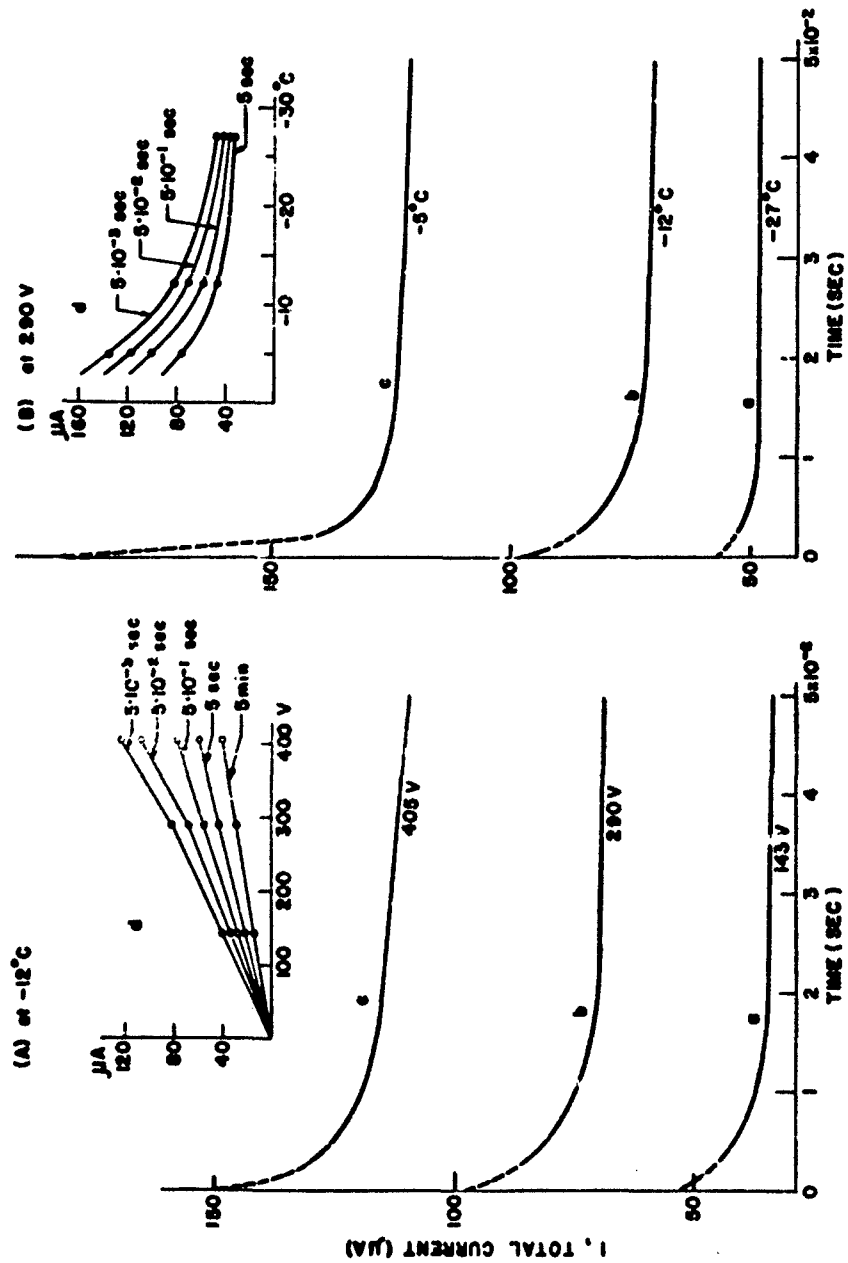


Figure J-6. Time dependence of direct current flowing through a snow condenser.

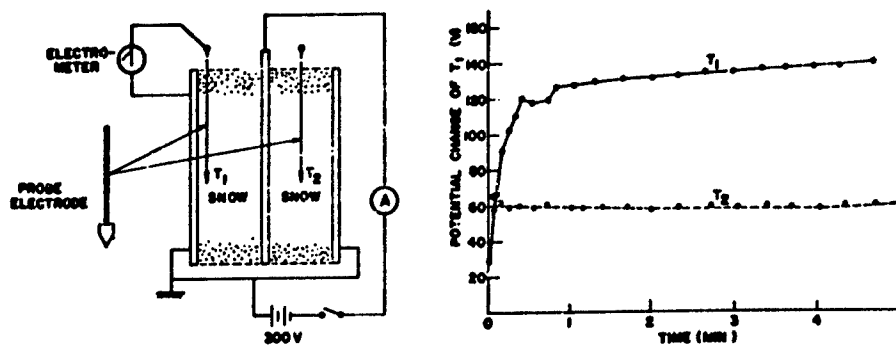


Figure J-7. Change of potential of probe electrodes inserted into snow condenser.

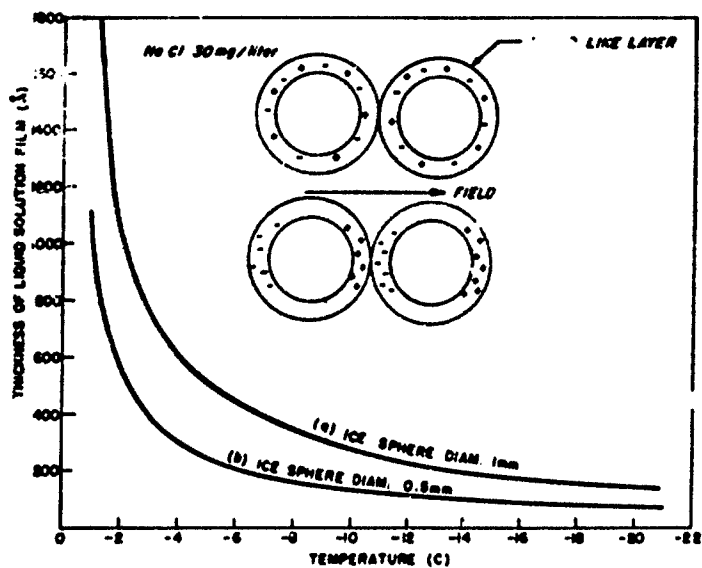


Figure J-8. Temperature dependence of the thickness of solution film in equilibrium with ice sphere.

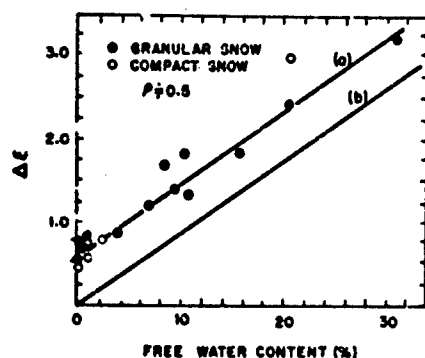


Figure J-9. Relation between $\Delta\epsilon$ and free water content in snow. $\Delta\epsilon$ = dielectric constant (wet snow) - dielectric constant (dry snow).

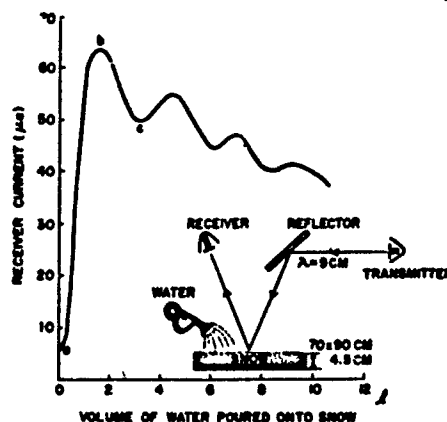


Figure J-10. An interference method for determining the dielectric constant of snow (Asami and Kurobe, 1949).

electrical paths formed by ice bonds. In Figure J-8, curves (a) and (b) represent the temperature dependence of the thickness of the solution film existing on the ice sphere surfaces. Approximate calculations were performed by assuming that: 1) 30 mg of NaCl are contained in one kilogram of snow, 2) snow is made of pure ice spheres having diameters of 0.5 mm and 1 mm, respectively, 3) each particle is covered with a concentrated NaCl solution in equilibrium with ice at a given temperature. The thickness of the solution film increases with increasing temperature; this fact may explain the temperature dependence of the electrical conductivity of snow.

Dielectric properties of snow in the high-frequency range - in relation to radio and microwave communication problems in a snowy district

Dielectric constant of wet snow. Since the dielectric constant of water is much larger than that of ice at high frequency (from 1 to 10^4 megacycles), namely about 80 for the former and 3.2 for the latter, it is to be anticipated that ϵ_{∞} of wet snow must increase in proportion to its free water content. The presence of even a small amount of liquid water will be of great importance for the dielectric behavior of snow. In Figure J-9, the difference $\Delta\epsilon$ between the high frequency dielectric constant of wet snow and that of dry snow is plotted against free water content. Wet snow having a density of about 0.5 g cm^3 was used in testing. The observed curve (a) does not pass through the origin of the coordinates, that is, $\Delta\epsilon$ remains finite, even when free water content is measured as zero. (This arose from the fact that the centrifugal separator was incapable of separating free water completely.) A true relationship between $\Delta\epsilon$ and water content should be expressed by curve (b). The dielectric constant of dry snow having a density of 0.5 g cm^3 , for example, is found to be 2.4 (Fig. J-3). If this snow becomes wet until it contains 20% water, its dielectric constant will become $2.4 + 1.8 = 4.2$. Figure J-10 shows another experiment concerning the determination of the dielectric constant of wet snow by the interference of an electromagnetic wave. An electromagnetic wave having a 9 cm wavelength was emitted horizontally from a transmitter and projected by a metallic reflector onto the surface of snow packed in a shallow box. Part of the incident wave is reflected at the snow surface, and another part is refracted into the snow and then reflected again at the base of the snow. Reflected and refracted waves combine to make an interference image on the receiver placed opposite the transmitter. When water was poured onto the snow surface, the signal received by the receiver changed as a function of the quantity of water. The dielectric constant of the snow increased with

increasing water content. The change of the dielectric constant of snow corresponds to the apparent increase of the thickness of snow. Therefore, it can be assumed that the following relations are satisfied between wavelength λ , thickness of snow d , and ϵ : $d\sqrt{\epsilon}/\lambda = 3/4$, $d\sqrt{\epsilon}/\lambda = 1$, and $d\sqrt{\epsilon}/\lambda = 1\frac{1}{4}$ at the points a, b, and c on the curve. One can easily calculate the dielectric constant of wet snow from these relations.

$$\begin{aligned}\epsilon &= 2.3 \text{ (at a, no water poured)} \\ \epsilon &= 4.0 \text{ (at b, 1.5 liters of water poured)} \\ \epsilon &= 6.0 \text{ (at c, 3.0 liters of water poured)}\end{aligned}$$

Loss factor, $\tan \delta$, of snow at high frequency range and absorption of the electromagnetic waves by snow. The loss factor, $\tan \delta$, of snow is needed in radio communications in a snowy district. In Figure J-11, values of $\tan \delta$ obtained by various authors for snow of 0.3 g/cm^3 are plotted in the frequency range between 10^5 cps and 10^{10} cps (100 kc and 10 gc*). Unfortunately, observed data are lacking in the frequency range between 10^7 and 8×10^9 cps (10 mc and 8 gc). There is no reason, however, to suppose that the frequency dependence of $\tan \delta$ in these ranges is not monotonic, so that the value of $\tan \delta$ can be estimated from a dotted line if required. As is expected from previous sections, $\tan \delta$ of snow is greatly influenced by a free water content. Typical data measured at 9.37 gc are given as a function of the free water content in Figure J-11. Black circles represent the values of $\tan \delta$ for ice obtained by various authors. No good agreement of the observed data is seen at the frequency of 10^{10} cps.

If the initial amplitude of the electromagnetic wave projected vertically onto the snow surface is expressed by I_0 (at $x = 0$) and that reached at a certain depth from the surface by I_x (at $x = x$), I_x is given by

$$I_x = I_0 \exp\left(\frac{2\pi x}{\lambda} a\right) \quad (9)$$

where

$$a = \frac{\epsilon'}{2} \left(\sqrt{1 + \tan^2 \delta} - 1 \right);$$

λ , the wavelength; ϵ' , the dielectric constant of snow. Using the ratio I_x/I_0 can be calculated as follows:

Depth	I_x/I_0 (for 1 mc)	I_x/I_0 (for 5 mc)	at -4.0C
1 m	0.999	0.985	
2 m	0.985	0.970	

Decrease of radiation power from high-frequency antenna due to icing or snow accretion. A common problem in snowy districts is snow accretion or icing on antennas. As mentioned above, the absorption of the electromagnetic wave in snow due to dielectric loss can be considered to be negligibly small, so long as the snow does not begin to melt. In order to study this problem, Asami and Kurobe (1949) made this laboratory experiment: A dipole antenna was enclosed in a glass tube, and snow was packed in it to create a situation analogous to natural snow accretion. A wavelength of 9 cm was used. When the air temperature was kept below 0C and the snow was maintained in a dry condition, no effect was observed, but when the antenna was placed in a warm room kept at +16C, a remarkable decrease of radiation took place with elapsed time. In Figure J-12a, curve I shows the decrease of receiver current with increasing time. The snow begins melting at the contact surface with the inside wall of the glass tube. Since water content of the snow should increase with time, it is quite natural to assume that the decrease of radiation of an electromagnetic wave can be attributed to the increase of free water content of snow. The same experiment was conducted using an iced antenna. When the surface of ice which covered the dipole antenna began to melt, the radiation power greatly decreased as shown in Figure J-12, curve II. Figure J-12b illustrates another experiment for an electromagnetic wave of 100 cm wavelength. In this case, only a slight decrease in radiation was observed at the melting point, though

*gigacycle

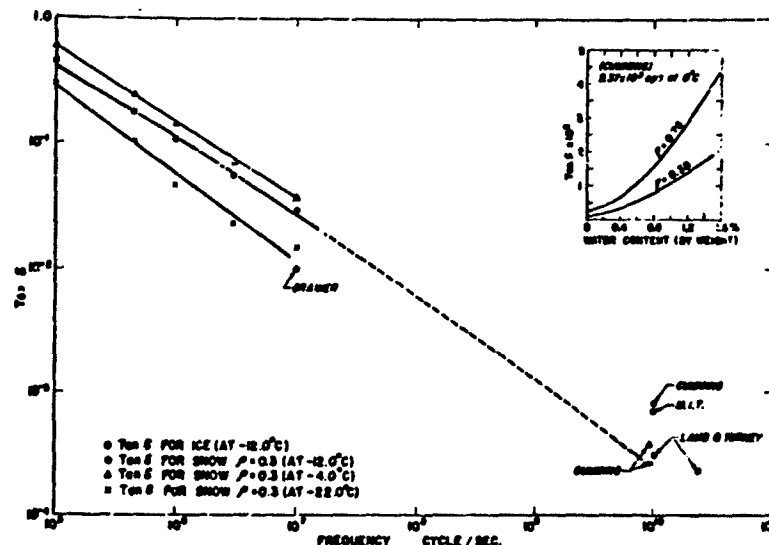


Figure J-11. $\tan \delta$ of snow at frequency range $10^3 - 10^6$ cps.
All values not otherwise marked were obtained by the author.

The surface of ice was covered with melted water. In above-mentioned experiments, the decrease of receiver current takes place mainly as a result of an impedance mismatching of the antenna and dielectric losses due to wet snow accretion or icing. When a complete matching of impedance was applied for the antenna, no decrease of radiation power was observed. From this fact, the inference can be drawn that the decrease of radiation of the electromagnetic waves must be attributed more to the impedance mismatching of antenna circuit than to the dielectric loss due to snow or ice.

Deflection of a beam of electromagnetic waves emitted from an iced feedhorn.
Microwave radiation is transmitted as a straight beam from a feedhorn. It is very important for microwave communication in snowy districts to know how much deflection of an emitted beam occurs as a result of icing or snow accretion on the feedhorn. In order to obtain some information about scattering of the beam under these conditions, microwave radiation of 12 cm wavelength was transmitted from a feedhorn having the dimensions shown in Figure J-11. A detector was fixed at a distance of 60 cm from the feedhorn, and the strength of the electric field emitted from the feedhorn was measured. The feedhorn could be rotated horizontally around a vertical axis to measure the distribution of the field strength of a scattered beam as a function of the angle of rotation. The typical distribution curves of a scattered beam are illustrated in Figure J-13. Curve (a) represents a normal distribution curve of the emitted beam from a non-iced feedhorn. When the horizontal axis of a feedhorn was directed toward the detector (in this case, angle = 0°), the strength of the electric field reached a maximum value; when the feedhorn was rotated around a vertical axis, the detector gave a sharp symmetrical distribution curve from side to side. Curves (b) through (f) illustrate the change in the distribution curve of the scattered beam emitted from the feedhorn when the snow block was attached in various ways to its inside surface. Curves (g) through (j) represent the cases where the snow blocks of various shapes were attached to the outside of the feedhorn. All experiments were carried out with wet snow. Dry snow kept below 0°C showed no influence on the transmission of a 12 cm wave. Figure J-9 suggests that wet snow accretion of irregular shape on the feedhorn greatly disturbs the direction of the emitted beam. Uniform snow accretion, e.g. (f) and (g), however, does not deflect the beam significantly.

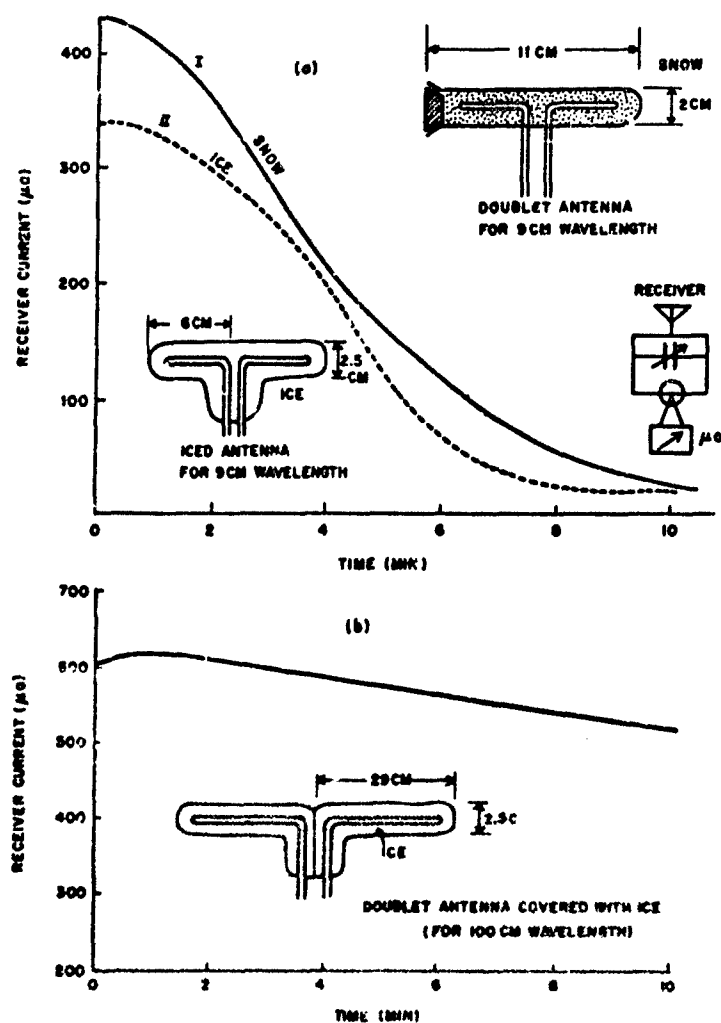


Figure J-12. Decrease of receiver current due to snow accretion or icing. (Asami and Kurobe, 1949).

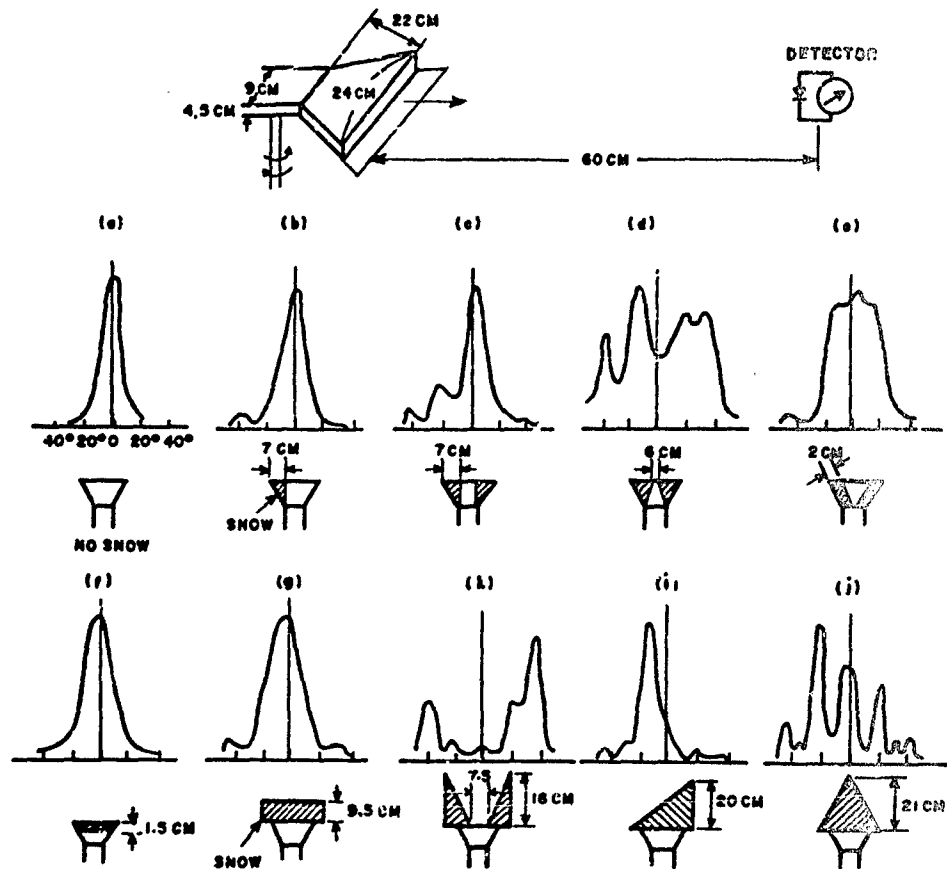


Figure J-13. Scattering of a 12 cm wave due to snow accretion on a feedhorn (Matsukawa and Kobayashi, 1955).

REFERENCES - Chapter J.

- Asami, Y. (1958) Microwave propagation in snowy districts, Research Institute of Applied Electricity of Hokkaido University, Monograph no. 6, (text in English).
- and Kurobe, T. (1949) Kyokusho tanppa antena ni oyobosu yuki, kori no aikyo (The effects of snow and ice on the antenna at ultra high frequencies), Mem. Faculty Eng. Hokkaido University, 8, no. 2 (text in Japanese), p. 123-132.
- Auty, R. P. and Cole, R. H. (1952) Dielectric properties of ice and solid D₂O, Journal of Chemical Physics, vol. 20, p. 1309-1314.
- Cole, K. S. and Cole, R. H. (1941) Dispersion and absorption in dielectrics, Journal of Chemical Physics, vol. 9, p. 341-351.
- Cumming, W. A. (1952) The dielectric properties of ice and snow at 3.2 cm, Journal of Applied Physics, vol. 23, p. 768-773.
- Errera, M. J. (1924) La dispersion des ondes hertziennes dans les solides au voisinage du point de fusion (Dispersion of Hertzian waves in solids near the melting point), Journal of Physical Radium, 5, p. 304-311.
- Gränicher, H.; Jaccard, C.; Scherrer, P.; and Steinemann, A. (1957) Dielectric relaxation and the electrical conductivity of ice crystals, Discussions Faraday Society, no. 23, p. 50-62.
- Granier, J. (1924) Absorption des ondes electromagnetiques par la glace (Absorption of electromagnetic waves by ice), Académie des sciences (Paris), Comptes Rendues, vol 179, p. 1313-1316.
- Humbel, F.; Jona, F.; and Scherrer, P. (1953) Anisotropie der Dielektrizitätskonstante des Eises (Anisotropy of the dielectric constant of ice) Helvetica Physica Acta, vol. 26, p. 17-32.
- Joffe, A. F. (1927) The physics of crystals. New York: McGraw-Hill, 11V.
- Kingery, W. D. (1960) Regelation, surface diffusion, and ice sintering, Journal of Applied Physics, vol. 31, p. 833-838.
- Kuroiwa, D. (1961) A study of ice sintering, Tellus, vol. 13, p. 253-259.
- (1951) Tekisetsu no yudenteki seishitsu (The dielectric behavior of snow covers), Low Temperature Science, vol. 8, p. 1-57, (text in Japanese).
- Lamb, L. and Turney, A. (1949) The dielectric properties of ice at 1.25 cm wavelength, Proceedings of the Physical Society of London, vol. 62B, p. 272-273.
- Matsukawa, K., and Kobayashi, S. (1955) Effects of snow on ultra high frequency wave, Studies on fallen snow, no. 5, (text in Japanese).
- Murphy, E. J. (1934) The temperature dependence of relaxation time of polarization in ice, Electrochemical Society, Transactions, vol. 65, p. 133-142.
- and Lowry, H. H. (1930) The complex nature of dielectric absorption and dielectric loss, Journal of Physical Chemistry, vol. 34, p. 598.
- Nakaya, U. and Matsumoto, A. (1954) Simple experiment showing existence of "a liquid water" film on the ice surface, Journal of Colloid Science, vol. 9, no. 1, p. 41-49.
- Saxton, J. A. (1950) Reflection coefficient of snow and ice at V.H.F., Wireless Engineering, p. 17-25.
- Sikena, R. (1957) Conduction of electricity through ice and snow I., Discharge of a condenser through ice crystals, Arkiv för Fysik, vol. 11, p. 495-510.

REFERENCES — Chapter J. (Cont'd)

- Smyth, C. P., and Hitchcock, C. S. (1932) Dipole rotation in crystalline solids, Journal of American Chemical Society, vol. 54, p. 4631-4647.
- Winnisch, H. (1932) Über Dielektrizitätskonstante, Widerstand und Phasenwinkel des Eises, (Dielectric constant, resistance, and phase angle of ice), Helvetica Physica Acta, vol. 5, p. 126-144.